WEAK GALERKIN FINITE ELEMENT METHODS FOR SOME INTERFACE PROBLEMS WITH NONHOMOGENEOUS JUMP CONDITIONS

by

PAPRI ROY

DEPARTMENT OF MATHEMATICS
INDIAN INSTITUTE OF TECHNOLOGY GUWAHATI
GUWAHATI-781039, INDIA

October, 2021

WEAK GALERKIN FINITE ELEMENT METHODS FOR SOME INTERFACE PROBLEMS WITH NONHOMOGENEOUS JUMP CONDITIONS

A thesis submitted

in partial fulfillment of the requirements

for the degree of

DOCTOR OF PHILOSOPHY

by

PAPRI ROY

(Roll No. 146123001)

Department of Mathematics

INDIAN INSTITUTE OF TECHNOLOGY GUWAHATI

October, 2021

Dedicated

to

my parents

CERTIFICATE

It is certified that the work contained in this thesis entitled **"Weak Galerkin finite element methods for some interface problems with nonhomogeneous jump conditions"** by **Papri Roy,** a student of Department of Mathematics, Indian Institute of Technology Guwahati, for the award of the degree of Doctor of Philosophy has been carried out under my supervision and that this work has not been submitted elsewhere for a degree.

October, 2021

Prof. Bhupen Deka
Professor
Department of Mathematics
Indian Institute of Technology Guwahati

ACKNOWLEDGEMENTS

It is my magnificent pleasure to write a note of thanks to all those who contributed in many ways to the successful completion of my Ph.D. and made it an unforgettable experience for me.

I would like to express my deep sense of gratitude and heartfelt appreciation to my supervisor Prof. Bhupen Deka who has introduced me to the research field and suggested this problem. For his encouragement, scholastic guidance, stimulating discussions, invaluable advice helped me immensely in completing this work. Without his active guidance, it would not have been possible for me to complete my research work. His guidance has helped me a lot during my Ph.D. work and during writing my thesis.

I want to convey my sincere gratitude to all the members of my doctoral committee: Prof. R. K. Sinha, Prof. R. Alam and Prof. S. N. Bora for their insightful comments and suggestions during the progress of my work. I also express my gratitude to all the faculty members of Mathematics Department for their help and cooperations.

I express my warm and sincere thanks to Prof. K. Kapoor, Head of the Department and Prof. M. G. P. Prasad, Swaroop Nandan Bora, Prof. N. Selvaraju, Prof. B. K. Sarma, former Heads of the Department for providing excellent research facilities during my Ph.D programme.

I take this opportunity to thank my research mates Dr. Jogen Dutta and Mr. Naresh Kumar for their help.

I sincerely acknowledge IIT Guwahati for providing me various facilities necessary to carry out my research. I am most grateful to Ministry of Human and Resource Development, Government of India, for providing me financial assistance for the completion of my thesis work. I am also grateful to all the technical and nontechnical staff members of the department for their help and cooperation throughout the period of my research.

Finally, I express my very profound gratitude to my grandfather Rajendranath Roy, my parents Bholen Roy and Puspa Dutta Roy, younger brother Arco Roy, my husband Biswanath Sarkar and all other family members for their continuous support, blessings, love and encouragement throughout my life. Words can never be enough to express my deepest sense of gratitude towards them.

Finally, I remain ever grateful to Almighty God for His blessings.

October, 2021

(Papri Roy)

Department of Mathematics

Indian Institute of Technology Guwahati

ABSTRACT

The objective of this thesis is to provide higher order convergence of weak Galerkin finite element solutions to the exact solutions of some time dependent partial differential equations with Lipschitz continuous interfaces. Due to low global regularity of the exact solution it is challenging to obtain higher order of convergence for interface problem. In this thesis, we have proposed non-conforming fitted weak Galerkin finite element methods (WG-FEMs) for some interface problems with nonhomogeneous jump conditions and related convergence analysis are carried out under low global regularity of the true solution.

The weak Galerkin finite element method is a numerical technique for partial differential equations where the differential operators (e.g., gradient, divergence, curl, Laplacian) are approximated by weak forms. Like the DG methods, WG-FEM makes use of discontinuous functions in the finite element procedure which endows WG-FEM with high flexibility to deal with geometric complexities and boundary conditions. WG-FEM enforces only weak continuity of variables naturally through well-defined discrete differential operators. Therefore, weak Galerkin methods avoid pending parameters resulted from the excessive flexibility given to individual elements. As a consequence, WG-FEMs are absolutely stable once properly constructed. The WG algorithm allows the use of finite element partitions consisting of general polygonal meshes.

In our first problem, we analyze WG-FEMs for parabolic interface problems. Both continuous time Galerkin method and discrete time Galerkin methods are discussed. Fully discrete schemes are based on backward Euler and Crank-Nicolson time discretizations. Optimal order error estimates in L^2 and H^1 norms are established for both semidiscrete and fully discrete schemes.

We next proceed to the a priori error analysis of wave equation with interfaces. Although various higher order finite element methods for elliptic and parabolic interface problems have been proposed and studied in the literature, but higher order finite element treatment of similar hyperbolic problems is mostly missing. In this work, we are able to prove optimal order point-wise-in-time error estimates in L^2 and H^1 norms for the wave equation with interfaces. Fully discrete scheme is based on backward Euler

method. Numerical experiments are reported for several test cases to confirm our theoretical convergence rate. Finite element algorithm presented here can be used to solve a wide variety of wave models for non-homogeneous inner structures.

In our last problem, we analyze WG-FEMs applied to pulsed electric model arising in biological tissue when a biological cell is exposed to an electric field. Considering the cell to be a conductive body, embedded in a more or less conductive medium, the governing system involves an electric interface (surface membrane), and heterogeneous permittivity and a heterogeneous conductivity. A fitted finite element method is proposed to approximate the voltage of the pulsed electric model across the physical media. Optimal pointwise-in-time error estimates in L^2-norm and H^1-norm are shown to hold for semidiscrete scheme even if the regularity of the solution is low on the whole domain. Further, a fully discrete finite element approximation based on backward Euler scheme is analyzed and related optimal error estimates are derived. Finally, we give numerical examples to verify the theoretical results.

Contents

List of Figures

List of Tables

1 Introduction

The objective of this thesis is to study higher order weak Galerkin finite element methods (WG-FEMs) for some interface problems with nonhomogeneous jump conditions. Interface problems are often referred to as differential equations with discontinuous coefficients. The typical mathematical models are the heat or wave type equations with discontinuous coefficients, which arise when the physical processes involve two or more materials or media with non-identical properties. Owing to its mathematical complexity and low regularity of its solutions, the study of interface problems has remained a major part of the mathematical study up to the present day. In the present work, we have used non-conforming fitted finite element methods to study the convergence of weak Galerkin finite element solutions to the exact solutions of some classes of interface problems.

1.1 Problem Description

In this section, we introduces the interface problems that to be studied in this thesis. It also contains a brief overview on the occurrence of these problems and their applications in many fields of science and engineering.

Parabolic Interface Problem: Let Ω be a convex polygonal domain in $\mathbb{R}^2$ with boundary $\partial\Omega$ and $\Omega_1 \subset \Omega$ be an open domain with Lipschitz boundary $\Gamma = \partial\Omega_1$. Let $\Omega_2 = \Omega \backslash \Omega_1$ be an another open domain contained in Ω with boundary $\Gamma \cup \partial\Omega$ (see, Figure 1.1). In $\Omega = \Omega_1 \cup \Gamma \cup \Omega_2$, we consider the following parabolic interface problem

$$u_t - \nabla \cdot (\beta \nabla u) = f \ \text{ in } \Omega \times (0, T],\ T < \infty, \tag{1.1.1}$$

with initial and Dirichlet boundary condition

$$u(x, 0) = u_0(x) \ \text{ in } \Omega; \ \ u = 0 \ \ \text{ on } \partial\Omega \times (0, T] \tag{1.1.2}$$

and interface conditions

$$[u] = \psi, \ \ \left[\beta \frac{\partial u}{\partial \mathbf{n}}\right] = \phi \ \ \text{ along } \Gamma \times (0, T]. \tag{1.1.3}$$

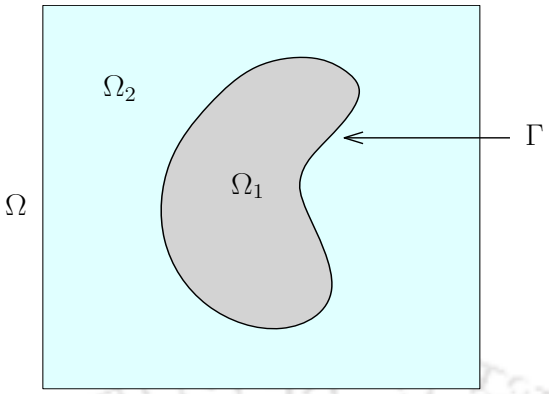

Figure 1.1: *Domain* Ω *and its sub domains* Ω_1, Ω_2 *with interface* Γ.

Here, $\mathbf{n}$ is the outward pointing unit normal to Ω_1 and $[v]$ denotes the jump of a quantity v across the interface Γ, i.e., $[v](x) = v_1(x) - v_2(x),\ x \in \Gamma$, where $v_i(x) = v(x)|_{\Omega_i}$, $i = 1, 2$. The coefficient function β is assumed to be positive and piecewise constant across Γ, i.e., $\beta(x) = \beta_k$ for $x \in \Omega_k,\ k = 1, 2$. Across the interface Γ, the source function $f : \Omega \times (0, T] \to \mathbb{R}$ can be singular. We assume that f is sufficiently smooth locally. Jump functions $\psi,\ \phi : \Gamma \times (0, T] \to \mathbb{R}$ and initial data $u_0 : \Omega \to \mathbb{R}$ are given.

The model equations of the form (1.1.1)-(1.1.3) involving discontinuous coefficients are sometimes called diffraction problems of parabolic type. Such problems arise in non-stationary heat conduction problems in two dimensions with a conduction coefficient which is discontinuous across a smooth interface. The study of parabolic interface problems is motivated by the models of heat conduction in composite materials [80], bio heat transfer in heterogenous media [132], heat-mass transfer problem [76], transport of a dissolved species in two-phase incompressible flow problems [122], viscoplasticity and plasticity with hardening as well as perfect plasticity [31], eddy current in electromagnetic field theory [8, 99] and cellular signal transduction [30].

Wave Interface Problem: Let Ω be a convex polygonal domain in $\mathbb{R}^2$ with boundary $\partial\Omega$ and $\Omega_1 \subset \Omega$ be an open domain with Lipschitz boundary $\Gamma = \partial\Omega_1$. Let $\Omega_2 = \Omega \backslash \Omega_1$ be an another open domain contained in Ω with boundary $\Gamma \cup \partial\Omega$ (see, Figure 1.1). In $\Omega = \Omega_1 \cup \Gamma \cup \Omega_2$, we consider the following wave interface problem

$$u_{tt} - \nabla \cdot (\beta \nabla u) = f \ \text{ in } \ \Omega \times (0, T], \tag{1.1.4}$$

with initial and boundary conditions

$$u(x, 0) = u_0(x), \ \ u_t(x, 0) = v_0(x) \ \text{ in } \Omega \ \ \& \ \ u(x, t) = 0 \ \ \text{ on } \partial\Omega \times (0, T] \tag{1.1.5}$$

and the jump conditions on the interface

$$[u] = \psi, \quad \left[\beta \frac{\partial u}{\partial \mathbf{n}}\right] = \phi \quad \text{along } \Gamma \times (0, T], \tag{1.1.6}$$

where the symbols $[v]$ and $\mathbf{n}$ are defined as before. The coefficient function $\beta(x)$ is assumed to be positive and piecewise constant across Γ, i.e., $\beta(x) = \beta_k$ for $x \in \Omega_k$, $k = 1, 2$. Source function $f : \Omega \times (0, T] \to \mathbb{R}$, jump functions $\psi,\ \phi : \Gamma \times (0, T] \to \mathbb{R}$ and initial data $u_0,\ v_0 : \Omega \to \mathbb{R}$ are given.

In the study of wave equations for some physical problems, such as acoustic or elastic waves traveling through heterogeneous media, there can be discontinuities in the coefficients of the equation at interfaces (e.g., [20, 21, 74] and references therein). For instance, an acoustic wave propagating at different speeds in different media is modeled by the second order wave equation with discontinuous coefficients. This wave propagation is modeled by the interface problem (1.1.4)-(1.1.6).

Electric Interface Model Problem: Let Ω be a convex polygonal domain in $\mathbb{R}^2$ with boundary $\partial\Omega$ occupied by the concerned physical media having conductivity $\sigma = \sigma(x)$ and permittivity $\epsilon = \epsilon(x)$. We now consider the pulsed electric field model for biological media [9, 102, 121, 147]

$$-\nabla \cdot \left(\epsilon \nabla u' + \sigma \nabla u\right) = f \quad \text{in } \Omega \times (0, T], \tag{1.1.7}$$

with initial and boundary conditions

$$u(x, 0) = u_0 \ \text{ in } \Omega; \quad u(x, t) = 0 \quad \text{on } \partial\Omega \times (0, T], \tag{1.1.8}$$

where u and f are the voltage potential and electric pulse of the model, respectively. Further, u_0 is the initial voltage and T is the finite terminal observation time, and u' denotes the derivative of u with respect to time variable.

The basic effects of an electric field on a biological cell can be described by considering the cell to be a conductive body (cytoplasm) surrounded by a dielectric layer (surface membrane), embedded in a more or less conductive medium. When an electric field is applied to this cell (by placing the cell in a conductive medium between two electrodes and applying an unipolar voltage pulse to the electrodes), the resulting current causes accumulation of electric charges at the membrane and consequently a voltage (transmembrane voltage) across the membrane. For details, we refer to [13, 100, 102, 117, 126] and references therein. In [102, 126], biological tissue is described as having a permittivity and a conductivity, and current flow through the biological medium is discussed in [13, 100, 117]. Figure 1.2 shows a cross-section of a single cell comprising of the cell cytoplasm and the cell membrane. Here, σ_j and ϵ_j define the conductivity and

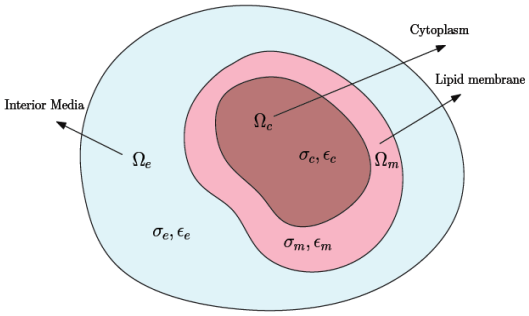

Figure 1.2: A cell comprising of the cell cytoplasm and the cell membrane.

permittivity of each medium with subscripts c, m and e describing the cell cytoplasm, membrane, and exterior media, respectively. Therefore the governing system involves interface (surface membrane) and discontinuous media parameters, which may find wide applications in electromagnetism, medicine, food sciences, and biotechnology. Of our special interest is the case when the physical coefficients are discontinuous and piecewise constant in Ω. Since generalization to multilayered media is straightforward, we can restrict ourselves to the case when domain Ω consists of two open subdomains Ω_1 and Ω_2 with Lipschitz interface Γ (see, Figure 1.2). We write

$$(\sigma, \epsilon) = \begin{cases} (\sigma_1, \epsilon_1) & \text{in } \Omega_1, \\ (\sigma_2, \epsilon_2) & \text{in } \Omega_2. \end{cases}$$

Then the information between both the domains are transferred via some interface conditions

$$[u] = \psi, \quad \left[\sigma \frac{\partial u}{\partial \mathbf{n}} + \epsilon \frac{\partial u'}{\partial \mathbf{n}}\right] = \phi \quad \text{along } \Gamma \times (0, T], \tag{1.1.9}$$

where $[u] := u_1|_\Gamma - u_2|_\Gamma$ and $\left[\sigma \frac{\partial u}{\partial \mathbf{n}} + \epsilon \frac{\partial u'}{\partial \mathbf{n}}\right] := \sigma_1 \frac{\partial u_1}{\partial \mathbf{n_1}} + \sigma_2 \frac{\partial u_2}{\partial \mathbf{n_2}} + \epsilon_1 \frac{\partial u_1'}{\partial \mathbf{n_1}} + \epsilon_2 \frac{\partial u_2'}{\partial \mathbf{n_2}}$. Here, u_i stands for the restrictions of u to Ω_i and $\frac{\partial}{\partial \mathbf{n}_i}$ denotes the outer normal derivative with respect to Ω_i, $i = 1, 2$. Further, jump functions ψ, $\phi : \Gamma \times (0, T] \to \mathbb{R}$ are given.

1.2 Preliminaries

1.2.1 Basic Notation

In this section, we shall introduce some basic notations, function spaces and preliminary materials to be used in this thesis. All functions considered here are real valued. For the purpose of introducing notations, we assume Ω to be a convex polygonal domain

in $\mathbb{R}^d$ (d-dimensional Euclidean space) and $\partial\Omega$ denote the boundary of Ω. For $x = (x_1, x_2, \ldots, x_d) \in \Omega$, set $dx = dx_1 \ldots dx_d$. Further, let $\alpha = (\alpha_1, \ldots, \alpha_d)$ be an d-tuple with nonnegative integer component and denote the order of α as $|\alpha| = \alpha_1 + \alpha_2 + \ldots + \alpha_d$. Then, by $D^\alpha\phi$, we shall mean the αth derivative of ϕ defined by

$$D^\alpha\phi = \frac{\partial^{|\alpha|}\phi}{\partial {x_1}^{\alpha_1} \ldots \partial {x_n}^{\alpha_d}}.$$

By support of a function ϕ, denoted by $\text{supp}(\phi)$, we mean the closure of all points x with $\phi(x) \neq 0$, i.e.,

$$\text{supp}(\phi) = \overline{\{x \in \Omega : \phi(x) \neq 0\}}.$$

For any nonnegative integer m, $C^m(\overline{\Omega})$ denotes the space of functions with continuous derivatives upto and including order m in $\overline{\Omega}$. $C_0^m(\Omega)$ is the space of all $C^m(\Omega)$ functions with compact support in Ω and $C_0^\infty(\Omega)$ is the space of all infinitely differentiable functions with compact support in Ω.

Now we introduce the following function spaces which we shall refer frequently. For any domain $\mathcal{M} \subseteq \Omega \subset \mathbb{R}^d$, $d = 2,\ 3$, with $1 \leq p \leq \infty$, $L^p(\mathcal{M})$ denotes the linear space of equivalence classes of measurable functions ϕ on Ω such that $\|\phi\|_{L^p(\mathcal{M})} < \infty$, where

$$\begin{aligned} \|\phi\|_{L^p(\mathcal{M})} &:= \left(\int_{\mathcal{M}} |\phi(x)|^p dx \right)^{\frac{1}{p}}, \quad 1 \leq p < \infty, \\ \|\phi\|_{L^\infty(\mathcal{M})} &:= \operatorname*{ess\,sup}_{x \in \mathcal{M}} |\phi(x)| < \infty. \end{aligned}$$

When $p = 2$, $L^2(\mathcal{M})$ is a Hilbert space with respect to the inner product

$$(\phi, \psi)_{\mathcal{M}} = \int_{\mathcal{M}} \phi(x)\psi(x)dx.$$

For simplicity of notation, we write the norm $\|\cdot\|_{L^2(\mathcal{M})}$ of $L^2(\mathcal{M})$ by $\|\cdot\|_{\mathcal{M}}$ and remove the subscript $\mathcal{M}$ whenever $\mathcal{M} = \Omega$.

We now introduce the notion of Sobolev spaces. For each integer $k \geq 0$ and real number p with $1 \leq p \leq \infty$, $W^{k,p}(\mathcal{M})$ denotes the standard Sobolev space of functions with their distributional derivatives of order up to k in the Lebesgue space $L^p(\mathcal{M})$, i.e.

$$W^{k,p}(\mathcal{M}) = \{\phi \in L^p(\mathcal{M}) :\ D^\alpha\phi \in L^p(\mathcal{M}) \text{ for } 0 \leq |\alpha| \leq k\}.$$

The spaces $W^{k,p}(\mathcal{M})$ are Banach spaces endowed with the norm

$$\begin{aligned} \|\phi\|_{k,p,\mathcal{M}} &:= \left(\sum_{0 \leq |\alpha| \leq k} \|D^\alpha\phi\|^p_{L^p(\mathcal{M})} \right)^{\frac{1}{p}}, \quad 1 \leq p < \infty, \\ \|\phi\|_{k,\infty,\mathcal{M}} &:= \max_{0 \leq |\alpha| \leq k} \|D^\alpha\phi(x)\|_{L^\infty(\mathcal{M})}, \quad p = \infty, \end{aligned}$$

also, the semi-norm on $W^{k,p}(\mathcal{M})$ is defined as

$$|\phi|_{k,p,\mathcal{M}} := \sum_{|\alpha|=k} \|D^\alpha \phi\|_{L^p(\mathcal{M})}.$$

When $p = 2$, we write $H^k(\mathcal{M})$ for $W^{k,2}(\mathcal{M})$ with the norm $\|\cdot\|_{k,2,\mathcal{M}} = \|\cdot\|_{k,\mathcal{M}}$ and the semi-norm $|\cdot|_{k,2,\mathcal{M}} = |\cdot|_{k,\mathcal{M}}$. For simplicity of notation, we skip the subscript $\mathcal{M}$ in the norm and inner product notation when $\mathcal{M} = \Omega$.

The space $H^k(\mathcal{M})$ is a Hilbert space with natural inner product defined by

$$(\phi, \psi)_{k,\mathcal{M}} = \sum_{0\le|\alpha|\le k} \int_{\mathcal{M}} D^\alpha \phi D^\alpha \psi dx, \quad \phi, \psi \in H^k(\mathcal{M}).$$

The Sobolev space $H_0^k(\Omega)$ is defined as the closure of $C_0^\infty(\Omega)$ with respect to the norm $\|\phi\|_k = \|\phi\|_{k,2}$. This result is true under some smoothness assumption on the boundary $\partial\Omega$. For a complete discussion on Sobolev spaces, see Adams and Fournier [1].

We shall also use the following space-time function spaces in our error analysis. For $1 \le p \le \infty$, we also define the standard Bôchner spaces $L^p(J;\mathcal{B})$, where $\mathcal{B}$ is a real Banach space with norm $\|\cdot\|_\mathcal{B}$ and $J = [0,T]$, consisting of all measurable functions $\phi : J \to \mathcal{B}$ for which

$$\begin{aligned} \|\phi\|_{L^p(0,T;\mathcal{B})} &= \Big(\int_0^T \|\phi(t)\|_\mathcal{B}^p dt\Big)^{\frac{1}{p}} < \infty \quad \text{for } 1 \le p < \infty, \\ \|\phi\|_{L^\infty(0,T;\mathcal{B})} &= \operatorname*{ess\,sup}_{t\in[0,T]} \|\phi(t)\|_\mathcal{B} < \infty \quad \text{for } p = \infty. \end{aligned}$$

We denote by $H^m(0,T;\mathcal{B})$, $1 \le m < \infty$, the space of all measurable functions $\phi : J \to \mathcal{B}$ for which

$$\|\phi\|_{H^m(0,T;\mathcal{B})} = \left(\sum_{j=0}^m \int_0^T \left\|\frac{\partial^j \phi(t)}{\partial t^j}\right\|_\mathcal{B}^2 dt\right)^{\frac{1}{2}} < \infty.$$

When no risk of confusion exists, we shall write $L^2(\mathcal{B})$ for $L^2(J;\mathcal{B})$, $L^\infty(\mathcal{B})$ for $L^\infty(J;\mathcal{B})$ and $H^m(\mathcal{B})$ for $H^m(J;\mathcal{B})$. Furthermore, $C(0,T;\mathcal{B})$ is defined as the space of continuous functions $\phi : [0,T] \to \mathcal{B}$ with norm $\|\phi\|_{C(0,T;B)} := \max_{t\in[0,T]} |\phi(t)| < \infty$. For a complete discussion on Sobolev Spaces, one may refer to Adams and Fourier [1], Dautray and Lions [42] and Evans [61].

For our notational convenience, we will be using $\frac{\partial u}{\partial t}$ or u_t or u' interchangeably to denote the first order time derivative of u with respect to t. Similar notions are used for higher order time derivatives.

Now we shall recall some important inequalities for our subsequent use (see Hardy *et al.* [71]):

Young's inequality. For $a, b \geq 0$ and $\mu > 0$, the following inequality holds

$$ab \leq \frac{a^2}{2\mu} + \frac{\mu b^2}{2}.$$

An important consequence of the Young's inequality is the Hölder's inequality. The discrete version of Hölder's inequality is stated below.

Hölder's inequality: Let $p > 1$ and q be such that $\frac{1}{p} + \frac{1}{q} = 1$. Then, for any real numbers $a_i, b_i \in \mathbb{R}, i = 1, 2, \cdots, d$,

$$\sum_{i=1}^{d} |a_i b_i| \leq \left(\sum_{i=1}^{d} |a_i|^p \right)^{\frac{1}{p}} \left(\sum_{i=1}^{d} |b_i|^q \right)^{\frac{1}{q}}.$$

In particular, for $p = q = 2$, the above inequality is known as the *Cauchy-Schwarz inequality* in $\mathbb{R}^d$.

The integral analogue of Hölder's inequality is as follows: Let $p > 1$ and q be such that $\frac{1}{p} + \frac{1}{q} = 1$. Then, for any measurable functions $\phi, \psi : \Omega \to \mathbb{R}$

$$\|\phi\psi\|_{L^1(\Omega)} \leq \|\phi\|_{L^p(\Omega)} \|\psi\|_{L^q(\Omega)}.$$

For $p = q = 2$, the above inequality is known as the *Cauchy-Schwarz inequality.*

Poincaré inequality: Let Ω be a bounded open domain in $\mathbb{R}^d$. Then there exists a positive constant $C = C(\Omega)$ such that

$$\|\phi\| \leq C \|\nabla \phi\| \quad \forall \phi \in H_0^1(\Omega).$$

In view of the Poincaré inequality, $\|\nabla(\cdot)\|$ defines a norm on $H_0^1(\Omega)$.

Next we state without proof, the following continuous version of Grownwall's lemma. For a proof, see Rao [118].

Lemma 1.2.1 (Gronwall's lemma)**.** *Let $G(t)$ be a continuous function and $H(t)$ a non-negative continuous function on its interval $t_0 \leq t \leq t_0 + a$. If a continuous function $F(t)$ has the property*

$$F(t) \leq G(t) + \int_{t_0}^{t} F(s)H(s)ds \quad \text{for } t \in [t_0, t_0 + a],$$

then

$$F(t) \leq G(t) + \int_{t_0}^{t} G(s)H(s) exp\left[\int_{s}^{t} H(\tau)d\tau \right] ds \quad \text{for } t \in [t_0, t_0 + a].$$

In particular, when $G(t) = C$ a nonnegative constant, we have

$$F(t) \leq C exp\left[\int_{t_0}^{t} H(s)ds \right] \quad \text{for } t \in [t_0, t_0 + a].$$

1.3 Background and Motivation

We now present a brief account of the relevant literature and motivation for the present study. Further, this section elucidates our contributions and motivation for the present study.

Interface problems are frequently encountered in scientific computing and many applied sciences. Typical examples are the elliptic, parabolic and hyperbolic equations with discontinuous coefficients. Numerical methods treating these interface problems have been investigated widely. Finite element method (FEM) is another class of important approaches for interface problems and a wide variety of FEM approaches have been proposed in the literature. There are two major classes of FEM depending on the choice of the discretization, namely, interface fitted FEMs and unfitted FEMs. In fitted FEMs, the discretization is made in such a way that the grid line is either follow the actual interface or an approximation of the smooth interface. In unfitted FEMs, the discretization is independent of the location of the interface. Numerical methods applied for interface problems based on finite element framework can be mainly grouped by conforming FEM, Mixed FEM, Discontinuous Galerkin (DG) and Immersed FEMs. More recently, weak Galerkin (WG) FEMs with polygonal meshes are applied to interface problems. Classical finite element methods for interface problems are mainly based on the interface-fitted discretization. The performance of such kind of interface-fitted FEMs depends not only on the quality of underlying finite element partition but also on the variational formulation of the problem. While the flux discontinuity of the solution can be captured in a variational formulation, the discontinuity of the solutions neither fit in the variational formulation nor satisfied in classical FEM solution spaces (see [9, 34, 43, 45, 46, 48, 49, 59, 85, 127], and references therein). Thus, conforming FEMs for interface problems assume continuity of the solutions along interfaces. Many efforts have been made to develop alternative finite element methods based on unfitted meshes for solving interface problems. Galerkin projections and numerical fluxes have been considered in discontinuous Galerkin (DG) variational formulations to weakly enforce the interface conditions (for instance, see [19, 26, 57, 70, 81, 82, 84, 101], and references therein). Surprisingly, there has been considerably less work on the mixed finite element methods for interface problems with non-homogeneous jump conditions (see [27, 157]). In fact, convergence analysis of mixed finite element methods for time-dependent interface problems is still open. More recently, local discontinuous Galerkin (LDG) method has been proposed to solve not only the homogeneous but also non-homogeneous parabolic interface problems in [11]. Using the LDG method for space

discretization, authors have derived the approximations for the potential and the flux at the same time. Moreover, unlike the conforming Galerkin methods which need special treatment for the discontinuity across an interface, the LDG method provides a natural framework to enforce the discontinuities in both the potential and the flux weakly in the discrete formulation. Theoretical convergence analysis of the LDG method for parabolic interface problems is still missing. Recently, it starts to gain more attention on developing Discontinuous Galerkin (DG) finite element methods for time dependent interface problems [11, 158]. Because the discontinuous approximation functions are employed, DG methods have many advantages such as high parallelizability, localizability, and easy handling of complicated geometries. Immersed FEMs is another popular class of numerical methods which allow the interface to cut through elements so that simple structured Cartesian meshes can be employed. Immersed FEMs can be regarded as the Galerkin formulations of finite difference based interface schemes. It is not surprising that the key ideas of many immersed FEMs actually come from the corresponding finite-difference based interface schemes. This renders immersed FEMs great popularity in solving a variety of interface problems (see [5, 6, 7, 35, 66, 69, 72, 75, 83, 92, 94, 95, 96, 154, 155], to name only a few). Further, combining immersed FEMs and DG methods (DG-IFE) together to solve PDEs has been proposed in [95] and subsequently it has been extended for parabolic interface problems in [96, 155] and hyperbolic interface problems [5, 6, 7]. For higher order finite element methods with sufficiently smooth interface, we refer to [3, 4, 24, 78, 81, 82, 85]. The existing work on FEMs for interface problems assume C^2-smooth interface Γ. The material interfaces in real applications can be geometrically complicated and very irregular. In some extreme cases with non-smooth interfaces or interfaces with Lipschitz continuity, geometric singularities, such as sharp edges, cusps and tips, could be encountered. It is challenging to obtain high order convergence when the interface geometries are arbitrarily complex. To achieve a higher order of convergence in the body fitted FEMs, in which unstructured meshes conform to the interfaces, a proper variational formulation that handles jumps in solution and flux is indispensable. On the other hand, discontinuity of the solution along interface adds more challenge than one would imagine. A higher order weak Galerkin (WG) method is introduced in [112] for the elliptic interface problem. The WG method in [112] has many new features including symmetric positive definite formulation, fewer unknowns and, more importantly, allowing the use of general meshes such as hybrid meshes, polygonal and polyhedral meshes and meshes with hanging nodes. These features make the new WG-FEM more flexible in handling complicated interface geometries. Further, the WG finite element algorithm allows interfaces with Lipschitz continuity. Then the author in [44] provides an optimal

combination for the polynomial spaces that minimize the number of unknowns in the WG scheme without affecting the accuracy of the numerical approximation.

Time evolution equations (which often lead to parabolic PDEs) are considered to study and understand the dynamics of nature. The best-known linear parabolic PDE is the heat (or diffusion) equation, where an interface problem occurs when two distinct materials or fluids with different conductivities or densities or diffusions are involved. In this thesis, a fitted WG-FEM is proposed and analyzed for the interface problem (1.1.1)-(1.1.3). Typical semidiscrete and fully discrete schemes are presented, and analyzed. The fully discrete space-time finite element discretization are based on backward Euler and Crank-Nicolson approximations. Optimal *a priori* error estimates for both semidiscrete and fully discrete schemes are proved in $L^\infty(H^1)$ and $L^\infty(L^2)$ norms for the weak finite element space $(\mathcal{P}_k(K),\ \mathcal{P}_{k-1}(\partial K),\ \left[\mathcal{P}_{k-1}(K)\right]^2),\ k \geq 1$. The new WG algorithm allows the use of finite element partitions consisting of general polygonal meshes and applicable to interface problems with Lipschitz interfaces.

Solving wave propagation problems within heterogeneous media has been of great interest and has drawn significant attention in a variety of fields such as the oil exploration industry and mineral finding as well as the study of earthquakes. Previous works on FEMs for wave equation with interfaces are concerned only on linear elements and assume continuity of the solution along interfaces. In this thesis, WG-FEM is introduced for solving the interface problem (1.1.4)-(1.1.6) on weak Galerkin finite element space $(\mathcal{P}_k(K), \mathcal{P}_{k-1}(\partial K), [\mathcal{P}_{k-1}(K)]^2)$. Optimal order a priori error estimates for both space-discrete scheme and implicit fully discrete scheme are derived in $L^\infty(L^2)$ norm. Our results are intended to enhance the numerical analysis of linear wave equations where physical domain consists of heterogenous media.

The equation (1.1.7) is numerically interesting as it does not belong to the well-studied classes of time-dependent equations. Numerical solutions of electric interface model (1.1.7)-(1.1.9) draw significant attention in a variety of fields such as neural activation during deep brain simulations, debacterization of liquids, food processing, biofouling prevention, selective spectroscopic imaging of the electrical properties of biological media. In this thesis, the weak Galerkin finite element method is applied to a pulsed electric model arising in biological tissue when a biological cell is exposed to an electric field. A fitted weak Galerkin finite element method is proposed to approximate the voltage of the pulsed electric model across the physical media involving an electric interface (surface membrane), and heterogeneous permittivity and a heterogeneous conductivity. Optimal pointwise-in-time error estimates in L^2-norm and H^1-norm are shown to hold for the semidiscrete scheme even if the regularity of the solution is low

on the whole domain. Further, a fully discrete approximation based on backward Euler scheme is analyzed and related optimal error estimates are derived.

1.4 WG Discretization for Interface Problems

In this section, we shall briefly introduce WG-FEMs for elliptic interface problem. More precisely, we discuss weak Galerkin discretization for interface problems, review the definition of the weak gradient operator and its discrete analogue.

In $\Omega = \Omega_1 \cup \Gamma \cup \Omega_2$ (see, Figure 1.1), we consider the following linear elliptic interface problem

$$-\nabla \cdot (\beta \nabla u) = f \ \text{ in } \Omega \tag{1.4.1}$$

with Dirichlet boundary conditions

$$u = 0 \quad \text{on } \partial\Omega \tag{1.4.2}$$

and interface conditions

$$[u] = \psi, \quad \left[\beta \frac{\partial u}{\partial \mathbf{n}}\right] = \phi \quad \text{along } \Gamma \times (0, T]. \tag{1.4.3}$$

Symbols $[v]$ and $\mathbf{n}$ are defined as before. The coefficient function $\beta(x)$ is assumed to be positive and piecewise constant across Γ, i.e., $\beta(x) = \beta_k$ for $x \in \Omega_k,\ k = 1, 2$. Source function $f : \Omega \to \mathbb{R}$ and jump functions $\psi,\ \phi : \Gamma \times (0, T] \to \mathbb{R}$ are given. Throughout this thesis, we assume that Ω is a convex polygon in $\mathbb{R}^2$ and interface Γ is sufficiently smooth so that solutions to the interface problems belong to desired Sobolev spaces.

The model equation of the form (1.4.1) is known as stationary heat conduction problems. Numerical methods treating these problems have been investigated widely. Finite element method (FEM) is another class of important approaches for partial differential equations and a wide variety of FEM approaches have been proposed in the literature. For details, we refer to Brenner *et al.* [22] and Ciarlet [36], and references therein. The classical finite element methods based on conforming finite element discretization, have limitations in practical computation. The conforming finite element space is restricted to piecewise polynomials with prescribed continuity that ensures conformity and stability of the corresponding weak formulation, which is often very difficult to implement, particularly for problems in high dimensions and/or on general polytopal partitions. In scientific computing, higher order of convergence is always one of the major research goals, because high order methods are more accurate and cost efficient. Although conforming finite element methods have simple formulations with many fewer unknowns, construction of conforming finite element spaces of any orders would be either challenging or impossible. Keeping in mind the applicability of numerical methods of higher

order with polygonal meshes, recently attempts have been made to develop certain technologies which make use of polygonal meshes, for instance, see [133, 134, 135] for virtual element methods, [15, 28, 29, 37, 39] for discontinuous Galerkin methods.

Recently, the weak Galerkin finite element method has attracted much attention in the field of numerical partial differential equations. The WG-FEM introduced in [143] refers to the numerical algorithms for differential equations where the differential operators appearing in the variational forms are to project into another appropriately chosen Sobolev space such that its approximation by polynomials is possible. More precisely, the WG finite element approximations are derived from the weak formulations of the problems by replacing differential operators involved by its weak forms and adding parameter free stabilizers. In fact, WG formulation is a natural extension of conforming finite element formulation when nonconforming elements are used. In [143], a weak Galerkin method was introduced and analyzed for second order elliptic equations based on a *discrete weak gradient* arising from local *RT* ([120]) or *BDM* ([23]) elements. Due to the use of the *RT* and *BDM* elements, the weak Galerkin finite element formulation of [143] was limited to classical finite element partitions of triangles ($d = 2$) and tetrahedra ($d = 3$). A computational study of the weak Galerkin method for second-order elliptic equations has been carried out in [105]. In [144], a WG-FEM was developed for the second order elliptic equation in mixed form. The use of stabilization for the flux variable in the mixed formulation is the key to the WG mixed finite element method of [144]. The resulting WG mixed finite element schemes turned out to be applicable for general finite element partitions consisting of shape regular polytopes, and the stabilization idea opened a new door for weak Galerkin method. The WG approach has been extended to a variety of PDEs arising from the mathematical modeling of practical problems in science and engineering. There is an abundant literature on such PDEs; see, e.g., elliptic equation [86, 87, 89, 97, 98, 109, 110, 129, 140, 142, 144], biharmonic equation [40, 56, 106, 108, 111, 138, 156, 159], parabolic equation [50, 65, 88, 149, 160, 161, 162], wave equation [73, 137], system of equations [32, 90, 93, 103, 104, 113, 139, 145, 146], interface problems [44, 52, 107, 112, 130] etc.

Let $\mathcal{T}_h$ be a partition of the domain Ω with mesh size h. We require that the edges of the elements in $\mathcal{T}_h$ align with the interface Γ. A simple and efficient interface fitted mesh generation algorithm has been proposed in [33]. Elements in such interface fitted meshes are not restricted to simplices but can be polygons or polyhedra. A typical element is presented in Figure 1.3. Thus, the partition $\mathcal{T}_h$ can be grouped into two sets of elements denoted by $\mathcal{T}_h^1 = \mathcal{T}_h \cap \Omega_1$ and $\mathcal{T}_h^2 = \mathcal{T}_h \cap \Omega_2$, respectively. Denote by $\mathcal{E}_h$ the set of all edges in $\mathcal{T}_h$ and let $\mathcal{E}_h^0 = \mathcal{E}_h \backslash \partial\Omega$ be the set of all interior edges. Let Γ_h be the

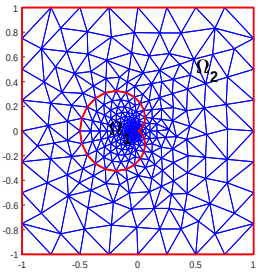

Figure 1.3: A typical fitted discretization

subset of $\mathcal{E}_h$ of all edges on Γ. For every element $K \in \mathcal{T}_h$, we denote by h_K its diameter and mesh size $h = \max_{K\in\mathcal{T}_h} h_K$ for $\mathcal{T}_h$. Note that

$$\begin{aligned} \mathcal{T}_h &= \{K \in \mathcal{T}_h : \ K \nsubseteq \Omega_2 \text{ or } \partial K \cap \Gamma = \emptyset\} \\ &\quad \cup \{K \in \mathcal{T}_h : \ K \subseteq \Omega_2 \text{ and } \partial K \cap \Gamma \neq \emptyset\} \\ &:= \mathcal{T}_1 \cup \mathcal{T}_2. \end{aligned} \tag{1.4.4}$$

Note that $\mathcal{T}_1$ contains all elements in Ω_1 and non-interface elements Ω_2. For more details, we refer to [112].

The key in weak Galerkin methods is the use of weak derivatives in the place of strong derivatives in the variational form for the underlying partial differential equations. Thus, it is essential to introduce a weak version for the gradient operator. Weak gradient operators and its discrete version were introduced in [143, 144], and the rest of the section will review them. Let K be any polygonal domain with interior K^0 and boundary ∂K. A weak function on the region K refers to a pair of scalar valued functions $v = \{v_0, v_b\}$ such that $v_0 \in L^2(K)$ and $v_b \in L^2(\partial K)$. Note that v_b may not be necessarily related to the trace of v_0 on ∂K. Denote by $\mathcal{V}(K)$ the space of weak scalar valued functions on K; i. e.,

$$\mathcal{V}(K) = \{v = \{v_0, v_b\} : v_0 \in L^2(K), v_b \in L^2(\partial K)\}. \tag{1.4.5}$$

For any weak function $v = \{v_0, v_b\}$, its weak gradient $\nabla_w v$ is defined (interpreted) as a linear functional on $H(\text{div}, K)$ whose action on each $q \in H(\text{div}, K)$ is given by

$$(\nabla_w v, q)_K = -\int_K v_0 \nabla \cdot q dK + \int_{\partial K} v_b q \cdot \eta ds, \tag{1.4.6}$$

where η is the outward normal to ∂K.

For any given integer $k \geq 0$, denote $\mathcal{P}_k(K)$ the space of polynomials of total degree k or less on the element $K \in \mathcal{T}_h$. Analogously, for any given integer $j \geq 0$, $\mathcal{P}_j(e)$ denotes

the space of polynomials of total degree j or less on the edge $e \in \mathcal{E}_h$. On each element $K \in \mathcal{T}_h$, define the following local weak finite element space

$$\mathcal{V}(k, j, K) = \{v_h = \{v_0, v_b\} : \ v_0 \in \mathcal{P}_k(K), \ v_b \in \mathcal{P}_j(\partial K)\}. \tag{1.4.7}$$

A global weak finite element space $\mathcal{V}_h$ is constructed by patching local space $\mathcal{V}(k, j, K)$ through a common value of v_b on all interior edges

$$\mathcal{V}_h = \{v_h = \{v_0, v_b\} : \ v_h|_K \in \mathcal{V}(k, j, K), \ [v_h]_e = 0, \ \forall e \in \mathcal{E}_h^0\}. \tag{1.4.8}$$

Here, $[v_h]_e = [v_b]$ denotes the jump of $v_h \in \mathcal{V} = \prod_{K \in \mathcal{T}_h} \mathcal{V}(k, j, K)$ across an interior edge $e \in \mathcal{E}_h^0$. Denote by $\mathcal{V}_h^0$ the subspace of $\mathcal{V}_h$ consisting of all finite element functions with vanishing boundary value

$$\mathcal{V}_h^0 = \{v_h \in \mathcal{V}_h : v_b|_{\partial\Omega} = 0\}. \tag{1.4.9}$$

Next, we introduce a discrete weak gradient operator, denoted by ∇_w, is defined as the unique polynomial $(\nabla_w v_h) \in [\mathcal{P}_l(K)]^2$ that satisfies the following equation

$$(\nabla_w v_h, \varphi)_K = -\int_K v_0(\nabla \cdot \varphi) dK + \int_{\partial K} v_b(\varphi \cdot \eta) ds \ \ \forall \varphi \in [\mathcal{P}_l(K)]^2. \tag{1.4.10}$$

where η is the outward normal to ∂K and $l \geq 0$ is prescribed non-negative integer. By applying the divergence theorem to the first term on the right-hand side of (1.4.10) we arrive at

$$(\nabla_w v_h, \phi)_K = (\nabla v_0, \phi)_K + \langle v_b - v_0, \phi \cdot \eta \rangle_{\partial K} \ \ \forall \phi \in [P_l(K)]^2. \tag{1.4.11}$$

Using the discrete weak gradient operator ∇_w, we define a bilinear map $\mathcal{A} : \mathcal{V}_h \times \mathcal{V}_h \to \mathbb{R}$ by

$$\mathcal{A}(u_h, v_h) = \sum_{K \in \mathcal{T}_h} \left(\beta \nabla_w u_h, \nabla_w v_h\right)_K + \mathcal{S}(u_h, v_h) \ \ \forall u_h, v_h \in \mathcal{V}_h. \tag{1.4.12}$$

Here, $\mathcal{S}(\cdot, \cdot)$ is known as stabilizer, which is a semi-positive definite bilinear form defined on $\mathcal{V}_h \times \mathcal{V}_h$. Stabilizer $\mathcal{S}(\cdot, \cdot)$ is often chosen in such a way that it fits well into the theory and implementation of the WG numerical scheme. For examples (cf. [142]):

Example 1.4.1. *(Projected Element-Boundary Discrepancy) For $v_h = \{v_0, v_b\} \in \mathcal{V}_h$, the continuity of v_h can be measured by the quantity $v_b - v_0|_{\partial K}$ for each element $K \in \mathcal{T}_h$. The projected element-boundary-discrepancy method is based on the following stabilizer*

$$\mathcal{S}(u_h, v_h) = \sum_{K \in \mathcal{T}_h} h_K^{-1} \langle \mathcal{Q}_m(u_b - u_0|_{\partial K}), \mathcal{Q}_m(v_b - v_0|_{\partial K}) \rangle_{\partial K}, \tag{1.4.13}$$

where $\mathcal{Q}_m : L^2(\partial K) \to \mathcal{P}_m(\partial K)$ is the usual L^2- projection operator and $m = \max\{j, l\}$.

Example 1.4.2. *(Element-Boundary Discrepancy) The element-boundary-discrepancy method is based on the following stabilizer*

$$\mathcal{S}(u_h, v_h) = \sum_{K\in\mathcal{T}_h} h_K^{-1}\langle u_b - u_0|_{\partial K}, v_b - v_0|_{\partial K}\rangle_{\partial K}. \tag{1.4.14}$$

In the WG methods, the polynomial degree and the stabilizer must be chosen so that the bilinear form $\mathcal{A}(\cdot,\cdot)$ is coercive with respect to the semi-norm $\|\cdot\|_{1,h}$ (cf. [142]) defined by

$$\|v_h\|_{1,h} = \Big(\sum_{K\in\mathcal{T}_h}(\|\nabla v_0\|_K^2 + h_K^{-1}\|v_0 - v_b\|_{\partial K}^2)\Big)^{\frac{1}{2}},\ v_h = \{v_0, v_b\} \in \mathcal{V}_h. \tag{1.4.15}$$

More precisely, there exist constants $C_1,\ C_2 > 0$ such that for any $v_h \in \mathcal{V}_h$, the following inequality holds true

$$C_1\|v_h\|_{1,h}^2 \le \mathcal{A}(v_h, v_h) \le C_2\|v_h\|_{1,h}^2. \tag{1.4.16}$$

The coercivity inequality (1.4.16), for both the stabilizers on weak Galerkin space $(\mathcal{P}_k(K),\ \mathcal{P}_j(\partial K),\ \big[\mathcal{P}_l(K)\big]^2)$, is stated below (cf. [142]).

Lemma 1.4.1. *Assume that $l \ge k-1$ and $m = \max\{j, l\}$. Then the coercivity inequality (1.4.16) holds true.*

In fact, $\mathcal{V}_h^0$ is a normed linear space with respect to discrete H^1-norm $\|\cdot\|_{1,h}$. For simplicity, we shall only verify the positive length property for $\|\cdot\|_{1,h}$. Assume that $\|w_h\|_{1,h} = 0$ for some $w_h = \{w_0, w_b\} \in \mathcal{V}_h^0$. It follows that $\nabla w_0 = 0$ on each element $K \in \mathcal{T}_h$ and $w_b = w_0$ on ∂K. It follows that $w_0 =$ constant on every $K \in \mathcal{T}_h$. This, together with the fact that $w_b = w_0$ on ∂K and $w_b = 0$ on $\partial\Omega$, implies that $w_0 = 0$ and $w_b = 0$.

Let K be an element with e as an edge. For any function $\varphi \in H^1(K)$, the following trace inequality holds true (see [144] for details)

$$\|\varphi\|_e^2 \le C(h_K^{-1}\|\varphi\|_K^2 + h_K\|\nabla\varphi\|_K^2). \tag{1.4.17}$$

For our later use, for any $v_h = \{v_0, v_b\} \in V_h$, we define following forms

$$\begin{aligned}
\langle\psi, \beta\nabla_w v_h\cdot\mathbf{n}\rangle_\Gamma &= \sum_{K\in\mathcal{T}_2}\langle\psi, \beta_2\nabla_w(v_h|_K).\mathbf{n}\rangle_{\partial K\cap\Gamma_h},\\
h^{-1}\langle\psi, v_0 - v_b\rangle_\Gamma &= \sum_{K\in\mathcal{T}_2} h^{-1}\langle\psi, v_0|_K - v_b\rangle_{\partial K\cap\Gamma_h},\\
h^{-1}\langle\psi, Q_b v_0 - v_b\rangle_\Gamma &= \sum_{K\in\mathcal{T}_2} h^{-1}\langle\psi, Q_b(v_0|_K) - v_b\rangle_{\partial K\cap\Gamma_h},\\
\langle\phi, v_b\rangle_\Gamma &= \sum_{e\in\Gamma_h}\langle\phi, v_b\rangle_e.
\end{aligned}$$

Here, $\langle \cdot, \cdot \rangle_M$ denotes the L^2 inner product on $M \subset \mathcal{E}_h$ and $\mathbf{n}$ is the outward pointing unit normal to Ω_1.

The usual L^2-inner product can be written locally on each element as follows

$$(\nabla_w v_h, \nabla_w w_h) = \sum_{K \in \mathcal{T}_h} (\nabla_w v_h, \nabla_w w_h)_K, \quad w_h, v_h \in \mathcal{V}_h. \tag{1.4.18}$$

1.5 Proposed Contents of the Thesis

This thesis consists of six chapters, and is organized as follows.

Chapter 1 contains the description of the problems, notations and preliminary materials to be used in the thesis. It also provides a brief survey on the relevant literature concerning the problems and their numerical solutions. Further, motivations for the present study is discussed.

In Chapter 2, we present a priori error estimates for the spatially semidiscrete scheme for the parabolic interface problem (1.1.1)-(1.1.3) on weak Galerkin finite element space $(\mathcal{P}_k(K),\ \mathcal{P}_{k-1}(\partial K),\ \left[\mathcal{P}_{k-1}(K)\right]^2)$. Optimal order of convergence in $L^\infty(L^2)$ and $L^\infty(H^1)$ norms are established. The derivation of the a priori error bound heavily depends on the approximation properties of the elliptic interface problems along with standard analytical tools and techniques. Some parts of this chapter are published in [51].

In Chapter 3, we extend the spatially discrete a priori error analysis to the fully discrete approximation for the parabolic interface problem (1.1.1)-(1.1.3). The time discretization are based on backward Euler and Crank-Nicolson schemes. Optimal a priori error estimates in L^2 and H^1 norms are derived for the fully discrete solutions. Further, numerical results are presented to validate our theoretical findings. Some parts of the Chapter 3 are published in [51, 54].

Chapter 4 deals with the a priori error analysis for hyperbolic model problem (1.1.4)-(1.1.6). Here, we extend the work of Chapter 3 to the interface problem (1.1.4)-(1.1.6). Optimal order of convergence in $L^\infty(L^2)$ norm is established for the semidiscrete solution. We have also studied stability of the semidiscrete solution and derived some estimates which are very crucial for the fully discrete error analysis. The fully discrete space-time finite element discretization, based on the backward Euler approximation, is analyzed and related optimal a priori error estimates are derived. Finally, numerical results are presented to consolidates our theoretical findings. Results and findings of this Chapter are communicated in [55].

Chapter 5 is devoted to the study of a priori error analysis for the electric interface problem (1.1.7)-(1.1.9). Optimal order of convergence in $L^\infty(L^2)$, $H^1(L^2)$ and $L^\infty(H^1)$ norms are established for the semidiscrete solution. We have also studied stability of

the semidiscrete solution and derived some estimates which are very crucial for the fully discrete error analysis. A discrete in time scheme based on backward Euler scheme is considered and analyzed for the fully discrete solution. Optimal a priori error estimates in L^2 and H^1 norms are derived for the fully discrete solution. Further, numerical results are discussed to validate our theoretical findings. Results and findings of this Chapter are published in [53].

Finally in Chapter 6, we discuss the critical evaluation of the results presented in this thesis. This chapter concludes with a brief discussion on the possible extensions and future work.

2

Semidiscrete WG-FEM for Parabolic Interface Problem with Non-homogeneous Jump Conditions

This chapter concerns a numerical solution of a second order linear parabolic interface problem. Although the solutions of interface problems exhibit higher regularities in each individual domains, regularity in the entire physical domain is H^1 only due to discontinuities across the interface. To handle this difficulty the weak Galerkin finite element method is used for the discretization since it allows the use of totally discontinuous functions in the approximation space. In the implementation, the weak partial derivatives and the weak functions are approximated by polynomials with various degrees of freedom. The accuracy and the computational complexity of the corresponding WG scheme is significantly impacted by the selection of such polynomials. This chapter presents an optimal combination for the polynomial spaces that minimize the number of unknowns in the numerical scheme without compromising the accuracy of the numerical approximation. More precisely, optimal order error estimates in both H^1 and L^2 norms are established for lowest order WG finite element space $(\mathcal{P}_k(K),\ \mathcal{P}_{k-1}(\partial K),\ \left[\mathcal{P}_{k-1}(K)\right]^2)$. Moreover, the new WG algorithm allows the use of finite element partitions consisting of general polygonal meshes.

2.1 Introduction

To begin with, let us first recall the parabolic interface interface problem of the form

$$u_t - \nabla \cdot (\beta \nabla u) = f \quad \text{in } \Omega \times (0, T], \tag{2.1.1}$$

Some parts of this chapter published online in *Numer. Funct. Anal. Optim. 40 (2019), no. 3, 259-279*

with initial and Dirichlet boundary condition

$$u(x,0) = u_0(x) \ \text{ in } \Omega; \quad u = 0 \quad \text{on } \partial\Omega \times (0,T] \tag{2.1.2}$$

and interface conditions

$$[u] = \psi, \quad \left[\beta \frac{\partial u}{\partial \mathbf{n}}\right] = \phi \quad \text{along } \Gamma \times (0,T]. \tag{2.1.3}$$

where Ω is a convex polygonal domain in $\mathbb{R}^2$ with boundary $\partial\Omega$ and $\Omega_1 \subset \Omega$ is an open domain with Lipschitz boundary $\Gamma = \partial\Omega_1$ and $\Omega_2 = \Omega \backslash \Omega_1$. Other symbols are as defined in Chapter 1. We assume that the physical coefficient is discontinuous along interface Γ and piecewise positive constant i.e., $\beta(x) = \beta_k$ for $x \in \Omega_k,\ k = 1, 2$. We assume that f is sufficiently smooth locally. Jump functions $\psi,\ \phi : \Gamma \times (0,T] \to \mathbb{R}$ and initial data $u_0 : \Omega \to \mathbb{R}$ are given.

Due to the mathematical complexity and essential importance in a number of application areas, the study of interface problems has evolved into a well defined field in applied and computational mathematics. The solutions of interface problems may show higher regularities in each individual material region than in the entire physical domain because of discontinuities across the interface (cf. [34, 78, 80, 127]). Thus, achieving higher-order accuracy may be difficult using a classical method, hence, there is a need to find the solution to the problem by variational formulations. Convergence analysis for parabolic interface problem via finite element procedure has been studied by several authors. Conforming fitted finite element methods for parabolic interface problems can be found in [2, 34, 47, 127, 128, 141, 152] and reference therein. Then the idea of immersed FEMs have been proposed to allow the interface to cut through elements so that simple structured Cartesian meshes can be employed. For parabolic interface problem, we refer to [91] and references therein. Discontinuous Galerkin (DG) finite element methods for time dependent interface problems can be found in [11, 158], and combining immersed FEMs and DG methods (DG-IFE) together to solve parabolic interface problem has been proposed in [96, 136, 154]. In [78], higher order spectral element method for parabolic interface problem has been discussed. The algorithm in [78] is restricted to simple interfaces. At present, to the best of our knowledge, there is no rigorous convergence analysis available for parabolic interface methods that deliver high order accuracy for nonsmooth interfaces. The objective of the present chapter is to propose and analyze higher weak Galerkin finite element method for parabolic interface problems. In this chapter, we extend the work of [44, 112] to parabolic interface problem for lowest order WG finite element space $(\mathcal{P}_k(K),\ \mathcal{P}_{k-1}(\partial K),\ \left[\mathcal{P}_{k-1}(K)\right]^2)$ based

on projected element-boundary discrepancy stabilizer. Optimal order error estimates in both $L^\infty(H^1)$ and $L^\infty(L^2)$ norms are established.

The rest of the chapter is organized as follows. In Sec. 2, we propose the semidiscrete weak Galerkin finite element approximation and derive an important error relation. Sec. 3 is devoted to the error analysis for the spatially semidiscrete scheme, which is based on elliptic projection.

2.2 Semidiscrete Approximation

This section deals with spatially discrete scheme for the parabolic interface problem (2.1.1)-(2.1.3).

Let $\mathcal{T}_h = \mathcal{T}_1 \cup \mathcal{T}_2$ be the fitted finite element discretization of Ω as described in Chapter 1. Based on the discretization $\mathcal{T}_h$, for $k \geq 1$, we define following weak Galerkin finite element space

$$V_h = \{v_h = \{v_0, v_b\} : \ v_h|_K \in \mathcal{V}(k, k-1, K), \ [v_h]_e = 0, \ \forall e \in \mathcal{E}_h^0, \ K \in \mathcal{T}_h\}. \tag{2.2.1}$$

Here, $[v_h]_e = [v_b]$ denotes the jump of $v_h \in \prod_{K\in\mathcal{T}_h} \mathcal{V}(k, k-1, K)$ across an interior edge $e \in \mathcal{E}_h^0$ and $\mathcal{V}(k, k-1, K)$ is the local weak Galerkin space as defined in (1.4.7). Denote by V_h^0 the subspace of V_h consisting of all finite element functions with vanishing boundary value

$$V_h^0 = \{v_h \in V_h : v_b|_{\partial\Omega} = 0\}. \tag{2.2.2}$$

For each $v_h = \{v_0, v_b\} \in V_h$, we recall its discrete weak gradient $(\nabla_w v_h) \in [\mathcal{P}_{k-1}(K)]^2$ that satisfies the following equation

$$(\nabla_w v_h, \varphi)_K = -\int_K v_0(\nabla \cdot \varphi)dK + \int_{\partial K} v_b(\varphi \cdot \eta)ds \ \ \forall \varphi \in [\mathcal{P}_{k-1}(K)]^2, \tag{2.2.3}$$

where η is the outward normal to ∂K.

A time-dependent weak function $v_h : [0, T] \to V_h$ is written as $v_h(t) := \{v_0(t), v_b(t)\}$ and subsequently we define $v_{ht}(t) := \{v_0'(t), v_b'(t)\}$, where '$\prime$' denotes the time derivatives. For simplicity, we use $v_h = \{v_0, v_b\}$ for $v_h(t)$ and $v_{ht} = \{v_0', v_b'\}$ for $v_{ht}(t)$. Similar remarks hold for other higher order time derivatives.

Remark 2.2.1. *As there may be confusion with the notation u_0 for the initial data and finite element approximation $u_h = \{u_0, u_b\}$, we write $u(0)$ for the initial data.* □

For each element $K \in \mathcal{T}_h$, denote by Q_0 the usual L^2 projection operator from $L^2(K)$ onto $\mathcal{P}_k(K)$ and by Q_b the L^2 projection from $L^2(e)$ onto $\mathcal{P}_{k-1}(e)$ for any $e \in \mathcal{E}_h$. We shall combine Q_0 with Q_b by writing $Q_h = \{Q_0, Q_b\}$. We define another L^2-projection $\mathbb{Q}_h$ from $[L^2(K)]^2$ onto $[\mathcal{P}_{k-1}(K)]^2$. We recall following crucial approximation properties for local projections Q_h (Lemma 3.4 in [144]).

Lemma 2.2.1. *Let $\mathcal{T}_h$ be a finite element partition of Ω satisfying the shape regularity assumption as specified in [144]. Then, for $u \in H^{k+1}(\Omega_i)$ with $i = 1,\ 2$, we have*

$$\sum_{K\in\mathcal{T}_h}\Big(\|u-Q_0u\|_K^2+h_K^2\|\nabla(u-Q_0u)\|_K^2\Big)\leq Ch^{2(k+1)}\sum_{i=1}^{2}\|u\|_{k+1,\Omega_i}^2,$$

$$\sum_{K\in\mathcal{T}_h}\Big(\|\nabla u-\mathbb{Q}_h(\nabla u)\|_K^2+h_K^2\|\nabla(\nabla u-\mathbb{Q}_h(\nabla u))\|_K^2\Big)\leq Ch^{2k}\sum_{i=1}^{2}\|u\|_{k+1,\Omega_i}^2. \quad \square$$

The continuous-time weak Galerkin finite element approximation to (2.1.1)-(2.1.3) can be obtained by seeking $u_h = \{u_0, u_b\} : [0, T] \to V_h^0$ satisfying both $u_h(0) = Q_hu(0) = \{Q_0u(0), Q_bu(0)\}$ and following equation for any $v_h = \{v_0, v_b\} \in V_h^0$

$$(u_{ht}, v_0) + a(u_h, v_h) = (f, v_0) + \langle\psi, \beta\nabla_w v_h \cdot \mathbf{n}\rangle_\Gamma + \langle\phi, v_b\rangle_\Gamma - \frac{1}{h}\langle\psi, Q_bv_0 - v_b\rangle_\Gamma. \quad (2.2.4)$$

The bilinear map $a(\cdot,\cdot)$ on V_h^0 is given by

$$a(u_h, v_h) = \sum_{K\in\mathcal{T}_h}(\beta\nabla_w u_h, \nabla_w v_h)_K + s(u_h, v_h), \quad (2.2.5)$$

where the stabilizer $s(\cdot,\cdot)$ is defined as

$$s(u_h, v_h) = \sum_{K\in\mathcal{T}_h} h_K^{-1}\langle Q_bu_0 - u_b, Q_bv_0 - v_b\rangle_{\partial K}. \quad (2.2.6)$$

Inner product $\langle\cdot,\cdot\rangle_\Gamma$ is as described in Sec. 1.4 of Chapter 1.

From the Lemma 1.4.1, it is easy to observe that the finite element space V_h^0 is a normed linear space with a triple-bar norm given by

$$|||w_h|||^2 = \sum_{K\in\mathcal{T}_h}\|\beta^{\frac{1}{2}}\nabla_w w_h\|_K^2 + \sum_{K\in\mathcal{T}_h} h_K^{-1}\|Q_bw_0 - w_b\|_{\partial K}^2 = a(w_h, w_h),\ w_h = \{w_0, w_b\} \in V_h^0. \quad (2.2.7)$$

As an immediate consequence, the following solvability holds true for weak Galerkin finite element scheme (2.2.4).

Lemma 2.2.2. *The weak Galerkin finite element scheme (2.2.4) has one and only one solution.* $\square$

Assume that the exact solution of (2.1.1)-(2.1.3) is given by u. For an $e \in \mathcal{E}_h$ shared by the two elements K_1 and K_2, if $e \notin \Gamma_h$, $u|_{K_1\cap e} = u|_{K_2\cap e}$ and if $e \in \Gamma_h$, $u|_{K_1\cap e} \neq u|_{K_2\cap e}$. Next, we like to define $Q_hu = \{Q_0u, Q_bu\} \in V_h$. To ensure $Q_hu \in V_h$, i.e. Q_bu takes single value on any $e \in \mathcal{E}_h$, we define Q_bu in the following way:

$$Q_bu = \begin{cases} Q_b(u|_{K\cap e}) & \text{if} \quad e \subseteq \Gamma\ \&\ K \subset \Omega_1, \\ Q_b(u|_{K\cap e}) + Q_b\psi & \text{if} \quad e \subseteq \Gamma\ \&\ K \subset \Omega_2, \\ Q_b(u|_{K\cap e}) & \text{if} \quad e \nsubseteq \Gamma\ \&\ K \in \mathcal{T}_h. \end{cases} \quad (2.2.8)$$

Then we have following result connecting Q_h and $\mathbb{Q}_h$ operators (see, Lemma 3.2 in [44]). We present the proof for the completeness of this work.

Lemma 2.2.3. *Let Q_h and $\mathbb{Q}_h$ be the L^2 projection operators as defined. Then, on each element $K \in \mathcal{T}_h$ and for any $\tau \in [\mathcal{P}_{k-1}(K)]^2$, we have*

$$(\nabla_w(Q_h u), \tau)_K = (\mathbb{Q}(\nabla u), \tau)_K + \langle \psi, \tau \cdot \eta \rangle_{\partial K \cap \Gamma}, \ K \in \mathcal{T}_2, \tag{2.2.9}$$

$$(\nabla_w(Q_h u), \tau)_K = (\mathbb{Q}(\nabla u), \tau)_K, \ K \in \mathcal{T}_1, \tag{2.2.10}$$

where $\mathcal{T}_1$ and $\mathcal{T}_2$ are as defined in (1.4.4).

Proof. Let $K \in \mathcal{T}_1$. Using (2.2.10) together with the definition (2.2.8) that for any $\tau \in [\mathcal{P}_{k-1}(K)]^2$

$$\begin{aligned}(\nabla_w(Q_h u), \tau)_K &= -(Q_0 u, \nabla \cdot \tau)_K + \langle Q_b u, \tau \cdot \eta \rangle_{\partial K} \\ &= -(u, \nabla \cdot \tau)_K + \langle u, \tau \cdot \eta \rangle_{\partial K} \\ &= (\nabla u, \tau)_K \\ &= (\mathbb{Q}(\nabla u), \tau)_K.\end{aligned}$$

Here, we have used the definitions of Q_h and $\mathbb{Q}_h$ operators. For any $K \in \mathcal{T}_2$, we obtain

$$\begin{aligned}(\nabla_w(Q_h u), \tau)_K &= -(Q_0 u, \nabla \cdot \tau)_K + \langle Q_b u, \tau \cdot \eta \rangle_{\partial K} \\ &= -(u, \nabla \cdot \tau)_K + \langle Q_b(u|_{\partial K}), \tau \cdot \eta \rangle_{\partial K} + \langle Q_b \psi, \tau \cdot \eta \rangle_{\partial K \cap \Gamma} \\ &= -(u, \nabla \cdot \tau)_K + \langle u, \tau \cdot \eta \rangle_{\partial K} + \langle \psi, \tau \cdot \eta \rangle_{\partial K \cap \Gamma} \\ &= (\nabla u, \tau)_K + \langle \psi, \tau \cdot \eta \rangle_{\partial K \cap \Gamma} \\ &= (\mathbb{Q}(\nabla u), \tau)_K + \langle \psi, \tau \cdot \eta \rangle_{\partial K \cap \Gamma}.\end{aligned}$$

This completes the rest of the proof. □

As in finite element method, we split our error into two components using an intermediate operator. We write

$$u - u_h = (u - Q_h u) + (Q_h u - u_h),$$

where $u_h = \{u_0, u_b\} \in V_h^0$ is the semidiscrete weak Galerkin solution defined by (2.2.4) and $Q_h u$ is as defined in (2.2.8). For simplicity, we introduce the following notation

$$e_h := \{e_0, e_b\} = u_h - Q_h u = \{u_0 - Q_0 u, u_b - Q_b u\}. \tag{2.2.11}$$

Then e_h satisfies following error equation which is crucial for our later analysis.

Lemma 2.2.4. *Let e_h be the error as defined in (2.2.11), then we have*

$$(e_{ht}, v_0) + a(e_h, v_h) = l_1(u, v_h) + l_2(u, v_h) \;\; \forall v_h = \{v_0, v_b\} \in V_h^0, \tag{2.2.12}$$

where bilinear forms $l_1(\cdot,\cdot)$ and $l_2(\cdot,\cdot)$ are given by

$$\begin{aligned} l_1(u, v_h) &= \sum_{K\in\mathcal{T}_h} \langle \beta(\nabla u - \mathbb{Q}_h(\nabla u)) \cdot \eta, v_0 - v_b\rangle_{\partial K}, \\ l_2(u, v_h) &= \frac{1}{h}\sum_{K\in\mathcal{T}_h} \langle Q_b(Q_0 u) - Q_b(u|_{\partial K}), Q_b v_0 - v_b\rangle_{\partial K}, \end{aligned}$$

where η is the outward normal to ∂K.

Proof. Testing (2.1.1) by using v_0 of $v_h = \{v_0, v_b\} \in V_h^0$ we arrive at

$$\begin{aligned} (f, v_0) &= (u_t, v_0) - \sum_{K\in\mathcal{T}_h} (\nabla\cdot(\beta\nabla u), v_0)_K \\ &= (Q_h u_t, v_0) + \sum_{K\in\mathcal{T}_h} (\beta\nabla u, \nabla v_0)_K - \sum_{K\in\mathcal{T}_h} \langle \beta\nabla u\cdot\eta, v_0\rangle_{\partial K} \\ &= (Q_h u_t, v_0) + \sum_{K\in\mathcal{T}_h} (\beta\nabla u, \nabla v_0)_K \\ &\quad - \sum_{K\in\mathcal{T}_h} \langle \beta\nabla u\cdot\eta, v_0 - v_b\rangle_{\partial K} - \sum_{K\in\mathcal{T}_h} \langle \beta\nabla u\cdot\eta, v_b\rangle_{\partial K} \\ &= (Q_h u_t, v_0) + \sum_{K\in\mathcal{T}_h} (\beta\nabla u, \nabla v_0)_K \\ &\quad - \sum_{K\in\mathcal{T}_h} \langle \beta\nabla u\cdot\eta, v_0 - v_b\rangle_{\partial K} - \langle \phi, v_b\rangle_\Gamma. \end{aligned} \tag{2.2.13}$$

It follows from the definitions of discrete weak gradient (2.2.3) and $\mathbb{Q}_h$ operator, and the integration by parts that

$$\begin{aligned} (\beta\mathbb{Q}_h(\nabla u), \nabla_w v_h)_K &= -(v_0, \nabla\cdot(\beta\mathbb{Q}_h\nabla u))_K + \langle v_b, (\beta\mathbb{Q}_h(\nabla u))\cdot\eta\rangle_{\partial K} \\ &= (\nabla v_0, \beta\mathbb{Q}_h\nabla u)_K - \langle v_0 - v_b, (\beta\mathbb{Q}_h(\nabla u))\cdot\eta\rangle_{\partial K} \\ &= (\nabla v_0, \beta\nabla u)_K - \langle v_0 - v_b, (\beta\mathbb{Q}_h(\nabla u))\cdot\eta\rangle_{\partial K}. \end{aligned} \tag{2.2.14}$$

Combining (2.2.13) and (2.2.14), we have

$$\begin{aligned} (f, v_0) &= (Q_h u_t, v_0) + \sum_{K\in\mathcal{T}_h} (\beta\mathbb{Q}_h(\nabla u), \nabla_w v_h)_K \\ &\quad + \sum_{K\in\mathcal{T}_h} \langle v_0 - v_b, \beta(\mathbb{Q}_h(\nabla u) - \nabla u)\cdot\eta\rangle_{\partial K} - \langle \phi, v_b\rangle_\Gamma. \end{aligned} \tag{2.2.15}$$

This together with (2.2.9) and (2.2.10) leads to

$$\begin{aligned}(Q_h u_t, v_0) + \sum_{K\in\mathcal{T}_h} (\beta\nabla_w Q_h u, \nabla_w v_h)_K \\ = (f, v_0) + \langle\psi, \beta\nabla_w v_h\cdot\mathbf{n}\rangle_\Gamma + \langle\phi, v_b\rangle_\Gamma \\ - \sum_{K\in\mathcal{T}_h} \langle v_0 - v_b, \beta(\mathbb{Q}_h(\nabla u) - \nabla u)\cdot\eta\rangle_{\partial K}. \end{aligned} \tag{2.2.16}$$

Adding $s(Q_h u, v_h)$ to both sides of the above equation gives

$$\begin{aligned}(Q_h u_t, v_0) + a(Q_h u, v_h) &= (f, v_0) + \langle\psi, \beta\nabla_w v_h\cdot\mathbf{n}\rangle_\Gamma + \langle\phi, v_b\rangle_\Gamma \\ &\quad + l_1(u, v_h) + s(Q_h u, v_h). \end{aligned} \tag{2.2.17}$$

It follows from (2.2.8) that

$$\begin{aligned} s(Q_h u, v_h) &= \frac{1}{h}\sum_{K\in\mathcal{T}_h} \langle Q_b(Q_0 u) - Q_b u, Q_b v_0 - v_b\rangle_{\partial K} \\ &= \frac{1}{h}\sum_{K\in\mathcal{T}_h} \langle Q_b(Q_0 u) - Q_b(u|_{\partial K}), Q_b v_0 - v_b\rangle_{\partial K} \\ &\quad -\frac{1}{h}\langle\psi, Q_b v_0 - v_b\rangle_\Gamma. \end{aligned}$$

Substituting the above equation in (2.2.17) yields

$$\begin{aligned}(Q_h u_t, v_0) + a(Q_h u, v_h) &= (f, v_0) + \langle\psi, \beta\nabla_w v_h\cdot\mathbf{n}\rangle_\Gamma + \langle\phi, v_b\rangle_\Gamma \\ &\quad + l_1(u, v_h) - \frac{1}{h}\langle\psi, Q_b v_0 - v_b\rangle_\Gamma \\ &\quad + \frac{1}{h}\sum_{K\in\mathcal{T}_h} \langle Q_b(Q_0 u) - Q_b(u|_{\partial K}), Q_b v_0 - v_b\rangle_{\partial K}. \end{aligned} \tag{2.2.18}$$

Subtracting (2.2.4) from (2.2.18) leads to desire result. □

Before proceeding further, we introduce following results from earlier literature for our later analysis (cf. [44, 112])

Lemma 2.2.5. *For any $v_h = \{v_0, v_b\} \in V_h^0$, we have*

$$\|v_0 - v_b\|_{\partial K} \le C(h_K^{\frac{1}{2}}\|\nabla v_0\|_K + \|Q_b v_0 - v_b\|_{\partial K}). \quad \square$$

Lemma 2.2.6. *Assume that $\mathcal{T}_h$ is shape regular. Then for $u \in H^{k+1}(\Omega_i)$, $i = 1, 2$ and $v_h = \{v_0, v_b\} \in V_h^0$, we have*

$$\begin{aligned} |l_1(u, v_h)| &\le Ch^k(\|u\|_{k+1,\Omega_1} + \|u\|_{k+1,\Omega_2})|||v_h|||, \\ |l_2(u, v_h)| &\le Ch^k(\|u\|_{k+1,\Omega_1} + \|u\|_{k+1,\Omega_2})|||v_h|||. \quad \square \end{aligned}$$

2.3 Semidiscrete Error Analysis

This section deals with the error analysis for the spatially discrete scheme (2.2.4). Optimal order of convergence in both $L^\infty(L^2)$ and $L^\infty(H^1)$ norms are established when the regularity of the solution is low on the entire domain.

Now, we are ready to discuss the main results of this section.

Theorem 2.3.1. *Let $u_h \in V_h^0$ be the weak Galerkin finite element solution of the problem (2.1.1)-(2.1.3) arising from (2.2.4). Assume the exact solution $u \in H^1(0,T;H^{k+1}(\Omega_i))$, $i = 1,2$. Then there exists a constant $C > 0$ such that*

$$\|\nabla(u-u_h)\| \leq Ch^k \sum_{i=1}^{2} \Big(\|u\|_{k+1,\Omega_i} + \|u\|_{H^1(0,t;H^{k+1}(\Omega_i))} \Big).$$

Proof. By letting $v_h = e_h$ in (2.2.12), we have

$$\frac{1}{2}\frac{d}{dt}(e_0,e_0) + |||e_h|||^2 = l_1(u,e_h) + l_2(u,e_h).$$

By integration over the time period $[0,t]$, we get

$$\frac{1}{2}\|e_0(t)\|^2 + \int_0^t |||e_h|||^2 ds \leq \int_0^t |l_1(u,e_h)|ds + \int_0^t |l_2(u,e_h)|ds.$$

Here, we have used the fact that $e_h(0) = 0$. It then follows from Lemma 2.2.6 that

$$\begin{aligned} &\frac{1}{2}\|e_0(t)\|^2 + \int_0^t |||e_h|||^2 ds \\ &\leq Ch^{2k} \int_0^t (\|u\|^2_{k+1,\Omega_1} + \|u\|^2_{k+1,\Omega_2}) ds + \frac{1}{2}\int_0^t |||e_h|||^2 ds. \end{aligned} \tag{2.3.1}$$

Hence, we have

$$\|e_0(t)\|^2 + \int_0^t |||e_h|||^2 ds \leq Ch^{2k} \int_0^t (\|u\|^2_{k+1,\Omega_1} + \|u\|^2_{k+1,\Omega_2}) ds. \tag{2.3.2}$$

In order to estimate $|||e_h|||$, we apply the error equation (2.2.12) with $v_h = e_{ht}$ to have

$$(e_{0t},e_{0t}) + \frac{1}{2}\frac{d}{dt}a(e_h,e_h) = \frac{d}{dt}l_1(u,e_h) + \frac{d}{dt}l_2(u,e_h) - l_1(u_t,e_h) - l_2(u_t,e_h).$$

Thus, integrating above equation with respect to t, we obtain

$$\begin{aligned} \int_0^t \|e_{0t}\|^2 ds + \frac{1}{2}a(e_h,e_h) \;&\leq\; l_1(u,e_h) + l_2(u,e_h) \\ &\quad + \int_0^t |l_1(u_t,e_h)|ds + \int_0^t |l_2(u_t,e_h)|ds, \end{aligned}$$

which together with Lemma 2.2.6 leads to

$$\begin{aligned}\int_0^t \|e_{0t}\|^2 ds + |||e_h|||^2 &\leq C(\nu)h^{2k}\sum_{i=1}^{2}(\|u\|^2_{k+1,\Omega_i} + \int_0^t \|u_t\|^2_{k+1,\Omega_i} ds) \\ &\quad + C_\nu\Big(|||e_h|||^2 + \int_0^t |||e_h|||^2 ds\Big). \end{aligned} \tag{2.3.3}$$

Here, we have used Young's inequality with parameter $\nu > 0$.

Combining (2.3.2)-(2.3.3), we obtain

$$\begin{aligned}&\int_0^t \|e_{0t}\|^2 ds + |||e_h|||^2 \\ &\leq Ch^{2k}\sum_{i=1}^{2}\|u\|^2_{k+1,\Omega_i} + Ch^{2k}\sum_{i=1}^{2}\int_0^t \Big(\|u\|^2_{k+1,\Omega_i} + \|u_t\|^2_{k+1,\Omega_i}\Big) ds. \end{aligned} \tag{2.3.4}$$

Now, triangle inequality, coercive property (1.4.16) and Lemma 2.2.1 leads to

$$\begin{aligned}\|\nabla(u - u_h)\| &\leq \|\nabla(u - Q_0u)\| + \|\nabla(Q_0u - u_0)\| \\ &\leq Ch^k(\|u\|_{k+1,\Omega_1} + \|u\|_{k+1,\Omega_2}) + \|e_h\|_{1,h} \\ &\leq Ch^k(\|u\|_{k+1,\Omega_1} + \|u\|_{k+1,\Omega_2}) + C|||e_h|||. \end{aligned} \tag{2.3.5}$$

The desire estimate follows from (2.3.4)-(2.3.5). This completes the proof. □

Next, we derive an optimal order of estimate for e_h in L^2-norm, the basic idea applied is to use elliptic projection. Let X^* be the collection of all $v \in L^2(\Omega)$ with the property that $v \in H^2(\Omega_1) \cup H^2(\Omega_2)\} \cap \{\psi : \psi = 0 \text{ on } \partial\Omega\}$ and $[v] = \psi_v$ and $\left[\beta\frac{\partial v}{\partial \eta}\right] = \phi_v$ along Γ. Define

$$f_v^* = \begin{cases} -\nabla\cdot(\beta_1\nabla v) & \text{in } \Omega_1, \\ -\nabla\cdot(\beta_2\nabla v) & \text{in } \Omega_2. \end{cases}$$

Clearly $f_v^* \in L^2(\Omega)$. Define $R_h : X^* \to V_h^0$ by

$$\begin{aligned}a(R_hv, w_h) &= (f_v^*, w_0) + \langle\psi_v, \beta\nabla_w w_h\cdot\mathbf{n}\rangle_\Gamma + \langle\phi_v, w_b\rangle_\Gamma \\ &\quad - h^{-1}\langle\psi_v, Q_bw_0 - w_b\rangle_\Gamma \ \ \forall w_h = \{w_0, w_b\} \in V_h^0, \ v \in X^*. \end{aligned} \tag{2.3.6}$$

It is easy to observe from the definition of elliptic projection and equation (2.2.4) that

$$(u_{ht}, v_h) + a(u_h, v_h) - a(R_hu, v_h) = (f, v_0) + (\nabla\cdot(\beta\nabla u), v_0) = (u_t, v_0), \tag{2.3.7}$$

for all $v_h = \{v_0, v_b\} \in V_h^0$. Here, we have used equation (2.1.1).

Arguing as in (2.2.18), we obtain

$$\begin{aligned} a(Q_h v, w_h) &= (f_v^*, w_0) + \langle \psi_v, \beta \nabla_w w_h \cdot \mathbf{n} \rangle_\Gamma + (\phi_v, w_b)_\Gamma + l_1(v, w_h) \\ &\quad + l_2(v, w_h) - \frac{1}{h} \langle \psi_v, Q_b w_0 - w_b \rangle_\Gamma. \end{aligned} \tag{2.3.8}$$

Further, in view of (2.3.6), this definition may be expressed by saying that $R_h v$ is the weak Galerkin finite element solution of the following elliptic interface problem with exact solution v (cf. [44, 112])

$$\begin{aligned} -\nabla \cdot (\beta(x) \nabla v) &= f_v^* \quad \text{in } \Omega, \\ v &= 0 \quad \text{on } \partial\Omega, \\ [v] = \psi_v, \quad \left[\beta \frac{\partial u}{\partial \eta}\right] &= \phi_v \quad \text{along } \Gamma. \end{aligned} \tag{2.3.9}$$

The error estimate for R_h, as shows in the following lemma (cf. [44, 112]), should be applied.

Lemma 2.3.1. *Let R_h be defined by (2.3.6). Assume that the exact solution of problem (2.3.9) is so regular that $v \in H^{k+1}(\Omega_i)$, $i = 1, 2$. Then there exists a constant $C > 0$ such that*

$$\begin{aligned} |||R_h v - Q_h v||| &\leq C h^k (\|v\|_{k+1,\Omega_1} + \|v\|_{k+1,\Omega_2}), \\ \|R_h v - Q_h v\| &\leq C h^{k+1} (\|v\|_{k+1,\Omega_1} + \|v\|_{k+1,\Omega_2}). \quad \square \end{aligned}$$

Corollary 2.3.1. *Let u be the exact solution of the interface problem (2.1.1)-(2.1.3), then*

$$\begin{aligned} \|R_h u - Q_h u\|_{L^2(\Omega)} + h|||R_h u - Q_h u||| &\leq C h^{k+1} \sum_{i=1}^{2} \|u\|_{k+1,\Omega_i}, \\ \|R_h u_t - Q_h u_t\|_{L^2(\Omega)} + h|||R_h u_t - Q_h u_t||| &\leq C h^{k+1} \sum_{i=1}^{2} \|u_t\|_{k+1,\Omega_i}. \quad \square \end{aligned}$$

We write the error $e_h = u_h - Q_h u$ in standard ρ and θ form as

$$e_h(t) = u_h(t) - Q_h u(t) = \theta(t) + \rho(t), \tag{2.3.10}$$

where $\rho = R_h u - Q_h u$ and $\theta = u_h - R_h u$. According to Corollary 2.3.1, we obtain

$$\|\rho\| \leq C h^{k+1} (\|u\|_{k+1,\Omega_1} + \|u\|_{k+1,\Omega_2}). \tag{2.3.11}$$

Again, subtracting (2.3.8) from (2.3.6), we obtain

$$a(R_h v, w_h) = a(Q_h v, w_h) - l_1(v, w_h) - l_2(v, w_h) \ \ \forall v \in X^*, \ w_h \in V_h^0. \tag{2.3.12}$$

Setting $v = u \in X^\star$ in (2.3.12) and further differentiating with respect to t, we have

$$a((R_h u)_t, w_h) = a((Q_h u)_t, w_h) - l_1(u_t, w_h) - l_2(u_t, w_h).$$

Also,

$$a(R_h u_t, w_h) = a(Q_h u_t, w_h) - l_1(u_t, w_h) - l_2(u_t, w_h).$$

From the above two equations, we have

$$a((R_h u - Q_h u)_t - (R_h u_t - Q_h u_t), w_h) = 0 \ \ \forall w_h \in V_h^0.$$

Setting $w_h = (R_h u - Q_h u)_t - (R_h u_t - Q_h u_t)$ in the above equation and applying positivity of the bilinear map $a(.,.)$, we obtain

$$\rho_t = R_h u_t - Q_h u_t.$$

Then, as a consequence of Corollary 2.3.1, we obtain

$$\|\rho_t\| \leq C h^{k+1}(\|u_t\|_{k+1,\Omega_1} + \|u_t\|_{k+1,\Omega_2}). \tag{2.3.13}$$

In order to estimate θ, for all $v_h \in V_h^0$, note that

$$\begin{aligned}
(\theta_t, v_h) + a(\theta, v_h) &= (u_{ht} - (R_h u)_t, v_h) + a(u_h - R_h u, v_h) \\
&= (u_{ht}, v_h) + a(u_h, v_h) - ((R_h u)_t, v_h) - a(R_h u, v_h) \\
&= (u_t, v_h) - ((R_h u)_t, v_h) \\
&= (Q_h u_t, v_h) - ((R_h u)_t, v_h) \\
&= ((Q_h u)_t, v_h) - ((R_h u)_t, v_h) = (-\rho_t, v_h). \qquad (2.3.14)
\end{aligned}$$

Here, we have used equation (2.3.7). For $v_h = \theta$ in (2.3.14), we have

$$(\theta_t, \theta) + C|||\theta|||^2 \ \leq \ \|\rho_t\|\|\theta\|,$$

which leads to

$$\|\theta\|^2 + C\int_0^t |||\theta|||^2 ds \leq \|\theta(0)\|^2 + C\int_0^t \|\rho_t\|^2 ds + C\int_0^t \|\theta\|^2 ds.$$

A simple application of Grownwall's inequality yields

$$\|\theta\|^2 \leq \|\theta(0)\|^2 + C\int_0^t \|\rho_t\|^2 ds. \tag{2.3.15}$$

Using Lemma 2.3.1, we find

$$\|\theta(0)\| = \|u_h(0) - R_h u(0)\| = \|Q_h u(0) - R_h u(0)\| \leq C h^{k+1}\|u(0)\|_{k+1}. \tag{2.3.16}$$

This together with (2.3.13) and (2.3.15) leads to

$$\begin{aligned}\|\theta\|^2 &\leq Ch^{2(k+1)}\|u(0)\|^2_{k+1} \\ &\quad +Ch^{2(k+1)}\int_0^t (\|u_t\|^2_{k+1,\Omega_1} + \|u_t\|^2_{k+1,\Omega_2})ds. \end{aligned} \tag{2.3.17}$$

Substituting (2.3.11) and (2.3.17) in (2.3.10), and applying Lemma 2.2.1, we obtain following optimal $L^\infty(L^2)$ norm error estimate

Theorem 2.3.2. *Let $u_h \in V_h^0$ be the weak Galerkin finite element solution of the problem (2.1.1)-(2.1.3) arising from (2.2.4). Assume the exact solution $u \in H^1(0,T;H^{k+1}(\Omega_i))$, $i = 1,2$. Then there exists a constant $C > 0$ such that*

$$\|u - u_h\| \leq Ch^{k+1}\Big\{\|u(0)\|_{k+1} + \sum_{i=1}^{2}\big(\|u\|_{k+1,\Omega_i} + \|u\|_{H^1(0,t;H^{k+1}(\Omega_i))}\big)\Big\}. \quad \square$$

3

Fully Discrete Error Analysis for Parabolic Interface Problem with Non-homogeneous Jump Conditions

This chapter is devoted to the extension of spatially semidiscrete a priori error analysis to the fully discrete approximation for the parabolic interface problem (1.1.1)-(1.1.3) in a convex polygonal domain. First order backward Euler and second order Crank-Nicolson schemes are applied for the temporal discretization. Optimal order of convergence in $L^\infty(L^2)$ norm is derived for the fully discrete solution. Finally, two dimensional test experiments are presented to testify our theoretical results.

3.1 Introduction

We shall begin with first recalling the parabolic interface problem of the form

$$u_t - \nabla \cdot (\beta \nabla u) = f \quad \text{in } \Omega \times (0, T], \tag{3.1.1}$$

with initial and Dirichlet boundary condition

$$u(x, 0) = u_0(x) \ \text{ in } \Omega; \ \ u = 0 \quad \text{on } \partial\Omega \times (0, T] \tag{3.1.2}$$

and interface conditions

$$[u] = \psi, \quad \left[\beta \frac{\partial u}{\partial \mathbf{n}}\right] = \phi \quad \text{along } \Gamma \times (0, T]. \tag{3.1.3}$$

where Ω is a convex polygonal domain in $\mathbb{R}^2$ with boundary $\partial\Omega$ and $\Omega_1 \subset \Omega$ is an open domain with Lipschitz boundary $\Gamma = \partial\Omega_1$ and $\Omega_2 = \Omega \backslash \Omega_1$. Other symbols are as defined

Some parts of this chapter published online in *Numer. Funct. Anal. Optim. 40 (2019), no. 3, 259-279 and J. Appl. Anal. Comput. 10 (2020), no. 4, 1433-1442.*

in Chapter 1. We assume that the physical coefficients are discontinuous along interface Γ and piecewise positive constant i.e., $\beta(x) = \beta_k$ for $x \in \Omega_k,\ k = 1, 2$. We assume that f is sufficiently smooth locally. Jump functions $\psi,\ \phi : \Gamma \times (0, T] \to \mathbb{R}$ and initial data $u_0 : \Omega \to \mathbb{R}$ are given.

In fluid dynamics and material sciences, we often encounter parabolic interface problems. These interface models happen in many practical applications, such as, heat conduction process in different heat media, electric field distribution in different electromagnetic media, blood flow of human heart, dynamics of biological cell membrane and so on. A considerable amount of numerical algorithms are developed for interface problems based on Finite Element Methods (FEMs). These methods can be divided into two categories via the meshes: fitted FEM [2, 34, 47, 127, 141, 152] and unfitted FEM [11, 91, 95, 96, 128, 136, 154, 158]. Under the low regularity of solutions for interface problems, the convergence analysis has remained a major part of the mathematical study up to the present day. The purpose of the present chapter is to extend the convergence analysis of fitted WG-FEMs for elliptic interface problems to parabolic interface problems. To derive optimal $\mathrm{O}(h^{r+1})$ $(r \geq 1)$ in the L^2 norm for WG-FEM, the minimum regularity assumption on the exact solution u should be $u \in H^1(0, T; H^{r+1}(\Omega))$ (for instance, see [88, 160, 161]). More recently, in [50], the authors have shown the convergence of WG finite element solution to the true solution at an optimal rate in $L^2(L^2)$ norm under the assumption that $u \in L^2(0, T; H^{r+1}(\Omega)) \cap H^1(0, T; H^{r-1}(\Omega))$. In fact, the error analysis in [50] can be extended for the parabolic interface problems to derive optimal error estimate in $L^2(L^2)$ norm with some more details arguments. In this chapter, assuming higher local regularity (cf. [78]) of the true solutions, we have shown the convergence of WG finite element solution to the true solution at an optimal rate in L^2 norm on WG finite element space $(\mathcal{P}_k,\ \mathcal{P}_{k-1},\ \mathcal{P}_{k-1}^2)$. The obtained results intend to enhance the fully discrete error analysis of linear parabolic equations on polygonal meshes with Lipschitz interfaces and non-homogeneous jump conditions.

We now turn our attention to some discrete time weak Galerkin procedures. First, we divide the interval $[0, T]$ into M equally-spaced subintervals by the following points

$$0 = t^0 < t^1 < \cdots < t^M = T$$

with $t^n = n\tau$, $\tau = T/M$ be the time step. For a smooth function ξ on $[0, T]$, define $\xi^n = \xi(t^n)$ and

$$\bar{\partial}\xi^n = \frac{\xi^n - \xi^{n-1}}{\tau},\ \ \hat{\xi}^n = \frac{\xi^n + \xi^{n-1}}{2}. \tag{3.1.4}$$

Let $U^n = U_h^n = \{U_0^n, U_b^n\} \in V_h^0$ be the fully discrete approximation of u at $t = t^n$ which we shall define through the following scheme: Given U^{n-1} in V_h^0, we now determine

$U^n \in V_h^0$ satisfying

$$\begin{aligned}(\bar{\partial}U^n, v_0) + a(U^n, v_h) &= (f^n, v_0) + \langle \psi^n, \beta \nabla_w v_h \cdot \mathbf{n}\rangle_\Gamma + \langle \phi^n, v_b\rangle_\Gamma \\ &\quad -h^{-1}\langle \psi^n, Q_b v_0 - v_b\rangle_\Gamma \ \forall v_h = \{v_0, v_b\} \in V_h^0, \quad (3.1.5)\end{aligned}$$

with $U^0 = U_h^0 = Q_h u(0) = \{Q_0 u(0), Q_b u(0)\}$. For other notations, we refer to Chapter 1 or Chapter 2.

The Crank-Nicolson scheme can be defined through the following scheme: Given U^{n-1} in V_h^0, we now determine $U^n \in V_h^0$ satisfying

$$\begin{aligned}(\bar{\partial}U^n, v_0) + a(\hat{U}^n, v_h) &= (\hat{f}^n, v_0) + \langle \hat{\psi}^n, \beta \nabla_w v_h \cdot \mathbf{n}\rangle_\Gamma + \langle \hat{\phi}^n, v_b\rangle_\Gamma \\ &\quad -h^{-1}\langle \hat{\psi}^n, Q_b v_0 - v_b\rangle_\Gamma \ \forall v_h = \{v_0, v_b\} \in V_h^0, \quad (3.1.6)\end{aligned}$$

with $U^0 = U_h^0 = Q_h u(0) = \{Q_0 u(0), Q_b u(0)\}$.

The layout of this chapter is as follows: Sec. 3.1 introduces the fully discrete schemes. While Sec. 3.2 discusses the convergence behavior of backward Euler scheme, we discuss error analysis of Crank-Nicolson scheme in Sec. 3.3. Finally, in Sec. 3.4 we present some numerical results to validate our theoretical findings.

3.2 Error Analysis for Backward Euler Scheme

This section is devoted to optimal pointwise-in-time error estimate in L^2 norm for the fully discrete approximation given by backward Euler scheme (3.1.5). The error analysis is highly influenced by the techniques in [131].

For fully discrete error estimates, we now split the errors at $t = t^n$ as follows

$$u^n - U^n = u^n - Q_h u^n + Q_h u^n - U^n.$$

Here, $Q_h u^n = \{Q_0 u^n, Q_b u^n\} \in V_h^0$ is as defined by (2.2.8).

At $t = t^n$, we denote our fully discrete approximation error as

$$e^n = U^n - Q_h u^n = \{e_0^n, e_b^n\}.$$

Using ρ and θ, error e^n can be further separated as

$$e^n = \theta^n + \rho^n, \quad (3.2.1)$$

where $\theta^n = U^n - R_h u^n$ and $\rho^n = R_h u^n - Q_h u^n$. Here, R_h is the elliptic projection as defined in (2.3.6).

For θ^n, we have the following error equation

$$\begin{aligned}(\bar{\partial}\theta^n, v_0) + a(\theta^n, v_h) &= -(\bar{\partial}R_h u^n - u_t^n, v_0) \\ &\equiv: -(w^n, v_0) \ \forall v_h = \{v_0, v_b\} \in V_h^0, \quad (3.2.2)\end{aligned}$$

where $w^n = \bar{\partial} R_h u^n - u_t^n$. For simplicity of the exposition, we write $w^n = w_1^n + w_2^n$, where $w_1^n = \bar{\partial} R_h u^n - \bar{\partial} u^n$ and $w_2^n = \bar{\partial} u^n - u_t^n$.

Now, setting $v_h = \theta^n$ in (3.2.2), we have

$$(\bar{\partial}\theta^n, \theta^n) + a(\theta^n, \theta^n) = -(w^n, \theta^n). \tag{3.2.3}$$

Since $a(\theta^n, \theta^n) \geq 0$, we have

$$\begin{aligned} \|\theta^n\| &\leq \tau\|w^n\| + \|\theta^{n-1}\| \\ &\leq \|\theta^0\| + \tau\sum_{j=1}^{n}\|w_1^j\| + \tau\sum_{j=1}^{n}\|w_2^j\|. \end{aligned} \tag{3.2.4}$$

The term w_1^j can be expressed as

$$\begin{aligned} w_1^j &= R_h\bar{\partial}u^j - \bar{\partial}u^j = (R_h - I)(\bar{\partial}u^j) \\ &= (R_h - I)\frac{1}{\tau}\int_{t^{j-1}}^{t^j} u_t dt = \frac{1}{\tau}\int_{t^{j-1}}^{t^j}(R_h u_t - u_t)dt. \end{aligned} \tag{3.2.5}$$

An application of Corollary 2.3.1 leads to

$$\tau\|w_1^j\| \leq Ch^{k+1}\int_{t^{j-1}}^{t^j}(\|u_t\|_{k+1,\Omega_1} + \|u_t\|_{k+1,\Omega_2})dt.$$

Using above estimate, we have

$$\tau\sum_{j=1}^{n}\|w_1^j\| \leq Ch^{k+1}\int_0^{t^n}(\|u_t\|_{k+1,\Omega_1} + \|u_t\|_{k+1,\Omega_2})dt. \tag{3.2.6}$$

Similarly, for the term w_2^j, we have

$$\tau w_2^j = u^j - u^{j-1} - \tau u_t^j = -\int_{t^{j-1}}^{t^j}(s - t^{j-1})u_{tt}ds, \tag{3.2.7}$$

and hence,

$$\tau\|w_2^j\|_{L^2(\Omega_i)} \leq \tau\int_{t_{j-1}}^{t_j}\|u_{tt}\|_{L^2(\Omega_i)}ds.$$

Summing over j from $j = 1$ to $j = n$, we obtain

$$\tau\sum_{j=1}^{n}\|w_2^j\| \leq C\tau\int_0^{t^n}\Big\{\|u_{tt}\|_{L^2(\Omega_1)} + \|u_{tt}\|_{L^2(\Omega_2)}\Big\}dt. \tag{3.2.8}$$

Combining (3.2.6), (3.2.8) and (3.2.4), and further using the fact that $\|\theta^0\| = \|Q_h u(0) - R_h u(0)\| \leq Ch^{k+1}\|u(0)\|_{k+1}$, we obtain

$$\|\theta^n\| \leq C(h^{k+1} + \tau)\Big(\|u(0)\|_{k+1} + \sum_{i=1}^{2}\int_0^{t^n}\big(\|u_t\|_{k+1,\Omega_i} + \|u_{tt}\|_{L^2(\Omega_i)}\big)dt\Big). \tag{3.2.9}$$

An application of Corollary 2.3.1 for ρ^n yields

$$\|\rho^n\| \leq Ch^{k+1} \sum_{i=1}^{2} \|u^n\|_{k+1,\Omega_i}.$$

Again, it is easy to verify that

$$\|u^n\|_{k+1,\Omega_i} \leq \|u(0)\|_{k+1,\Omega_i} + \int_0^{t^n} \|u_t\|_{k+1,\Omega_i} dt.$$

Thus, we have

$$\|\rho^n\| \leq Ch^{k+1}\Big(\|u(0)\|_{k+1} + \sum_{i=1}^{2} \int_0^{t^n} \|u_t\|_{k+1,\Omega_i} dt\Big). \tag{3.2.10}$$

Combining estimates (3.2.9) and (3.2.10) along with Lemma 2.2.1, we obtain following optimal L^2 norm error estimate

Theorem 3.2.1. *Let u and U be the solutions of the problem (3.1.1)-(3.1.3) and (3.1.5), respectively. Assume the exact solution $u \in H^1(0,T;H^{k+1}(\Omega_i)) \cap H^2(0,T;L^2(\Omega_i))$, $i = 1,2$. Then there exists a constant $C > 0$ such that*

$$\begin{aligned}&\|U^n - u^n\| \\ &\leq C(h^{k+1} + \tau)\Big\{\|u(0)\|_{k+1} + \sum_{i=1}^{2}(\|u\|_{H^1(H^{k+1}(\Omega_i))} + \|u_{tt}\|_{L^2(L^2(\Omega_i))})\Big\}. \quad \square\end{aligned}$$

Standard inverse inequality (Lemma A.4, [144]), together with estimates (3.2.9) and (3.2.10), and Lemma 2.2.1 leads to following discrete H^1 norm error estimate

Theorem 3.2.2. *Let u and U be the solutions of the problem (3.1.1)-(3.1.3) and (3.1.5), respectively. Assume the exact solution $u \in H^1(0,T;H^{k+1}(\Omega_i)) \cap H^2(0,T;L^2(\Omega_i))$, $i = 1,2$. Then there exists a constant $C > 0$ such that*

$$\begin{aligned}&\|U^n - u^n\|_{1,h} \\ &\leq C(h^{k} + \tau)\Big\{\|u(0)\|_{k+1} + \sum_{i=1}^{2}(\|u\|_{H^1(H^{k+1}(\Omega_i))} + \|u_{tt}\|_{L^2(L^2(\Omega_i))})\Big\}. \quad \square\end{aligned}$$

3.3 Error Analysis for Crank-Nicolson Scheme

Optimal pointwise-in-time error estimate in L^2 norm is established for the Crank-Nicolson scheme (3.1.6).

From the definition (2.3.6), for all $w_h = \{w_0, w_b\} \in V_h^0$, it is easy to notice that

$$\begin{aligned} a\left(\frac{R_h u^n + R_h u^{n-1}}{\tau}, w_h\right) &= \sum_{i=1}^{2}(-\nabla\cdot(\beta\nabla\hat{u}^n), w_0)_{\Omega_i} + \langle\hat{\psi}^n, \beta\nabla_w w_h\cdot\mathbf{n}\rangle_\Gamma \\ &\quad +\langle\hat{\phi}^n, w_b\rangle_\Gamma - h^{-1}\langle\hat{\psi}^n, Q_b w_0 - w_b\rangle_\Gamma. \end{aligned} \tag{3.3.1}$$

Above equation and (3.1.1) leads to following error equation for θ^n

$$\begin{aligned} (\bar{\partial}\theta^n, v_0) + a(\hat{\theta}^n, v_h) &= (\hat{f}^n, v_0) + \sum_{i=1}^{2}(\nabla\cdot(\beta\nabla\hat{u}^n), v_0)_{\Omega_i} - (\bar{\partial}R_h u^n, v_0) \\ &= (\hat{u}_t^n, v_0) - (\bar{\partial}R_h u^n, v_0) \\ &:= -(w^n, v_0)\ \forall v_h = \{v_0, v_b\} \in V_h^0, \end{aligned} \tag{3.3.2}$$

where $w^n = \bar{\partial}R_h u^n - \hat{u}_t^n$. For simplicity of the exposition, we write $w^n = w_1^n + w_2^n$, where $w_1^n = \bar{\partial}R_h u^n - \bar{\partial}u^n$ and $w_2^n = \bar{\partial}u^n - \hat{u}_t^n$.

Now, setting $v_h = \hat{\theta}^n$ in (3.3.2), we have

$$(\bar{\partial}\theta^n, \hat{\theta}^n) + a(\hat{\theta}^n, \hat{\theta}^n) = -(w^n, \hat{\theta}^n). \tag{3.3.3}$$

Since $a(\hat{\theta}^n, \hat{\theta}^n) \geq 0$, we have

$$\frac{1}{2\tau}\big(\|\theta^n\|^2 - \|\theta^{n-1}\|^2\big) \leq \frac{1}{2}\|w^n\|\big(\|\theta^n\| + \|\theta^{n-1}\|\big),$$

which implies

$$\begin{aligned} \|\theta^n\| &\leq \|\theta^{n-1}\| + \tau\|w^n\| \\ &\leq \|\theta^0\| + \tau\sum_{j=1}^{n}\|w_1^j\| + \tau\sum_{j=1}^{n}\|w_2^j\|. \end{aligned} \tag{3.3.4}$$

The term w_1^j can be expressed as

$$\begin{aligned} w_1^j &= R_h\bar{\partial}u^j - \bar{\partial}u^j = (R_h - I)(\bar{\partial}u^j) \\ &= (R_h - I)\frac{1}{\tau}\int_{t^{j-1}}^{t^j} u_t dt = \frac{1}{\tau}\int_{t^{j-1}}^{t^j}(R_h u_t - u_t)dt. \end{aligned} \tag{3.3.5}$$

An application of Corollary 2.3.1 leads to

$$\tau\|w_1^j\| \leq Ch^{k+1}\int_{t^{j-1}}^{t^j}(\|u_t\|_{k+1,\Omega_1} + \|u_t\|_{k+1,\Omega_2})dt.$$

Using above estimate, we have

$$\tau\sum_{j=1}^{n}\|w_1^j\| \leq Ch^{k+1}\int_0^{t^n}(\|u_t\|_{k+1,\Omega_1} + \|u_t\|_{k+1,\Omega_2})dt. \tag{3.3.6}$$

Now, it remains to determine estimates for w_2^j. To find an estimate for w_2^j, we consider the following two parts separately

$$\begin{aligned}\sigma_1^j &:= \frac{u(t^j)-u(t^{j-1})}{\tau} - u'\Big(t^{j-1}+\frac{\tau}{2}\Big),\\ \sigma_2^j &:= u'\Big(t^{j-1}+\frac{\tau}{2}\Big) - \frac{u'(t^j)+u'(t^{j-1})}{2}.\end{aligned}$$

Using the Taylor's expansion, we obtain

$$\|\sigma_1^j\|_{\Omega_i} + \|\sigma_2^j\|_{\Omega_i} \le C\tau \int_{t^{j-1}}^{t^j} \|u_{ttt}(s)\|_{\Omega_i} ds,\ i=1,2. \tag{3.3.7}$$

Summing over j from $j=1$ to $j=n$ in (3.3.7), we obtain

$$\tau \sum_{j=1}^{n} \|w_2^j\| \le C\tau^2 \int_0^{t^n} \Big\{ \|u_{ttt}\|_{\Omega_1} + \|u_{ttt}\|_{\Omega_2} \Big\} dt. \tag{3.3.8}$$

Combining (3.3.6), (3.3.8) and (3.3.4), and further using the fact that $\|\theta^0\| = \|Q_h u(0) - R_h u(0)\| \le Ch^{k+1}\|u(0)\|_{k+1}$, we obtain

$$\|\theta^n\| \le C(h^{k+1}+\tau^2)\Big(\|u(0)\|_{k+1} + \sum_{i=1}^{2} \int_0^{t^n} \big(\|u_t\|_{k+1,\Omega_i} + \|u_{ttt}\|_{\Omega_i} \big) dt \Big). \tag{3.3.9}$$

An application of Lemma 2.3.1 for ρ^n yields

$$\|\rho^n\| \le Ch^{k+1} \sum_{i=1}^{2} \|u^n\|_{k+1,\Omega_i}.$$

Again, it is easy to verify that

$$\|u^n\|_{k+1,\Omega_i} \le \|u(0)\|_{k+1,\Omega_i} + \int_0^{t^n} \|u_t\|_{k+1,\Omega_i} dt.$$

Thus, we have

$$\|\rho^n\| \le Ch^{k+1}\Big(\|u(0)\|_{k+1} + \sum_{i=1}^{2} \int_0^{t^n} \|u_t\|_{k+1,\Omega_i} dt \Big). \tag{3.3.10}$$

Combining estimates (3.3.9) and (3.3.10) along with Lemma 2.2.1, we obtain following optimal L^2 norm error estimate

Theorem 3.3.1. *Let u and U be the solutions of the problem (3.1.1)-(3.1.3) and (3.1.6), respectively. Assume the exact solution $u \in H^1(H^{k+1}(\Omega_i)) \cap H^3(L^2(\Omega_i))$, $i=1,2$. Then there exists a constant $C>0$ such that*

$$\begin{aligned}&\|U^n - u^n\|\\ &\le C(h^{k+1}+\tau^2)\Big\{ \|u(0)\|_{k+1} + \sum_{i=1}^{2} \big(\|u\|_{H^1(H^{k+1}(\Omega_i))} + \|u_{ttt}\|_{L^2(L^2(\Omega_i))} \big) \Big\}. \quad \square\end{aligned}$$

Standard inverse inequality (Lemma A.4, [144]), together with estimates (3.3.9) and (3.3.10), and Lemma 2.2.1 leads to following discrete H^1 norm error estimate

Theorem 3.3.2. *Let u and U be the solutions of the problem (3.1.1)-(3.1.3) and (3.1.6), respectively. Assume the exact solution $u \in H^1(H^{k+1}(\Omega_i)) \cap H^3(L^2(\Omega_i))$, $i = 1, 2$. Then there exists a constant $C > 0$ such that*

$$\begin{aligned}&\|U^n - u^n\|_{1,h}\\ &\leq C(h^k + \tau^2)\Big\{\|u(0)\|_{k+1} + \sum_{i=1}^{2}(\|u\|_{H^1(H^{k+1}(\Omega_i))} + \|u_{ttt}\|_{L^2(L^2(\Omega_i))})\Big\}. \quad \square\end{aligned}$$

Remark 3.3.1. *The proposed fully discrete finite element scheme can be easily extended for the numerical approximation of the solutions to the following IBVP*

$$\begin{cases} \sigma u_t - \nabla.(\beta \nabla u) = f & \text{in } \Omega \times (0, T], \\ u(x, 0) = u_0, \quad u_t(x, 0) = v_0 & \text{in } \Omega, \\ u(x, t) = 0 & \text{on } \partial\Omega \times (0, T], \end{cases} \tag{3.3.11}$$

coupled with the jump conditions (3.1.3). For numerical validation, we refer to numerical example 3.4.2.

3.4 Numerical Results

We present in this section a numerical result to validate the theoretical estimates presented in Section 3.3. For our numerical experiment, we use lowest order weak Galerkin space $(\mathcal{P}_1(K),\ \mathcal{P}_0(\partial K),\ [\mathcal{P}_0(K)]^2)$ based on uniform triangulations of Ω_i, $i = 1, 2$. The nodes of the triangulations of Ω_1 and Ω_2 coincide on the interface Γ. Note that for each iteration, the spatial mesh size becomes half of the previous mesh size. We choose the uniform time step $\tau = \frac{1}{10}h$.

For the L^2 norm error with $\tau = \mathrm{O}(h)$, we observe its experimental order of convergence (EOC). For each run i, EOC of a given sequence of L^2 norm errors $e(i)$ defined on a sequence of meshes of size $h(i)$ by

$$\mathrm{EOC}(e(i)) = \frac{\log\Big(e(i+1)/e(i)\Big)}{\log\Big(h(i+1)/h(i)\Big)}.$$

Similarly, we have calculated the EOC for the discrete H^1-norm.

Example 3.4.1. We consider the two dimensional domain $\Omega = (-1,1) \times (-1,1)$ and the interface is taken to be the circle $x^2 + y^2 = \frac{1}{4}$. We select the data appearing in (3.1.1)-(3.1.3) by setting exact solution as

$$\begin{aligned} u_1(x,y,t) &= t(0.25 - x^2 - y^2) \quad \text{in } \Omega_1 \times (0,1], \\ u_2(x,y,t) &= t(0.25 - x^2 - y^2)\sin(\pi x)\sin(\pi y) \quad \text{in } \Omega_2 \times (0,1], \end{aligned}$$

with $\beta_1 = 10^{-4}$ and $\beta_2 = 1$.

Table 3.4.1: Numerical results for L^2-norm error in Example 3.4.1 at final time

l $(runs)$	h	$Error$	EOC
1	$\frac{1}{8}$	8.38744×10^{-2}	–
2	$\frac{1}{16}$	3.05176×10^{-2}	1.45
3	$\frac{1}{32}$	7.04421×10^{-3}	2.11
4	$\frac{1}{64}$	1.84338×10^{-3}	1.93
5	$\frac{1}{128}$	4.40906×10^{-4}	2.01

Table 3.4.2: Numerical results for discrete H^1-norm error in Example 3.4.1 at final time

l $(runs)$	h	$Error$	EOC
1	$\frac{1}{8}$	1.17124	–
2	$\frac{1}{16}$	6.84037×10^{-1}	0.77
3	$\frac{1}{32}$	3.17659×10^{-1}	1.10
4	$\frac{1}{64}$	1.59264×10^{-1}	0.99
5	$\frac{1}{128}$	7.93007×10^{-2}	1.00

The convergence behavior of the fully discrete weak Galerkin solutions at final time $T = 1$ with respect to the L^2-norm and discrete H^1 norm are also depicted in Tables 3.4.1-3.4.2. It is clear from these tables that we have achieved optimal order of convergence in both the norms, which confirm the theoretical prediction as proved in Theorems 3.3.1-3.3.2.

Example 3.4.2. In our second numerical example, we consider the square domain $\Omega = (-1,1)\times(-1,1)$ and the interface is taken to be the ellipse $\{(x,y) : 4x^2+16y^2 = r^2 = 1\}$. We select the data in (3.3.11) such that the exact solution u is given by

$$u(x,y,t) = \begin{cases} 10^{-1}(1-r^2)t^2\exp(-t) & \text{if } r^2 \leq 1, \\ 10^{-2}(1-r^2)\sin(0.25\pi t)\sin(\pi x)\sin(\pi y) & \text{if } r^2 > 1. \end{cases}$$

The second set of physical coefficients borrowed from Dai *et.al.* [41] that corresponds to the classical Pennes bio heat transfer model is given by

$$(\sigma,\beta) = \begin{cases} (4.08, 0.0052) & \text{in } 4x^2+16y^2 \leq 1, \\ (3.06, 0.0021) & \text{in } 4x^2+16y^2 > 1. \end{cases}$$

Table 3.4.3: Numerical results for L^2-norm error in Example 3.4.2 at final time

l $(runs)$	h	$Error$	EOC
1	$\frac{1}{4}$	2.3268×10^{-2}	–
2	$\frac{1}{8}$	5.68903×10^{-3}	2.03
3	$\frac{1}{16}$	1.48856×10^{-3}	1.93
4	$\frac{1}{32}$	3.60021×10^{-4}	2.04
5	$\frac{1}{64}$	9.6392×10^{-5}	2.01

Table 3.4.4: Numerical results for discrete H^1-norm error in Example 3.4.2 at final time

l $(runs)$	h	$Error$	EOC
1	$\frac{1}{4}$	2.037×10^{-1}	–
2	$\frac{1}{8}$	1.32786×10^{-1}	0.61
3	$\frac{1}{16}$	6.59948×10^{-2}	1.00
4	$\frac{1}{32}$	3.17777×10^{-2}	1.05
5	$\frac{1}{64}$	1.57923×10^{-2}	1.01

Tables 3.4.3-3.4.4 represent the numerical solution errors and convergence rates in L^2 and discrete H^1 norms, respectively. In both cases, errors are calculated at time $t = 1$ and clearly demonstrates the second order of convergence in L^2 norm and first order of convergence in discrete H^1 norm.

4

Convergence of WG-FEMs for Wave Equation with Interfaces

Weak Galerkin finite element method is proposed for solving wave equation with interface on the weak Galerkin finite element space $(\mathcal{P}_k(K), \mathcal{P}_{k-1}(\partial K), [\mathcal{P}_{k-1}(K)]^2)$. Optimal order a priori error estimates for both space-discrete scheme and implicit fully discrete scheme are derived in $L^\infty(L^2)$ norm. Finite element algorithm presented here can contribute to a variety of hyperbolic problems where physical domain consists of heterogeneous media. Finally, numerical results are presented to validate our theoretical findings.

4.1 Introduction

To begin with, let us first recall the electric interface interface problem of the form

$$u_{tt} - \nabla \cdot (\beta(x)\nabla u) = f(x,t) \quad \text{in } \Omega \times (0,T], \tag{4.1.1}$$

with initial and boundary conditions

$$u(x,0) = u(0) \;\; \& \;\; u_t(x,0) = v(0) \;\; \text{in } \Omega; \;\; u(x,t) = 0 \quad \text{on } \partial\Omega \times (0,T] \tag{4.1.2}$$

and the jump conditions on the interface

$$[u] = \psi, \;\; \left[\beta \frac{\partial u}{\partial \mathbf{n}}\right] = \phi \quad \text{along } \Gamma \times (0,T]. \tag{4.1.3}$$

where Ω is a convex polygonal domain in $\mathbb{R}^2$ with boundary $\partial\Omega$ and $\Omega_1 \subset \Omega$ is an open domain with Lipschitz boundary $\Gamma = \partial\Omega_1$ and $\Omega_2 = \Omega \backslash \Omega_1$. Other symbols are as defined in Chapter 1. We assume that the physical coefficients are discontinuous along interface Γ and piecewise positive constant i.e., $\beta(x) = \beta_k$ for $x \in \Omega_k, \; k = 1, 2$. We assume that

f is sufficiently smooth locally. Jump functions $\psi,\ \phi : \Gamma \times (0,T] \to \mathbb{R}$ and initial data $u(0),\ v(0) : \Omega \to \mathbb{R}$ are given.

The numerical solution of the wave equation is of fundamental importance to the simulation of time dependent acoustic, electromagnetic, or elastic waves. For such wave phenomena the scalar second order wave equation often serves as a model problem. In the study of wave equations for some physical problems, such as acoustic or elastic waves traveling through heterogeneous media, there can be discontinuities in the coefficients of the equation at interfaces (e.g., [20, 21, 74] and references therein). For instance, an acoustic wave propagating at different speeds in different media is modeled by the second order wave equation with discontinuous coefficients. In the past few decades there has been remarkable progress in understanding and analyzing numerical algorithms for solving hyperbolic equations. A substantial amount of research on a priori and a posteriori error estimates in the design of finite element methods for the hyperbolic equations without interfaces is available in literature (e.g., [16, 17, 38, 58, 60, 63, 64, 68, 77, 114, 119] and references therein). Solving wave propagation problems within heterogeneous media has been of great interest and has drawn significant attention in a variety of fields such as the oil exploration industry and mineral finding as well as the study of earthquakes. Finite element approximations of wave equation with interfaces via interface fitted conforming finite element algorithms are carried out in [43, 45, 46]. To avoid interface fitted mesh, immersed FEMs have been proposed to allow the interface to cut through elements so that simple structured Cartesian meshes can be employed that are not necessarily body-fitted (cf. [5, 7, 154]). Previous works on FEMs for wave equation with interfaces are concerned only on linear elements and assume continuity of the solution along interfaces. On the other hand it is challenging to obtain high order convergence when the interface geometries are arbitrarily complex. In this chapter, we extend the work of [112] to the interface problem (4.1.1)-(4.1.3). Typical semidiscrete and fully discrete schemes are presented. The fully discrete space-time finite element discretizations are based on the backward Euler approximations. Optimal a priori error estimates for both semidiscrete and fully discrete schemes are proved in $L^\infty(H^1)$ and $L^\infty(L^2)$ norms. Our results are intended to enhance the numerical analysis of linear wave equations where physical domain consists of heterogenous media.

The rest of the paper is organized as follows. Sec. 4.2 is devoted to the optimal order error estimates of semidiscrete WG-FEM algorithm. In Sec. 4.3, a implicit backward scheme is described along with a priori error bounds in $L^\infty(L^2)$ norm. Sec. 4.4 focuses on some numerical results that confirm the convergence theory developed in earlier section.

4.2 Error Analysis for the Semidiscrete Scheme

This section deals with the error analysis for the spatially discrete scheme. Optimal order of convergence in $L^\infty(L^2)$ norm is established when the regularity of the solution is low on the entire domain.

Let V_h^0 be the weak Galerkin finite element space defined by (2.2.2) based on the fitted finite element discretization $\mathcal{T}_h$ of Ω as described in Chapter 1. For each $v_h = \{v_0, v_b\} \in V_h$, we introduce a discrete weak gradient operator, denoted by ∇_w, is defined as the unique polynomial $(\nabla_w v_h) \in [\mathcal{P}_{k-1}(K)]^2$ that satisfies the following equation

$$(\nabla_w v_h, \varphi)_K = -\int_K v_0(\nabla \cdot \varphi) dK + \int_{\partial K} v_b(\varphi \cdot \eta) ds \;\; \forall \varphi \in [\mathcal{P}_{k-1}(K)]^2. \tag{4.2.1}$$

Using the discrete weak gradient operator ∇_w, we define a bilinear map $A : V_h \times V_h \to \mathbb{R}$ by

$$A(v_h, w_h) = \sum_{K \in \mathcal{T}_h} \left(\beta \nabla_w v_h, \nabla_w w_h\right)_K + S(v_h, w_h) \;\; \forall v_h, w_h \in V_h, \tag{4.2.2}$$

where $S(\cdot, \cdot)$ is known as stabilizer, which is a semi-positive definite bilinear form defined on $V_h \times V_h$. Stabilizer $S(\cdot, \cdot)$ is often chosen in such a way that it fits well into the theory and implementation of the WG numerical scheme. Here, the stabilizer $S(\cdot, \cdot)$ is defined as

$$S(v_h, w_h) = \sum_{K \in \mathcal{T}_h} h_K^{-1} \langle Q_b v_0 - v_b, Q_b w_0 - w_b \rangle_{\partial K}. \tag{4.2.3}$$

Notation $\langle \cdot, \cdot \rangle_{\partial K}$ denotes the L^2 inner product on ∂K and accordingly, we write

$$\langle \cdot, \cdot \rangle_{\partial K} = \sum_{e \in \partial K} \langle \cdot, \cdot \rangle_e,$$

where $\langle \cdot, \cdot \rangle_e$ denotes the L^2 inner product on $e \in \mathcal{E}_h$.

Recall that the weak Galerkin finite element space V_h^0 is a normed linear space with respect to following triple-bar norm given by (cf. [44])

$$|||w_h|||^2 = \sum_{K \in \mathcal{T}_h} \|\beta^{\frac{1}{2}} \nabla_w w_h\|_K^2 + \sum_{K \in \mathcal{T}_h} h_K^{-1} \|Q_b w_0 - w_b\|_{\partial K}^2 = A(w_h, w_h) \;\; w_h \in V_h^0. \tag{4.2.4}$$

Based on the space V_h^0, we are now in a position to define the semidiscrete approximation of the interface problem (4.1.1)-(4.1.3). The continuous-time weak Galerkin finite element approximation to (4.1.1)-(4.1.3) is defined as follows: Find $u_h = \{u_0, u_b\} : [0, T] \to V_h^0$ satisfying

$$\begin{aligned} (u_{htt}, v_0) + A(u_h, v_h) &= (f, v_0) + \langle \psi, \beta \nabla_w v_h \cdot \mathbf{n} \rangle_\Gamma + \langle \phi, v_b \rangle_\Gamma \\ &\quad - \frac{1}{h} \langle \psi, Q_b v_0 - v_b \rangle_\Gamma, \end{aligned} \tag{4.2.5}$$

for all $v_h \in V_h^0$ with $u_h(0) = R_h u(0)$ and $u_{ht}(0) = R_h v(0)$. Well-posedness of the scheme (4.2.5) can be verified from the fact that weak finite element space V_h^0 is a normed linear space with respect to the triple-bar norm. Here, $R_h : X^* \to V_h^0$ is the elliptic projection defined by (2.3.6).

Now, like earlier, we split our error into two components using L^2 projection as an intermediate operator. We write

$$u - u_h = (u - Q_h u) + (Q_h u - u_h),$$

where $Q_h u = \{Q_0 u, Q_b u\} \in V_h^0$ is defined by (2.2.8). For simplicity, we introduce the following notation

$$e_h := \{e_0, e_b\} = Q_h u - u_h. \tag{4.2.6}$$

Now, we further split our error $e_h = u_h - Q_h u$ into standard ρ and θ form as

$$e_h(t) = u_h(t) - Q_h u(t) := \theta(t) + \rho(t), \tag{4.2.7}$$

where $\rho := R_h u - Q_h u$ and $\theta := u_h - R_h u$. According to Corollary 2.3.1, we obtain

$$\|\rho\| \leq Ch^{k+1}(\|u\|_{k+1,\Omega_1} + \|u\|_{k+1,\Omega_2}). \tag{4.2.8}$$

Again, from the identity (2.3.12) it is easy to note that

$$\rho_t = R_h u_t - Q_h u_t.$$

Then, as a consequence of Corollary 2.3.1, we obtain

$$\|\rho_t\| \leq Ch^{k+1}(\|u_t\|_{k+1,\Omega_1} + \|u_t\|_{k+1,\Omega_2}). \tag{4.2.9}$$

Next, using the definitions of projection operators R_h and Q_h along with the semidiscrete approximation (4.2.5), we arrive at following important identity

$$\begin{aligned}
&(\theta_{tt}, v_h) + A(\theta, v_h) \\
&= (u_{htt}, v_h) + A(u_h, v_h) - ((R_h u)_{tt}, v_h) - A(R_h u, v_h) \\
&= (f, v_h) - ((R_h u)_{tt}, v_h) + (\nabla \cdot (\beta \nabla u), v_h) \\
&= (u_{tt}, v_h) - ((R_h u)_{tt}, v_h) \\
&= (Q_h u_{tt}, v_h) - ((R_h u)_{tt}, v_h) \\
&= ((Q_h u)_{tt}, v_h) - ((R_h u)_{tt}, v_h) = -(\rho_{tt}, v_h) \quad \forall v_h \in V_h^0.
\end{aligned} \tag{4.2.10}$$

Now, for some suitable $\xi \in (0, T)$, we define

$$\hat{\theta}(., t) = \int_t^\xi \theta(., s) ds, \quad 0 \leq t \leq T.$$

Clearly, we observe that

$$\hat{\theta}(\xi) = 0 \ \text{ and } \ \hat{\theta}_t = -\theta(.,t), \ t \in [0,T]. \tag{4.2.11}$$

Now, set $\phi_h = \hat{\theta}$ in (4.2.10), integrate between 0 to ξ with respect to the variable t to obtain

$$\begin{aligned} &-\int_0^\xi (\theta_t, \hat{\theta}_t)ds + (\theta_t(\xi), \hat{\theta}(\xi)) - (\theta_t(0), \hat{\theta}(0)) + \int_0^\xi A(\theta, \hat{\theta})ds \\ &= \int_0^\xi (\rho_t, \hat{\theta}_t)ds - (\rho_t(\xi), \hat{\theta}(\xi)) + (\rho_t(0), \hat{\theta}(0)). \end{aligned}$$

Using (4.2.11), we have

$$\begin{aligned} &\int_0^\xi \frac{1}{2}\frac{d}{dt}\|\theta(t)\|^2 dt - (\theta_t(0), \hat{\theta}(0)) - \int_0^\xi \frac{1}{2}\frac{d}{dt}A(\hat{\theta}, \hat{\theta})dt \\ &= -\int_0^\xi (\rho_t, \theta)dt + (\rho_t(0), \hat{\theta}(0)). \end{aligned}$$

Since θ is continuous in the time variable, we select ξ such that $\|\theta(\xi)\| = \max_{0\le t\le T}\|\theta(t)\|$. Then observe that $\theta(0) = 0$ and $\|\hat{\theta}(0)\| \le \xi\|\theta(\xi)\|$, which together with Young's inequality gives

$$\begin{aligned} &\frac{1}{2}\|\theta(\xi)\|^2 + \frac{1}{2}\mathcal{A}(\hat{\theta}(0), \hat{\theta}(0)) \\ &= (e_{ht}(0), \hat{\theta}(0)) - \int_0^\xi (\rho_t, \theta)dt \\ &\le \|e_{ht}(0)\|\|\hat{\theta}(0)\| + \max_{0\le t\le T}\|\theta(t)\| \int_0^\xi \|\rho_t\|dt \\ &\le \xi\|e_{ht}(0)\|\|\theta(\xi)\| + \|\theta(\xi)\|\sqrt{T}\|\rho_t\|_{L^2(L^2)} \\ &\le \frac{\epsilon}{2}\xi^2\|e_{ht}(0)\|^2 + \frac{1}{\epsilon}\|\theta(\xi)\|^2 + \frac{\epsilon}{2}T\|\rho_t\|^2_{L^2(L^2)}, \end{aligned} \tag{4.2.12}$$

for some $\epsilon > 0$. Now, combine estimates (4.2.9) and (4.2.12) to obtain

$$\|\theta(\xi)\|^2 \le Ch^{2(k+1)}\Big(\|v(0)\|^2_{k+1} + \sum_{i=1}^{2}\|u_t\|^2_{L^2(H^{k+1}(\Omega_i))}\Big). \tag{4.2.13}$$

Thus, we have proved the following optimal $L^\infty(L^2)$ norm estimate.

Theorem 4.2.1. *Let u and u_h be the solutions of problems (4.1.1)-(4.1.3) and (4.2.5), respectively. Assume that the solution of (4.1.1)-(4.1.3) is so regular that $u \in H^1(H^{k+1}(\Omega_1) \cap H^{k+1}(\Omega_2))$. Then there exists a constant C such that*

$$\begin{aligned} \|Q_h u(t) - u_h(t)\| \ \le \ Ch^{k+1}\Big(&\|v(0)\|_{k+1} + \sum_{i=1}^{2}\|u(t)\|_{k+1,\Omega_i} \\ &+ \sum_{i=1}^{2}\|u_t\|_{L^2(H^{k+1}(\Omega_i))}\Big), \ t \in (0,T]. \end{aligned}$$

4.3 Fully Discrete Error Analysis

We now turn our attention to discrete time weak Galerkin procedure. A discrete-in-time implicit scheme based on backward Euler method for approximating exact solution u is discussed in this section. Optimal pointwise-in-time error estimate in L^2 norm is established. The basic error analysis technique is highly influenced by the works in [43, 63]. It is worth to note that [43] has discussed only linear conforming finite element method for homogeneous wave equation with homogeneous jump conditions.

Before proceeding further, we now prove a stability result for the semidiscrete solution u_h given by (4.2.5). Regarding the stability of u_h, we have the following result.

Lemma 4.3.1. *Let u_h satisfy (4.2.5). Then, we have*

$$\begin{aligned}&\|u_{htttt}(t)\|\\&\leq C\Big(\|u(0)\|_4+\|v(0)\|_3+\|f\|_{H^3(H^2(\Omega))}+\sum_{i=1}^{2}\|u_t\|_{H^2(H^3(\Omega_i))}\Big).\end{aligned}$$

Proof. We differentiate (4.2.10) with respect to t and substitute $v_h=\theta_{tt}$ to have

$$\frac{1}{2}\frac{d}{dt}\|\theta_{tt}\|^2+\frac{1}{2}\frac{d}{dt}|||\theta_t|||^2=-(\rho_{ttt},\theta_{tt}).$$

Integration from 0 to t yields

$$\begin{aligned}&\|\theta_{tt}(t)\|^2+|||\theta_t(t)|||^2\\&\leq\|\theta_{tt}(0)\|^2+|||\theta_t(0)|||^2+\int_0^t\|\rho_{ttt}\|^2ds+\int_0^t\|\theta_{tt}\|^2ds.\end{aligned}$$

Then standard Gronwall's inequality yields

$$\|\theta_{tt}(t)\|^2\leq C\Big(\|\theta_{tt}(0)\|^2+|||\theta_t(0)|||^2+\int_0^T\|\rho_{ttt}\|^2dt\Big). \tag{4.3.1}$$

Similarly, we obtain

$$\|\theta_{tttt}(t)\|^2\leq C\Big(\|\theta_{tttt}(0)\|^2+|||\theta_{ttt}(0)|||^2+\int_0^T\|\rho_{ttttt}\|^2dt\Big). \tag{4.3.2}$$

Setting $t\to 0^+$ in (4.2.10) and using the fact that $\theta(0)=u_h(0)-R_hu(0)=0$, we obtain

$$(\theta_{tt}(0),v_h)=-(\rho_{tt}(0),v_h)\ \ \forall v_h\in V_h^0. \tag{4.3.3}$$

Then Lemma 2.3.1 leads to

$$\begin{aligned}\|\theta_{tt}(0)\| &\leq C\|\rho_{tt}(0)\| \\ &\leq Ch^2(\|u_{tt}(0)\|_{2,\Omega_1} + \|u_{tt}(0)\|_{2,\Omega_2}) \\ &\leq Ch^2(\|u(0)\|_4 + \|f(0)\|_2) \\ &\leq Ch^2(\|u(0)\|_4 + \|f\|_{H^1(H^2(\Omega))}). \end{aligned} \tag{4.3.4}$$

In the previous estimate, we have used the fact that (cf. [123], Proposition 7.1)

$$\sup_{0\leq t\leq T} \|v(t)\|_{\mathcal{B}} \leq C(T)\|v\|_{H^1(J;\mathcal{B})} \ \forall v \in H^1(J;\mathcal{B}), \tag{4.3.5}$$

for any Banach space $\mathcal{B}$. As a consequence of above estimate together with inverse inequality, we obtain

$$|||\theta_{tt}(0)||| \leq Ch^{-1}\|\theta_{tt}(0)\| \leq Ch(\|u(0)\|_4 + \|f\|_{H^1(H^2(\Omega))}). \tag{4.3.6}$$

We differentiate (4.2.10) with respect to t and then take $t \to 0^+$ to have

$$(\theta_{ttt}(0), v_h) = -(\rho_{ttt}(0), v_h) \ \ \forall v_h \in V_h^0. \tag{4.3.7}$$

Here, we have used the fact that $\theta_t(0) = u_{ht}(0) - R_h u_t(0) = 0$. Now, using Lemma 2.3.1 we arrive at

$$\begin{aligned}\|\rho_{ttt}(0)\| &= \|R_h u_{ttt}(0) - Q_h u_{ttt}(0)\| \\ &\leq Ch(\|u_{ttt}(0)\|_{1,\Omega_1} + \|u_{ttt}(0)\|_{1,\Omega_2}) \\ &\leq Ch(\|v(0)\|_3 + \|f_t(0)\|_1) \\ &\leq Ch(\|v(0)\|_3 + \|f\|_{H^2(H^1(\Omega))}). \end{aligned} \tag{4.3.8}$$

Now, we combine estimates (4.3.7)-(4.3.8) to have

$$\|\theta_{ttt}(0)\| \leq Ch(\|v(0)\|_3 + \|f\|_{H^2(H^1(\Omega))}). \tag{4.3.9}$$

Then use inverse inequality (Lemma A.4, [144]) to have

$$|||\theta_{ttt}(0)||| \leq Ch^{-1}\|\theta_{ttt}(0)\| \leq C(\|v(0)\|_3 + \|f\|_{H^2(H^1(\Omega))}). \tag{4.3.10}$$

Differentiating (4.2.10) twice with respect to t and then take $t \to 0^+$ to have

$$\begin{aligned}(\theta_{tttt}(0), v_h) &= -A(\theta_{tt}(0), v_h) - (\rho_{ttt}(0), v_h) \\ &\leq C(|||\theta_{tt}(0)|||\,|||v_h||| + \|\rho_{ttt}(0)\|\|v_h\|) \\ &\leq C(h^{-1}|||\theta_{tt}(0)||| + \|\rho_{ttt}(0)\|)\|v_h\| \\ &\leq C(\|u(0)\|_4 + \|v(0)\|_3 + \|f\|_{H^2(H^2(\Omega))}), \end{aligned}$$

In the last inequality, we have used standard inverse inequality. Further, using the estimates (4.3.6) and (4.3.8), we have

$$(\theta_{tttt}(0), v_h) \leq C(\|u(0)\|_4 + \|v(0)\|_3 + \|f\|_{H^2(H^2(\Omega))}),$$

which yields

$$\|\theta_{tttt}(0)\| \leq C(\|u(0)\|_4 + \|v(0)\|_3 + \|f\|_{H^2(H^2(\Omega))}). \tag{4.3.11}$$

Using estimates (4.3.10) and (4.3.11) in (4.3.2), we find that

$$\begin{aligned}
&\|\theta_{tttt}(t)\|^2 \\
&\leq C\Big(\|u(0)\|_4^2 + \|v(0)\|_3^2 + \|f\|^2_{H^2(H^2(\Omega))} + \int_0^T \|\rho_{ttttt}\|^2 dt\Big).
\end{aligned}$$

Using above estimate in (4.2.7), we obtain

$$\begin{aligned}
&\|u_{htttt}(t)\| \\
&\leq \|\rho_{tttt}\| + \|\theta_{tttt}\| + \|Q_h u_{tttt}\| \\
&\leq C\Big(\|u(0)\|_4 + \|v(0)\|_3 + \|f\|_{H^2(H^2(\Omega))} + \sum_{i=1}^{2} \|u\|_{H^5(H^1(\Omega_i))}\Big).
\end{aligned}$$

In the last inequality, we have used Lemma 2.3.1. □

Now, we turn our attention towards fully discrete approximation. We first divide the interval $[0, T]$ into N equally-spaced subintervals by the following points

$$0 = t^0 < t^1 < \cdots < t^N = T$$

with $t^n = n\tau$, $\tau = T/N$ be the time step. For a smooth function $\nu \in C(0, T; L^2(\Omega))$, we denote ν^n be the value of ν at $t = t^n$.

Let $U_h^n = \{U_0^n, U_b^n\} \in V_h^0$ be the fully discrete approximation of u at $t = t^n$, which we shall define through the following scheme: For each $n = 1, 2, \ldots, N$, we now determine $U_h^n \in V_h^0$ satisfying

$$\begin{aligned}
(\partial^2 U_h^n, v_h) + A(U_h^n, v_h) &= (f^n, v_0) + \langle \psi^n, \beta \nabla_w v_h \cdot \mathbf{n} \rangle_\Gamma + \langle \phi^n, v_b \rangle_\Gamma \\
&\quad - h^{-1} \langle \psi^n, Q_b v_0 - v_b \rangle_\Gamma,
\end{aligned} \tag{4.3.12}$$

for all $v_h = \{v_0, v_b\} \in V_h^0$. The backward second and first finite differences are defined as

$$\partial^2 U_h^n = \frac{\partial U_h^n - \partial U_h^{n-1}}{\tau}, \text{ for } n = 1, 2, \ldots, N, \tag{4.3.13}$$

with

$$\partial U_h^n = \begin{cases} (U_h^n - U_h^{n-1})/\tau, & \text{for } n = 1, 2, \ldots, N, \\ R_h v(0), & \text{for } n = 0, \end{cases} \tag{4.3.14}$$

where $U_h^0 = R_h u(0)$.

To connect both fully discrete and semidiscrete solutions, we define $U : (0, T] \times \Omega \to \mathbb{R}$ by

$$U(t) = \frac{t - t^{n-1}}{\tau} U_h^n + \frac{t^n - t}{\tau} U_h^{n-1} - \frac{(t - t_{n-1})(t_n - t)^2}{k} \partial^2 u_h^n, \tag{4.3.15}$$

for $t \in (t^{n-1}, t^n]$, $n = 1, 2, \ldots, N$, with $\partial^2 u_h^n$ is defined as in (4.3.13)-(4.3.14). Time reconstruction $U(t)$ has been introduced to setup a bridge between continuous time error analysis and discrete time error analysis. Note that U is a C^1 function in the time variable, with $U(t^n) = U_h^n$ and $U_t(t^n) = \partial U_h^n$ for $n = 0, 1, \ldots, N$. Further, for $t \in (t^{n-1}, t^n]$, $n = 1, 2, \ldots, N$, we obtain

$$\begin{aligned} U_{tt}(t) &= (1 + \mu^n(t)) \partial^2 u_h^n, \quad \text{with} \\ \mu^n(t) &= -\frac{6}{k}(t - t^{n-1/2}), \; t^{n-1/2} = \frac{1}{2}(t^n + t^{n-1}). \end{aligned} \tag{4.3.16}$$

Next, in order to bound the error $U - Q_h u$, we decompose it as

$$U - Q_h u = (U - u_h) + (u_h - Q_h u),$$

where $u_h : [0, T] \to V_h^0$ is the semidiscrete solution defined by (4.2.5).

Then fully discrete error relation in $\alpha := (U - u_h)$ is given by

$$(\alpha_{tt}, v_h) = (\mu^n(t) \partial^2 u_h^n, v_h) + (\partial^2 u_h^n - u_{htt}^n, v_h) - (u_{htt} - u_{htt}^n, v_h), \tag{4.3.17}$$

for $t \in (t^{n-1}, t^n]$, $1 \le n \le N$. In the last equality, we have used (4.3.16).

Setting $\omega_1^n = \mu^n(t) \partial^2 u_h^n$, $\omega_2^n = \partial^2 u_h^n - u_{htt}^n$ and $\omega_3^2 = u_{htt}^n - u_{htt}$ in (4.3.17), we have

$$(\alpha_{tt}, v_h) = (\omega_1^n, v_h) + (\omega_2^n, v_h) + (\omega_3^n, v_h) \;\; \forall v_h \in V_h^0. \tag{4.3.18}$$

Let $\hat{\alpha} : [0, T] \times \Omega \to \mathbb{R}$ be defined as

$$\hat{\alpha}(t, .) = \hat{\alpha}(t) = \int_t^\lambda \alpha(s, .) ds, \; t \in [0, T].$$

Here, $\lambda \in (t^{m-1}, t^m]$ is fixed for some integer m with $1 \le m \le N$ such that $\|\alpha(\lambda)\| = \max_{0 \le t \le T} \|\alpha(t)\|$. Next, we set $v_h = \hat{\alpha}$ in (4.3.18) and integrate the resulting equation with respect to t between 0 and λ to arrive at

$$\int_0^\lambda (\alpha_{tt}, \hat{\alpha}) dt = T_1 + T_2 + T_3, \tag{4.3.19}$$

where

$$\begin{aligned} T_1 &= \sum_{j=1}^{m-1}\int_{t^{j-1}}^{t^j}\Big(\omega_1^j,\hat{\alpha}\Big)dt+\int_{t^{m-1}}^{\lambda}\Big(\omega_1^m,\hat{\alpha}\Big)dt,\\ T_2 &= \sum_{j=1}^{m-1}\int_{t^{j-1}}^{t^j}\Big(\omega_2^j,\hat{\alpha}\Big)dt+\int_{t^{m-1}}^{\lambda}\Big(\omega_2^m,\hat{\alpha}\Big)dt, \qquad (4.3.20)\\ T_3 &= \sum_{j=1}^{m-1}\int_{t^{j-1}}^{t^j}(\omega_3^j,\hat{\alpha})dt+\int_{t^{m-1}}^{\lambda}(\omega_3^m,\hat{\alpha})dt. \end{aligned}$$

Integrate by parts the left-hand side in (4.3.19) to obtain

$$\begin{aligned} \frac{1}{2}\|\alpha(\lambda)\|^2 &= T_1+T_2+T_3+(\alpha_t(0),\hat{\alpha}(0))+\frac{1}{2}\|\alpha(0)\|^2\\ &= T_1+T_2+T_3+(\alpha_t(0),\hat{\alpha}(0)). \qquad (4.3.21) \end{aligned}$$

Here, we have used the fact that $\hat{\alpha}_t=-\alpha$ and

$$\begin{aligned} &\alpha_t(0)=U_t(0)-u_{ht}(0)=\partial U_h^0-R_hv(0)=0 \ \ \&\\ &\alpha(0)=U(0)-u_h(0)=U_h(0)-R_hu(0)=0. \end{aligned}$$

Now, we borrow following estimates from [43]. For the terms T_i $(1\le i\le 3)$, we obtain

$$\begin{aligned} T_1 &\le C\tau^2\|\alpha\|_{L^\infty(L^2(\Omega))}\\ &\quad\times\Big(\|u_{htttt}\|_{L^\infty(L^2(\Omega))}+\|u_{httt}\|_{L^\infty(L^2(\Omega))}+\|u_{htt}\|_{L^\infty(L^2(\Omega))}\Big),\\ T_2 &\le C\tau^2\|u_{htttt}\|_{L^\infty(L^2(\Omega))}\|\alpha\|_{L^\infty(L^2(\Omega))},\\ T_3 &\le C\tau^{\frac{5}{2}}\big(\|u_{htttt}\|_{L^\infty(L^2(\Omega))}+\|u_{httt}\|_{L^\infty(L^2(\Omega))}\big)\|\alpha\|_{L^\infty(L^2(\Omega))}. \end{aligned}$$

Using above estimates in (4.3.21), we obtain

$$\|\alpha(\lambda)\|^2\le C\tau^4\sum_{i=2}^{4}\Big\|\frac{\partial^i}{\partial t^i}u_h(t)\Big\|^2.$$

Above estimate together with Lemma 4.3.1 yields

$$\begin{aligned} \|\alpha(\lambda)\|^2 &\le C\tau^4\Big(\|u(0)\|_4^2+\|v(0)\|_3^2+\|f\|^2_{H^2(H^2(\Omega))}+\|f\|^2_{H^3(H^1(\Omega))}\\ &\qquad+\sum_{i=1}^{2}\|u_{tt}\|^2_{H^1(H^3(\Omega_i))}\Big). \end{aligned}$$

Finally, above estimate together with Theorem 4.2.1 leads to following optimal L^2 norm error estimate.

Theorem 4.3.1. *Let u and U_h^n be the solution of (4.1.1)-(4.1.3) and (4.3.12), respectively. Assume that the solution of (4.1.1)-(4.1.3) is so regular that $u \in H^1(H^{k+1}(\Omega_i)) \cap H^2(H^3(\Omega_i))$, $i = 1, 2$. Then, there exists a constant $C > 0$ such that*

$$\begin{aligned}&\|U(t) - Q_h u(t)\| \\ &\leq C(h^{k+1} + \tau^2)\Big(\|u(0)\|_4 + \|v(0)\|_3 + \|v(0)\|_{k+1} + \|f\|_{H^3(H^2(\Omega))} \\ &\qquad + \sum_{i=1}^{2} \left(\|u\|_{H^1(H^{k+1}(\Omega_i))} + \|u_t\|_{H^2(H^3(\Omega_i))}\right)\Big). \quad \square\end{aligned}$$

Remark 4.3.1. *Recently, linear immersed finite element method for second order wave equation in inhomogeneous media has been discussed in [5] with homogeneous jump conditions. The authors have established optimal order $O(h^2 + \tau^2)$ error estimate for the fully discrete scheme under the assumption that $u_{tttt} \in L^\infty(H^2(\Omega_1) \cap H^2(\Omega_2))$ or equivalently $u_{tt} \in L^\infty(H^4(\Omega_1) \cap H^4(\Omega_2))$ (see, Theorem 4.1 therein). In the previous result, for linear elements, we have derived same optimal order error estimate assuming $u_{tt} \in H^1(H^3(\Omega_1) \cap H^3(\Omega_2))$.*

4.4 Numerical Results

In this section, we will explore the performance of proposed weak Galerkin method in solving second order wave equation with discontinuous coefficients. We present some numerical illustrations to validate the theoretical findings reported in the previous section. Here, our main significance is to numerically analyze the standard L^2 norm convergence, which is obtained in the Theorem 4.3.1. To demonstrate the flexibility and efficiency of the method, different forms of interfaces along with a large scale of variation in the physical coefficients are considered. All the numerical computations are done in the time interval $J = (0, 1]$.

Let U_h^n be the weak Galerkin solution defined by (4.3.12). Then, we have calculated the following error

$$e_h := Q_h u(t_n) - U_h^n$$

at final time $t_n = T$ with respect to L^2-norm.

The experimental order of convergence (EOC) for a given finite sequence of successive runs (indexed by i)) is computed by

$$\mathrm{EOC}(e(i)) = \frac{\log(e(i+1)/e(i))}{\log(h(i+1)/h(i))},$$

where $e(i)$ is the error corresponding to the L^2 norm and $h(i)$ is the mesh size of the run i.

Table 4.4.1: The history of L^2 error convergence with time step $\tau = h$

	Example 4.4.1		Example 4.4.2	
h	$\|e_h\|$	EOC	$\|e_h\|$	EOC
1/2	5.725347e-01	-	2.635670e-01	-
1/4	2.674987e-01	1.09	7.841587e-02	1.74
1/8	8.489914e-02	1.65	1.890224e-02	2.05
1/16	2.283136e-02	1.89	4.992931e-03	1.92
1/32	5.818861e-03	1.97	1.23735e-03	2.01
1/64	1.461836e-03	1.99	3.017352e-04	2.03

Example 4.4.1. We have considered a line interface as $x = 1$ in the computational domain $\Omega = (0, 2) \times (0, 1)$, which is being considered in this numerical example. The exact solution is selected as

$$u(x, y, t) = \begin{cases} t^2 \sin(\pi x) \sin(\pi y) & \text{if } x \leq 1, \\ -t^2 \sin(2\pi x) \sin(2\pi y) & \text{if } x > 1. \end{cases}$$

The source function f, interface functions (ψ, ϕ) and the initial data $(u(0), v(0))$ that appear in (4.1.1)-(4.1.3) are determined from the choice of u with following physical coefficients

$$\beta = \begin{cases} 1 \text{ if } x \leq 1, \\ \frac{1}{2} \text{ otherwise.} \end{cases}$$

In this example, we have used rectangular mesh with line interface. We have reported errors in L^2 norm and the order of accuracy for linear WG space at time $t = 1$ for

different values of h in Table 4.4.1 (left). The time step is intentionally selected as $\tau = h$.

Example 4.4.2. In our second numerical example, we have considered a line interface given by $y = 1/2$ in the computational domain $\Omega = (0,1) \times (0,1)$. The true solution is given by

$$u(x,y,t) = \begin{cases} t^2 \exp(-t)\sin(\pi x)\sin(2\pi y) & \text{if } y \leq 1/2, \\ t\sin(t)\sin(\pi x)\sin(2\pi y) & \text{if } y > 1/2, \end{cases}$$

with the diffusion coefficient

$$\beta = \begin{cases} 2 \text{ if } y \leq 1/2, \\ 5 \quad \text{otherwise.} \end{cases}$$

The order of convergence in L^2 norm at the final time $t = 1$ is evaluated for linear WG space $(\mathcal{P}_1(K),\ \mathcal{P}_0(\partial K),\ \left[\mathcal{P}_0(K)\right]^2)$ on uniform triangular meshes, which is reported in Table 4.4.1 (right) for time step $\tau = h$.

Example 4.4.3. This example is concerned with the higher order WG methods for the interface problem (4.1.1)-(4.1.3). Here, we have considered a square interface. Let $\Omega = (-1,1)^2$ with $\Omega_1 = [-0.5, 0.5]^2$ and $\Omega_2 = \Omega \setminus \Omega_1$, as shown in Figure 4.1. We select the data appearing in (4.1.1)-(4.1.3) setting the exact solution as

$$u(x,y,t) = \begin{cases} t^2(x^2 - \frac{1}{4})(y^2 - \frac{1}{4}) & \text{in } \Omega_1, \\ t^2 \exp(-t)\sin(\pi x)\sin(2\pi y) & \text{in } \Omega_2 \end{cases}$$

with following set of diffusion coefficient

$$\beta = \begin{cases} 3.02 \text{ in } \Omega_1, \\ 4.06 \quad \text{in } \Omega_2. \end{cases}$$

Here, we have observed that the proposed WG-FEM scheme still achieved the optimal rate of convergence in L^2 norm at the final time $t = 1$ for the WG space of the form $(\mathcal{P}_2(K),\ \mathcal{P}_1(\partial K),\ \left[\mathcal{P}_1(K)\right]^2)$ on triangular meshes as depicted in Table 4.4.2 (left). We have selected the time step as $\tau = h^2$. Table 4.4.2 (left) clearly demonstrates the $\mathrm{O}(h^3)$ in L^2 norm.

Table 4.4.2: The history of L^2 error convergence

	Example 4.4.3		Example 4.4.4	
h	$\|e_h\|$	EOC	$\|e_h\|$	EOC
1/8	3.52536e-01	-	8.93151e-01	-
1/16	4.76792e-02	2.88	4.32018e-01	1.04
1/32	9.00415e-03	2.40	8.94715e-02	2.27
1/64	1.37947e-03	2.70	1.98659e-02	2.17
1/128	1.90361e-04	2.85	4.99063e-03	1.99
1/256	2.58287e-005	2.93	1.26788e-03	1.97

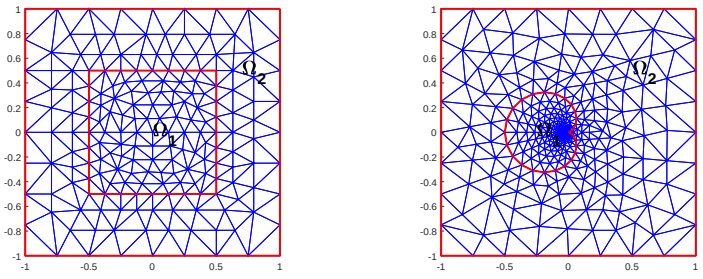

Figure 4.1: Triangulation of Ω (left) in Example 4.4.3 and a curved interface Γ (right) in Example 4.4.4.

Example 4.4.4. Here, we are considering a curved interface Γ in the given domain $\Omega = (-1,1)\times(-1,1)$ to examine the ability of the WG method to accommodate complex geometries. The interface and sub-domains are illustrated in the Figure 4.1 and its

parametric form is given as

$$\begin{cases} x(\theta) = a\cos\theta(1-\cos\theta), \\ y(\theta) = a\sin\theta(1-\cos\theta), \end{cases}$$

for $\theta \in [0, 2\pi]$. Here we have chosen $a = 0.25$.

We select the data in (4.1.1)-(4.1.3) such that the exact solution u is given by

$$u(x,y,t) = \begin{cases} t^2\exp(-t)\Big((x^2+y^2+ax)^2 - a^2(x^2+y^2)\Big) & \text{in } \Omega_1, \\ \sin(t\pi/4)\sin(\pi x)\sin(2\pi y)\Big((x^2+y^2+ax)^2 - a^2(x^2+y^2)\Big) & \text{in } \Omega_2, \end{cases}$$

along with the diffusion coefficient

$$\beta = \begin{cases} 10^{-1} \text{ in } \Omega_1, \\ 10^{-4} \text{ in } \Omega_2. \end{cases}$$

We have achieved optimal rate of convergence in L^2 norm at the final time $t = 1$ evaluated on linear WG space for uniform triangular meshes described in Table 4.4.2 (right) with time step $\tau = h$.

Example 4.4.5. We consider following initial boundary value problem

$$\begin{cases} \gamma u_{tt} - \nabla\cdot(\beta\nabla u) = f \text{ in } \Omega\times J, \\ u(x,0) = u(0), \quad u_t(x,0) = v(0) \text{ in } \Omega, \\ u(x,t) = 0 \quad \text{on } \partial\Omega\times J, \end{cases}$$

where $\Omega = (-1,1)\times(-1,1)$ with interface Γ as a circle centered at $(0,0)$ with radius 0.5, as shown in Figure 4.2 (top right). We set the exact solution u as

$$u(x,y,t) = \begin{cases} (r_0^2 - r^2)\sin t\exp(-t) & \text{if } r \le r_0, \\ (r_0^2 - r^2)t^2\sin(\pi x)\sin(\pi y) & \text{if } r > r_0, \end{cases}$$

where $r^2 = x^2 + y^2$ and $r_0 = 0.5$. Then, we select the interface functions and the data appearing in the above problem from the choice of u with the following physical coefficients

$$(\gamma,\ \beta) = (K^{-1},\ \rho^{-1}) = \begin{cases} \big(1, 1500\big) \text{ if } r \le r_0, \\ \big(10, 3000\big) \text{ if } r > r_0. \end{cases}$$

Here, K represents the bulk modulus and ρ the density. In this numerical example, physical coefficients (γ, β) are borrowed from Xu *et al.* [150, 151]. A large variation in the coefficients is a common occurrence in study of acoustic wave propagation through heterogeneous media in geophysical prospecting [18, 79]. Errors in L^2 norm and the convergence rate at time $t = 1$ for different values of h are listed in Table 4.4.3 (left). The time step is consciously taken as $\tau = h$. It is clear from the Table 4.4.3 (left) that we have achieved optimal order of convergence in L^2 norm which consolidates our theoretical findings. Figure 4.2 (top left) clearly demonstrates the second order of convergence in L^2 norm.

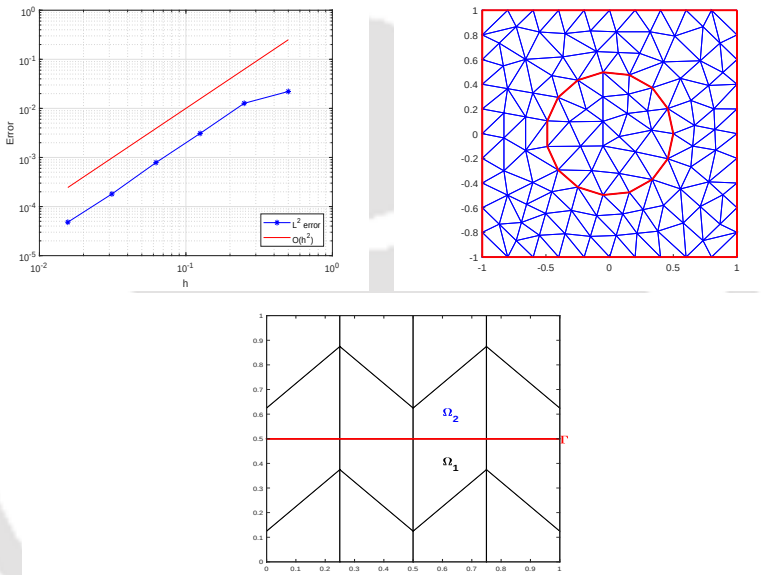

Figure 4.2: Log-log plot of the L^2 error versus the mesh size at time $t = 1$ (top left) along with the triangulation of Ω (top right) in Example 4.4.5, and polygonal mesh with $h = 1/4$ (bottom) in Example 4.4.6.

Example 4.4.6. In our last numerical example, we have considered a polygonal mesh with a line interface given by $y = 1/2$ in the computational domain $\Omega = (0, 1) \times (0, 1)$. A typical polygonal mesh is depicted in Figure 4.2 (bottom), where given domain Ω consists of two sub-domains Ω_1 and Ω_2 with line interface Γ. Necessary data appearing in equations (4.1.1)-(4.1.3) are selected from the following exact solution

$$u(x, y, t) = \begin{cases} t^2 \sin(2\pi t)(x^2 - 1/4)(y^2 - 1/4) & \text{if } y \leq 1/2, \\ \exp(-t)\cos(t^2)\sin(\pi x)\sin(2\pi y) & \text{if } y > 1/2, \end{cases}$$

Table 4.4.3: The history of L^2 error convergence with time step $\tau = h$

	Example 4.4.5		Example 4.4.6	
h	$\|e_h\|$	EOC	$\|e_h\|$	EOC
1/2	2.208641e-02	-	3.863172e-01	-
1/4	1.269432e-02	0.79	1.711643e-01	1.17
1/8	3.087225e-03	2.03	3.87092e-02	2.14
1/16	7.871982e-04	1.97	9.331984e-03	2.05
1/32	1.804471e-04	2.12	2.257593e-03	2.04
1/64	4.803721e-05	1.90	5.270162e-04	2.09

and the diffusion coefficient

$$\beta = \begin{cases} 1 \text{ if } y \leq 1/2, \\ 10^{-2} \text{ otherwise.} \end{cases}$$

We have evaluated the rate of convergence in L^2 norm at the final time $t = 1$ for linear WG space $(\mathcal{P}_1(K),\ \mathcal{P}_0(\partial K),\ \left[\mathcal{P}_0(K)\right]^2)$, which is reported in Table 4.4.3 (right) for $\tau = h$.

5

WG-FEMs for Electric Interface Problem with Non-homogeneous Jump Conditions

In this chapter, we study a priori error estimates for the spatially semidiscrete scheme for the electric interface problem (1.1.7)-(1.1.9). Optimal order of convergence for $L^\infty(L^2)$ and $L^\infty(H^1)$ norms are established when the global regularity of the solution is low on the entire domain. We have also established some a priori estimates for the semidiscrete solution which are very crucial to prove optimal convergence rate of the fully discrete solution. The fully discrete scheme is based on first order in time backward Euler discretization.

5.1 Introduction

To begin with, let us first recall the electric interface interface problem of the form

$$-\nabla \cdot \big(\epsilon \nabla u' + \sigma \nabla u\big) = f \ \text{ in } \Omega \times (0,T],\ T < \infty, \tag{5.1.1}$$

with initial and boundary conditions

$$u(x,0) = u_0 \ \text{ in } \Omega; \ \ u(x,t) = 0 \quad \text{on } \partial\Omega \times (0,T] \tag{5.1.2}$$

and jump conditions on the interface

$$[u] = \Phi, \ \ \Big[\epsilon \frac{\partial u'}{\partial \mathbf{n}} + \sigma \frac{\partial u}{\partial \mathbf{n}}\Big] = \Psi \quad \text{along } \Gamma \times (0,T], \tag{5.1.3}$$

where Ω is a convex polygonal domain in $\mathbb{R}^2$ with boundary $\partial\Omega$ and $\Omega_1 \subset \Omega$ is an open domain with Lipschitz boundary $\Gamma = \partial\Omega_1$ and $\Omega_2 = \Omega \backslash \Omega_1$. Other symbols are as defined

Published online in *Numer. Methods Partial Differential Equations 36 (2020), no. 4, 734-755.*

in Chapter 1. We assume that the physical coefficients are discontinuous along interface Γ and piecewise positive constant. We write

$$(\sigma, \epsilon) = \begin{cases} (\sigma_1, \epsilon_1) & \text{in } \Omega_1, \\ (\sigma_2, \epsilon_2) & \text{in } \Omega_2. \end{cases}$$

Several electrical models have been developed for biological cells exposed to an external electric field to obtain the distribution of the transmembrane voltage in [124]. The value and the spatial distribution of the transmembrane voltage are of significant interest in the electroporation of the cell membrane. Once the required voltage of electroporation is achieved the lipid bilayer molecules of the membrane rearrange themselves and form pores in the membrane through which ions and impermeable molecules can pass and enter the cytoplasm [148]. Electroporation is gaining increased importance because of its clinical applications in gene therapy and drug delivery as a method to introduce new DNA and drugs into a cell in order to change its function [12]. Numerical solutions of electric interface model (5.1.1)-(5.1.3) draw significant attention in a variety of fields such as neural activation during deep brain simulations [25, 67], debacterization of liquids, food processing [153], biofouling prevention [125], selective spectroscopic imaging of the electrical properties of biological media [10]. One of the first finite element methods treating electric interface problem has been studied by Ammari *et al.* in [9]. Well-posedness of the model interface problem and the regularity of its solutions have been established. A fully discrete finite element scheme based on backward Euler discretization has been proposed for the numerical approximation of the potential distribution. Optimal convergence order in both $L^2(H^1)$ and $L^2(L^2)$ norms have been obtained with homogeneous jump conditions. In [9], authors have used fitted finite element discretization. More recently, $L^\infty(H^1)$-norm and $L^\infty(L^2)$-norm error estimates are derived in [48] assuming solutions are continuous along interface. As far as we know, the other classes of finite element methods which are developed for interface problems yet to be discussed for the electric interface model. In this work, we consider an electric interface model with non-homogeneous jump conditions and solve it numerically using recently developed weak Galerkin finite element method. In this article, we extend the work of [112] to the electric interface model (5.1.1)-(5.1.3). Typical semidiscrete and fully discrete schemes are presented. The fully discrete space-time finite element discretizations are based on the backward Euler approximations. Optimal a priori error estimates for both semidiscrete and fully discrete schemes are proved in $L^\infty(H^1)$ and $L^\infty(L^2)$ norms. Finally, numerical results are reported to confirm our theoretical convergence rate. The present work not only discusses the electric interface model with

non-homogeneous jump conditions but also confirm the optimal point-wise-in time error estimates with respect to L^2 and H^1 norms.

The rest of the chapter is organized as follows. In Sect. 5.2, we review the definitions of weak gradient and its discrete analogs in suitable polynomial spaces. Sec. 5.3 is devoted to the convergence analysis of semidiscrete WG-FEM algorithm. In Sec. 5.4, a backward Euler scheme is described along with a priori error bounds in $L^\infty(H^1)$ and $L^\infty(L^2)$ norms. Sec. 5.5 focuses on some numerical examples.

5.2 Preliminaries

In this section, we shall describe the weak Galerkin finite element discretization for the problem (5.1.1)-(5.1.3) and review the definition of the weak gradient operator for our convenience.

Let $\mathcal{T}_h = \mathcal{T}_1 \cup \mathcal{T}_2$ be the fitted finite element discretization of Ω as described in Chapter 1. Based on the discretization $\mathcal{T}_h$, for $k \geq 1$, we define following weak Galerkin finite element space

$$V_h = \{v_h = \{v_0, v_b\} : \ v_h|_K \in \mathcal{V}(k,k,K), \ [v_h]_e = 0, \ \forall e \in \mathcal{E}_h^0, \ K \in \mathcal{T}_h\}. \tag{5.2.1}$$

Here, $[v_h]_e = [v_b]$ denotes the jump of $v_h \in \mathcal{V} = \prod_{K\in\mathcal{T}_h} \mathcal{V}(k,k,K)$ across an interior edge $e \in \mathcal{E}_h^0$ and $\mathcal{V}(k,k,K)$ is the local weak Galerkin space as defined in (1.4.7). Denote by V_h^0 the subspace of V_h consisting of all finite element functions with vanishing boundary value

$$V_h^0 = \{v_h = \{v_0, v_b\} \in V_h : v_b|_{\partial\Omega} = 0\}. \tag{5.2.2}$$

For each $v_h = \{v_0, v_b\} \in V_h$, we recall its discrete weak gradient $(\nabla_w v_h) \in [\mathcal{P}_{k-1}(K)]^2$ that satisfies the following equation

$$(\nabla_w v_h, \varphi)_K = -\int_K v_0(\nabla\cdot\varphi)dK + \int_{\partial K} v_b(\varphi\cdot\eta)ds \ \ \forall\varphi \in [\mathcal{P}_{k-1}(K)]^2, \tag{5.2.3}$$

where η is the outward normal to ∂K.

For each element $K \in \mathcal{T}_h$, denote by Q_0 the usual L^2 projection operator from $L^2(K)$ onto $\mathcal{P}_k(K)$ and by Q_b the L^2 projection from $L^2(e)$ onto $\mathcal{P}_k(e)$ for any $e \in \mathcal{E}_h$. In addition, let $\mathbb{Q}_h$ be an another local L^2 projection from $[L^2(K)]^2$ onto $[\mathcal{P}_{k-1}(K)]^2$.

We recall following crucial approximation properties for local projections Q_h and $\mathbb{Q}_h$. For details, we refer to [144].

Lemma 5.2.1. *Let $\mathcal{T}_h$ be a finite element partition of Ω satisfying the shape regularity*

assumption as specified in [144]. Then, for $u \in H^{k+1}(\Omega_i)$ with $i = 1,\ 2$, we have

$$\sum_{K\in\mathcal{T}_h}\Big(\|u-Q_0u\|_K^2+h_K^2\|\nabla(u-Q_0u)\|_K^2\Big) \ \leq\ Ch^{2(k+1)}\sum_{i=1}^{2}\|u\|_{k+1,\Omega_i}^2,$$

$$\sum_{K\in\mathcal{T}_h}\Big(\|\nabla u-\mathbb{Q}_h(\nabla u)\|_K^2+h_K^2\|\nabla(\nabla u-\mathbb{Q}_h(\nabla u))\|_K^2\Big) \ \leq\ Ch^{2k}\sum_{i=1}^{2}\|u\|_{k+1,\Omega_i}^2. \quad \square$$

Now, for $u_h=\{u_0,u_b\},\ v_h=\{v_0,v_b\}\in V_h$, we introduce following bilinear maps to be used in this chapter

$$a_1(u_h,v_h) := (\sigma(x)\nabla_w u_h,\nabla_w v_h) = \sum_{K\in\mathcal{T}_h}\big(\sigma(x)\nabla_w u_h,\nabla_w v_h\big)_K,$$

$$a_2(u_h,v_h) := (\epsilon(x)\nabla_w u_h,\nabla_w v_h) = \sum_{K\in\mathcal{T}_h}\big(\epsilon(x)\nabla_w u_h,\nabla_w v_h\big)_K,$$

$$s(u_h,v_h) := \sum_{K\in\mathcal{T}_h} h^{-1}\langle u_0-u_b,v_0-v_b\rangle_{\partial K} \ \ \&\ \ \langle\Psi,v_b\rangle_{\Gamma_h} := \sum_{e\in\Gamma_h}\langle\Psi,v_b\rangle_e.$$

Further, we define following bilinear forms

$$\langle\Phi,\sigma(x)\nabla_w v_h\cdot\mathbf{n}\rangle_{\Gamma_h} = \sum_{K\in\mathcal{T}_2}\langle\Phi,\sigma_2\nabla_w v_h\cdot\mathbf{n}\rangle_{\partial K\cap\Gamma_h},$$

$$\langle\Phi,\epsilon(x)\nabla_w v_h\cdot\mathbf{n}\rangle_{\Gamma_h} = \sum_{K\in\mathcal{T}_2}\langle\Phi,\epsilon_2\nabla_w v_h\cdot\mathbf{n}\rangle_{\partial K\cap\Gamma_h},$$

$$h^{-1}\langle\Phi,v_0-v_b\rangle_{\Gamma_h} = \sum_{K\in\mathcal{T}_2}h^{-1}\langle\Phi,v_0-v_b\rangle_{\partial K\cap\Gamma_h} = \sum_{e\in\Gamma_h}h^{-1}\langle\Phi,v_0|_{K_2}-v_b\rangle_e.$$

Here, $\langle\cdot,\cdot\rangle_e$ denotes the L^2 inner product on $e\in\mathcal{E}_h$ and we write

$$\langle\cdot,\cdot\rangle_{\partial K} = \sum_{e\in\partial K}\langle\cdot,\cdot\rangle_e.$$

To deal with the interface problem, we introduce a Banach space

$$\mathcal{Y} = \{u\in H_0^1(\Omega):\ u|_{\Omega_i}\in H^2(\Omega_i),\ i=1,\ 2\}$$

with the norm

$$\|u\|_{\mathcal{Y}} = \|u\|_{H^1(\Omega)}+\|u\|_{H^2(\Omega_1)}+\|u\|_{H^2(\Omega_2)}.$$

5.3 Semidiscrete Scheme

This section deals with the error analysis for the spatially discrete scheme. Optimal order of convergence in both $L^\infty(L^2)$ and $L^\infty(H^1)$ norms are established.

The continuous-time weak Galerkin finite element approximation to (5.1.1)-(5.1.3) is stated as follows: Find $u_h : [0,T] \to V_h^0$ such that

$$\begin{aligned} a(u_h, v_h) + b(u_h', v_h) &= (f, v_0) + \langle \Psi, v_b\rangle_{\Gamma_h} + \langle \Phi, \sigma\nabla_w v_h \cdot \mathbf{n}\rangle_{\Gamma_h} + \langle \Phi', \epsilon\nabla_w v_h \cdot \mathbf{n}\rangle_{\Gamma_h} \\ &\quad -h^{-1}\langle \Phi + \Phi', v_0 - v_b\rangle_{\Gamma_h} \quad \forall v_h = \{v_0, v_b\} \in V_h^0 \end{aligned} \tag{5.3.1}$$

and $u_h(0) = Q_h u(0) = (Q_0 u(0), Q_b u(0))$. Bilinear maps $a(\cdot,\cdot)$ and $b(\cdot,\cdot)$ on V_h^0 are given by

$$a(u_h, v_h) = a_1(u_h, v_h) + s(u_h, v_h),$$

$$b(u_h, v_h) = a_2(u_h, v_h) + s(u_h, v_h).$$

Recall that a time dependent weak function $v_h : [0,T] \to V_h^0$ is written as $v_h(t) := \{v_0(t), v_b(t)\}$ and subsequently $v_h'(t) := \{v_0'(t), v_b'(t)\}$. For simplicity, we use $v_h = \{v_0, v_b\}$ for $v_h(t)$ and $v_h' = \{v_0', v_b'\}$ for $v_h'(t)$. With above notations and from the definition of weak gradient (5.2.3), it is easy to note that $(\nabla_w v_h)' = \nabla_w v_h'$ and $(\nabla_w v_h)|_{t=0} = \nabla_w v_h(0)$ for all $v_h \in V_h$.

Well-posedness of the scheme (5.3.1) can be verified from the fact that finite element space V_h^0 is a normed linear space with respect to the triple norm

$$|||v_h||| := \Big[(\nabla_w v_h, \nabla_w v_h) + s(v_h, v_h)\Big]^{\frac{1}{2}}, \quad v_h \in V_h^0.$$

It is easy to see that $|||\cdot|||$ is equivalent to the norms $|||\cdot|||_1$ and $|||\cdot|||_2$ associated with the bilinear maps $a(\cdot,\cdot)$ and $b(\cdot,\cdot)$, respectively.

Remark 5.3.1. *We define following energy norm*

$$|||\xi(t)|||_E^2 = \frac{1}{2}a(\xi(t),\xi(t)) + \frac{1}{2}b(\xi(t),\xi(t)) + \int_0^t \{a(\xi,\xi) + b(\xi',\xi')\}ds, \quad \xi \in V_h^0.$$

In the absence of source function and jump functions, for $v_h = u_h'$, we obtain

$$\frac{1}{2}a(u_h(t), u_h(t)) + \int_0^t b(u_h', u_h')ds = \frac{1}{2}a(u_h(0), u_h(0)). \tag{5.3.2}$$

Similarly we derive

$$\int_0^t a(u_h, u_h)ds + \frac{1}{2}b(u_h(t), u_h(t)) = \frac{1}{2}b(u_h(0), u_h(0)). \tag{5.3.3}$$

Adding equations (5.3.2) and (5.3.3), we have

$$|||u_h(t)|||_E^2 = |||u_h(0)|||_E^2 \quad \forall t \in (0,T]. \quad \square$$

Remark 5.3.2. *A simple application of trace inequality (1.4.17) and discrete weak gradient (5.2.3), it is easy to verify that the triple bar norm is equivalent to following discrete H^1- norm*

$$\|v_h\|_{1,h} = \Big(\sum_{K\in\mathcal{T}_h} (\|\nabla v_0\|_K^2 + h_K^{-1}\|v_0 - v_b\|_{\partial K}^2)\Big)^{\frac{1}{2}},\ v_h = \{v_0, v_b\} \in V_h^0. \tag{5.3.4}$$

Thus, for the projection operator $Q_h : H^1(K) \to V_h^0$ on each element $K \in \mathcal{T}_h$ defined by $Q_h v = \{Q_0 v, Q_b v\}$, we have

$$\begin{aligned}
|||Q_h v|||^2 &\leq C \sum_{K\in\mathcal{T}_h} (\|\nabla Q_0 v\|_K^2 + h_K^{-1}\|Q_0 v - Q_b v\|_{\partial K}^2) \\
&\leq C \sum_{K\in\mathcal{T}_h} (\|\nabla Q_0 v\|_K^2 + h_K^{-1}\|Q_0 v - v\|_{\partial K}^2) \\
&\leq C \sum_{K\in\mathcal{T}_h} (\|\nabla Q_0 v\|_K^2 + h_K^{-2}\|Q_0 v - v\|_K^2 + \|\nabla(Q_0 v - v)\|_K^2) \\
&\leq C \sum_{i=1}^{2} \|v\|_{H^2(\Omega_i)} \quad \forall v \in \mathcal{Y}.
\end{aligned}$$

Here, we have used the fact that $\|Q_0 u - Q_b u\|_{\partial K} \leq \|Q_0 u - u\|_{\partial K}$ and standard approximation properties of L^2 projection. □

Moreover, the following Poincaŕe-type inequality holds true (see, Lemma 7.1 in [109])

$$\|v_0\| \leq C|||v_h|||,\ v_h = \{v_0, v_b\} \in V_h^0. \tag{5.3.5}$$

Next, we recall the definition for $Q_h u = \{Q_0 u, Q_b u\} \in V_h$. To ensure $Q_h u \in V_h$, *i. e.* $Q_b u$ takes single value on any $e \in \mathcal{E}_h$, we define $Q_b u$ in the following way

$$Q_b u = \begin{cases} Q_b(u|_{K\cap e}) & \text{if} \quad e \subseteq \Gamma\ \&\ K \subset \Omega_1, \\ Q_b(u|_{K\cap e}) + Q_b\Phi & \text{if} \quad e \subseteq \Gamma\ \&\ K \subset \Omega_2, \\ Q_b(u|_{K\cap e}) & \text{if} \quad e \nsubseteq \Gamma\ \&\ K \in \mathcal{T}_h. \end{cases} \tag{5.3.6}$$

Then we have the following lemma connecting Q_h and $\mathbb{Q}_h$ operators ([112]). We omit the details.

Lemma 5.3.1. *Let Q_h and $\mathbb{Q}_h$ be the L^2 projection operators as defined. Then, on each element $K \in \mathcal{T}_h$ and for any $\tau \in [\mathcal{P}_{k-1}(K)]^2$, we have*

$$(\nabla_w(Q_h u), \tau)_K = (\mathbb{Q}(\nabla u), \tau)_K + \langle \Phi, \tau\cdot\mathbf{n}\rangle_{\partial K\cap\Gamma},\ K \in \mathcal{T}_2, \tag{5.3.7}$$

$$(\nabla_w(Q_h u), \tau)_K = (\mathbb{Q}(\nabla u), \tau)_K,\ K \in \mathcal{T}_1, \tag{5.3.8}$$

where $\mathcal{T}_1$ and $\mathcal{T}_2$ are as defined in (1.4.4). □

It is easy to observe from the definition of local L^2 projection and definition (5.3.6) that

$$(Q_b u)' = \begin{cases} Q_b(u'|_{K\cap e}) & \text{if} \quad e \subseteq \Gamma \ \& \ K \subset \Omega_1, \\ Q_b(u'|_{K\cap e}) + Q_b\Phi' & \text{if} \quad e \subseteq \Gamma \ \& \ K \subset \Omega_2, \\ Q_b(u'|_{K\cap e}) & \text{if} \quad e \nsubseteq \Gamma \ \& \ K \in \mathcal{T}_h \end{cases} \tag{5.3.9}$$

and hence $(Q_h u)' = \{(Q_0 u)', (Q_b u)'\} = \{Q_0 u', (Q_b u)'\} \in V_h$ in which $(Q_b u)'$ is given by the relation (5.3.9).

Remark 5.3.3. *Using the relation (5.3.9), on each element $K \in \mathcal{T}_h$ and for any $\tau \in [\mathcal{P}_{k-1}(K)]^2$, we have*

$$\begin{aligned} (\nabla_w(Q_h u'), \tau)_K &= (\mathbb{Q}(\nabla u'), \tau)_K + \langle \Phi', \tau \cdot \mathbf{n}\rangle_{\partial K\cap\Gamma}, \ K \in \mathcal{T}_2, \\ (\nabla_w(Q_h u'), \tau)_K &= (\mathbb{Q}(\nabla u'), \tau)_K, \ K \in \mathcal{T}_1. \ \square \end{aligned}$$

Now, we define $Q_h u' := \{Q_0 u', Q_b u'\}$ with

$$Q_b u' = \begin{cases} Q_b(u'|_{K\cap e}) & \text{if} \quad e \subseteq \Gamma \ \& \ K \subset \Omega_1, \\ Q_b(u'|_{K\cap e}) + Q_b\Phi' & \text{if} \quad e \subseteq \Gamma \ \& \ K \subset \Omega_2, \\ Q_b(u'|_{K\cap e}) & \text{if} \quad e \nsubseteq \Gamma \ \& \ K \in \mathcal{T}_h, \end{cases} \tag{5.3.10}$$

so that $Q_h u' = \{Q_0 u', Q_b u'\} \in V_h$ and $Q_h u' = (Q_h u)'$.

Remark 5.3.4. *Let $u \in H^1(J; \mathcal{Y})$ be the solution to the problem (5.1.1)-(5.1.3). Then it follows from the definition of bilinear map $s(\cdot,\cdot)$ that*

$$\begin{aligned} s(Q_h u, v_h) &= \sum_{K\in\mathcal{T}_h} h^{-1}\langle Q_0 u - Q_b u, v_0 - v_b\rangle_{\partial K} \\ &= \sum_{K\in\mathcal{T}_1} h^{-1}\langle Q_0 u - Q_b u, v_0 - v_b\rangle_{\partial K} \\ &\quad + \sum_{K\in\mathcal{T}_2} h^{-1}\langle Q_0 u - Q_b u, v_0 - v_b\rangle_{\partial K\setminus\Gamma_h} \\ &\quad + \sum_{e\in\Gamma_h} h^{-1}\langle Q_0 u - Q_b u, v_0 - v_b\rangle_e \\ &= \sum_{K\in\mathcal{T}_h} h^{-1}\langle Q_0 u - Q_b(u|_{\partial K}), v_0 - v_b\rangle_{\partial K} - h^{-1}\langle \Phi, v_0 - v_b\rangle_{\Gamma_h}. \end{aligned}$$

Similar arguments and definition (5.3.10) leads to

$$\begin{aligned} s((Q_h u)', v_h) = s(Q_h u', v_h) &= \sum_{K\in\mathcal{T}_h} h^{-1}\langle Q_0 u' - Q_b(u'|_{\partial K}), v_0 - v_b\rangle_{\partial K} \\ &\quad - h^{-1}\langle \Phi', v_0 - v_b\rangle_{\Gamma_h}. \ \square \end{aligned}$$

Below, we shall prove the following stability result for the solution u_h satisfying (5.3.1)

Lemma 5.3.2. *Assume $u_h \in V_h^0$ satisfies (5.3.1). Then, for f, $\Psi \in L^2(J; L^2(\Omega))$ and $\Phi \in H^1(J; H^2(\Gamma))$, we have*

$$|||u_h(t)|||^2 \leq |||Q_h u(0)|||^2 + C\int_0^t (\|f\|^2 + \|\psi\|^2_{L^2(\Gamma)} + \|\Phi\|^2_{H^2(\Gamma)} + \|\Phi'\|^2_{H^2(\Gamma)})ds.$$

Proof. Putting $v_h = u_h = \{u_0, u_b\}$ in (5.3.1), we obtain

$$a(u_h, u_h) + b(u_h', u_h) = (f, u_0) + \langle \Psi, u_b\rangle_{\Gamma_h} + \langle \Phi, \sigma\nabla_w u_h \cdot \mathbf{n}\rangle_{\Gamma_h} + \langle \Phi', \epsilon\nabla_w u_h \cdot \mathbf{n}\rangle_{\mathbf{\Gamma_h}} - h^{-1}\langle \Phi + \Phi', u_0 - u_b\rangle_{\Gamma_h}.$$

Now, integrate with respect to t from 0 to t to have

$$\begin{aligned}
&\int_0^t |||u_h|||_1^2 ds + \frac{1}{2}|||u_h(t)|||_2^2 - \frac{1}{2}|||u_h(0)|||_2^2 \\
&\leq \int_0^t \|f\|\|u_0\|ds + \int_0^t \|\Psi\|_{\Gamma_h}\|u_0 - u_b\|_{\Gamma_h}ds + \int_0^t \|\Psi\|_{\Gamma_h}\|u_0\|_{\Gamma_h}ds \\
&\quad + C\int_0^t \|\Phi\|_{\Gamma_h}\|\nabla_w u_h \cdot \mathbf{n}\|_{\Gamma_h}ds + C\int_0^t \|\Phi'\|_{\Gamma_h}\|\nabla_w u_h \cdot \mathbf{n}\|_{\Gamma_h}ds \\
&\quad + C\int_0^t h^{-1}\|\Phi + \Phi'\|_{\Gamma_h}\|u_0 - u_b\|_{\Gamma_h}ds. \qquad (5.3.11)
\end{aligned}$$

From (5.3.5), we observe that

$$\int_0^t \|f\|\|u_0\|ds \leq \int_0^t \|f\|\|u_h\|ds \leq \Big(\int_0^t \|f\|^2 ds\Big)^{\frac{1}{2}}\Big(\int_0^t |||u_h|||^2 ds\Big)^{\frac{1}{2}}. \qquad (5.3.12)$$

Similarly, we obtain

$$\begin{aligned}
\int_0^t \|\Psi\|_{\Gamma_h}\|u_0 - u_b\|_{\Gamma_h}ds &\leq \Big(\int_0^t h\|\Psi\|^2_{\Gamma_h}ds\Big)^{\frac{1}{2}}\left(\int_0^t \sum_{K\in\mathcal{T}_h} h^{-1}\|u_0 - u_b\|^2_{\partial K}ds\right)^{\frac{1}{2}} \\
&\leq C\|\Psi\|_{L^2(0,t;L^2(\Gamma))}\|u_h\|_{L^2(0,t;|||\cdot|||)}. \qquad (5.3.13) \\
\int_0^t \|\Psi\|_{\Gamma_h}\|u_0\|_{\Gamma_h}ds &\leq C\Big(\int_0^t \|\Psi\|^2_{\Gamma_h}ds\Big)^{\frac{1}{2}}\left(\int_0^t \sum_{K\in\mathcal{T}_h} \|u_0\|^2_{1,K}ds\right)^{\frac{1}{2}} \\
&\leq C\|\Psi\|_{L^2(0,t;L^2(\Gamma))}\Big(\int_0^t \sum_{K\in\mathcal{T}_h} (\|u_0\|^2_K + \|\nabla u_0\|^2_K)ds\Big)^{\frac{1}{2}} \\
&\leq C\|\Psi\|_{L^2(0,t;L^2(\Gamma))}\Big(\int_0^t (|||u_h|||^2 + \|u_h\|^2_{1,h})ds\Big)^{\frac{1}{2}} \\
&\leq C\|\Psi\|_{L^2(0,t;L^2(\Gamma))}\|u_h\|_{L^2(0,t;|||\cdot|||)}. \qquad (5.3.14)
\end{aligned}$$

Here, we have used (5.3.5) and Remark 5.3.2. For $\Phi \in L^2(J; H^2(\Gamma))$, we note that

$$\begin{aligned}
&\int_0^t \|\Phi\|_{\Gamma_h}\|\nabla_w u_h \cdot \mathbf{n}\|_{\Gamma_h} ds \\
&\leq \left(\int_0^t \sum_{e\in\Gamma_h} \frac{1}{h_e}\|\Phi\|_e^2 ds\right)^{\frac{1}{2}} \left(\int_0^t \sum_{e\in\Gamma_h} h_e\|\nabla_w u_h \cdot \mathbf{n}\|_e^2 ds\right)^{\frac{1}{2}} \\
&\leq C\left(\int_0^t \sum_{e\in\Gamma_h} h_e^{-1}\mathrm{meas}(e)\|\Phi\|_{L^\infty(e)}^2 ds\right)^{\frac{1}{2}} \left(\int_0^t \sum_{K\in\mathcal{T}_h} h_K\|\nabla_w u_h \cdot \mathbf{n}\|_{\partial K}^2 ds\right)^{\frac{1}{2}} \\
&\leq C\left(\int_0^t \|\Phi\|_{H^2(\Gamma)}^2 ds\right)^{\frac{1}{2}} \left(\int_0^t \sum_{K\in\mathcal{T}_h} \|\nabla_w u_h\|_K^2 ds\right)^{\frac{1}{2}} \\
&\leq C\|\Phi\|_{L^2(0,t;H^2(\Gamma))}\|u_h\|_{L^2(0,t;|||\cdot|||)}. \qquad (5.3.15)
\end{aligned}$$

In the derivation of above inequality, we have used the fact that $\mathrm{meas}(e) = \mathrm{O}(h_e)$ and standard inequality $\|\Phi\|_{L^\infty(e)} \leq \|\Phi\|_{H^2(e)}$ along with trance inequality (1.4.17) and inverse inequality (*cf.* Lemma A.6 in [144]).

Arguing as in (5.3.15), we obtain

$$\begin{aligned}
&\int_0^t \|\Phi'\|_{\Gamma_h}\|\nabla_w u_h \cdot \mathbf{n}\|_{\Gamma_h} ds + \int_0^t h^{-1}\|\Phi + \Phi'\|_{\Gamma_h}\|u_0 - u_b\|_{\Gamma_h} ds \\
&\leq C\big(\|\Phi\|_{L^2(0,t;H^2(\Gamma))} + \|\Phi'\|_{L^2(0,t;H^2(\Gamma))}\big)\|u_h\|_{L^2(0,t;|||\cdot|||)}. \qquad (5.3.16)
\end{aligned}$$

Finally, estimates (5.3.11)-(5.3.16) leads to desire inequality. □

Remark 5.3.5. *Setting $v_h = u_h'$ in (5.3.1) and arguing as in Lemma 5.3.2, we derive following stability for u_h satisfying (5.3.1)*

$$|||u_h'(t)|||^2 \leq |||Q_h u(0)|||^2 + C\int_0^t (\|f\|^2 + \|\psi\|_{L^2(\Gamma)}^2 + \|\Phi\|_{H^2(\Gamma)}^2 + \|\Phi'\|_{H^2(\Gamma)}^2) ds. \quad \square$$

For the error analysis, we split our error into two components using an intermediate operator. We write

$$u - u_h = (u - Q_h u) + (Q_h u - u_h).$$

For simplicity, we introduce the following notation

$$e_h := \{e_0, e_b\} = Q_h u - u_h = \{Q_0 u - u_0, Q_b u - u_b\}, \quad u_h = \{u_0, u_b\}. \qquad (5.3.17)$$

As an usual technique, we try to derive some error equation involving e_h which is crucial for our later analysis.

Lemma 5.3.3. *Let e_h be the error as defined in (5.3.17) and $u \in H^1(J;\mathcal{Y})$ be the solution to the problem (5.1.1)-(5.1.3). Then, for any $v_h = \{v_0, v_b\} \in V_h^0$, we have*

$$a(e_h, v_h) + b(e_h', v_h) = l_1(u, v_h) + l_2(u', v_h) + l_3(u, v_h) + l_3(u', v_h), \tag{5.3.18}$$

where bilinear forms $l_1(\cdot,\cdot)$, $l_2(\cdot,\cdot)$ and $l_3(\cdot,\cdot)$ are given by

$$\begin{aligned} l_1(u, v_h) &= \sum_{K\in\mathcal{T}_h} \langle \sigma(\nabla u - \mathbb{Q}_h(\nabla u)) \cdot \eta, v_0 - v_b\rangle_{\partial K}, \\ l_2(u, v_h) &= \sum_{K\in\mathcal{T}_h} \langle \epsilon(\nabla u - \mathbb{Q}_h(\nabla u)) \cdot \eta, v_0 - v_b\rangle_{\partial K}, \\ l_3(u, v_h) &= \sum_{K\in\mathcal{T}_h} h^{-1}\langle Q_0 u - Q_b(u|_{\partial K}), v_0 - v_b\rangle_{\partial K}, \end{aligned}$$

where η is the outward normal to ∂K.

Proof. For any $K \in \mathcal{T}_h$, either $K \subseteq \bar{\Omega}_1$ or $K \subseteq \bar{\Omega}_2$. When K belongs to $\bar{\Omega}_i, i = 1, 2$, we obtain

$$\begin{aligned} -(\nabla \cdot \sigma\nabla u, v_0)_K &= -(\nabla \cdot (\sigma_i \nabla u), v_0)_K \\ &= (\sigma_i \nabla u, \nabla v_0)_K - \langle \sigma_i \nabla u \cdot \eta, v_0\rangle_{\partial K}. \end{aligned}$$

Now, summing over $K \in \mathcal{T}_h$ leads to

$$\begin{aligned} -(\nabla \cdot \sigma\nabla u, v_0) &= \sum_{K\in\mathcal{T}_h} (\sigma\nabla u, \nabla v_0)_K - \sum_{K\in\mathcal{T}_h} \langle \sigma\nabla u \cdot \eta, v_0 - v_b\rangle_{\partial K} \\ &\quad - \sum_{K\in\mathcal{T}_h} \langle \sigma\nabla u \cdot \eta, v_b\rangle_{\partial K}. \end{aligned} \tag{5.3.19}$$

Here, $\sigma\nabla u \cdot \eta = \sigma_i \nabla u \cdot \eta$ on ∂K when K belongs to $\bar{\Omega}_i, i = 1, 2$. It follows from (5.2.3) and the definition of $\mathbb{Q}_h$ operator that

$$\begin{aligned} (\sigma\mathbb{Q}_h(\nabla u), \nabla_w v_h)_K &= -(v_0, \nabla \cdot (\sigma\mathbb{Q}_h\nabla u))_K + \langle v_b, (\sigma\mathbb{Q}_h(\nabla u)) \cdot \eta\rangle_{\partial K} \\ &= (\nabla v_0, \sigma\mathbb{Q}_h\nabla u)_K - \langle v_0 - v_b, (\sigma\mathbb{Q}_h(\nabla u)) \cdot \eta\rangle_{\partial K} \\ &= (\nabla v_0, \sigma\nabla u)_K - \langle v_0 - v_b, (\sigma\mathbb{Q}_h(\nabla u)) \cdot \eta\rangle_{\partial K}. \end{aligned} \tag{5.3.20}$$

Combining (5.3.19) and (5.3.20), we have

$$\begin{aligned} -(\nabla \cdot \sigma\nabla u, v_0) &= \sum_{K\in\mathcal{T}_h} (\sigma\mathbb{Q}_h(\nabla u), \nabla_w v_h)_K - \sum_{K\in\mathcal{T}_h} \langle \sigma\nabla u \cdot \eta, v_b\rangle_{\partial K} \\ &\quad + \sum_{K\in\mathcal{T}_h} \langle v_0 - v_b, \sigma(\mathbb{Q}_h(\nabla u) - \nabla u) \cdot \eta\rangle_{\partial K}. \end{aligned} \tag{5.3.21}$$

In a similar way, we obtain

$$\begin{aligned} -(\nabla\cdot\epsilon\nabla u', v_0) &= \sum_{K\in\mathcal{T}_h}(\epsilon\mathbb{Q}_h(\nabla u'), \nabla_w v_h)_K - \sum_{K\in\mathcal{T}_h}\langle\epsilon\nabla u'\cdot\eta, v_b\rangle_{\partial K} \\ &\quad + \sum_{K\in\mathcal{T}_h}\langle v_0 - v_b, \epsilon(\mathbb{Q}_h(\nabla u') - \nabla u')\cdot\eta\rangle_{\partial K}. \end{aligned} \tag{5.3.22}$$

Now, taking L^2-inner product of

$$-\nabla\cdot(\sigma(x)\nabla u + \epsilon(x)\nabla u') = f$$

with v_0 and using above equations (5.3.21)-(5.3.22), we obtain

$$\begin{aligned} (f, v_0) &= \sum_{K\in\mathcal{T}_h}(\sigma\mathbb{Q}_h(\nabla u), \nabla_w v_h)_K + \sum_{K\in\mathcal{T}_h}(\epsilon\mathbb{Q}_h(\nabla u'), \nabla_w v_h)_K \\ &\quad -\langle\Psi, v_b\rangle_{\Gamma_h} - l_1(u, v_h) - l_2(u', v_h). \end{aligned} \tag{5.3.23}$$

This together with identities (5.3.7)-(5.3.8) and Remark 5.3.3 leads to

$$\begin{aligned} &\sum_{K\in\mathcal{T}_h}(\sigma\nabla_w Q_h u, \nabla_w v_h)_K + \sum_{K\in\mathcal{T}_h}(\epsilon\nabla_w Q_h u', \nabla_w v_h)_K \\ &= (f, v_0) + \langle\Phi, \sigma\nabla_w v_h\cdot\mathbf{n}\rangle_{\Gamma_h} + l_1(u, v_h) + l_2(u', v_h) \\ &\quad +\langle\Phi', \epsilon\nabla_w v_h\cdot\mathbf{n}\rangle_{\Gamma_h} + \langle\Psi, v_b\rangle_{\Gamma_h}. \end{aligned} \tag{5.3.24}$$

Adding $s(Q_h u, v_h)$ and $s((Q_h u)', v_h)$ to both sides of the above equation gives

$$\begin{aligned} a(Q_h u, v_h) + b((Q_h u)', v_h) &= (f, v_0) + \langle\Phi, \sigma\nabla_w v_h\cdot\mathbf{n}\rangle_{\Gamma_h} + \langle\Phi', \epsilon\nabla_w v_h\cdot\mathbf{n}\rangle_{\Gamma_h} \\ &\quad +\langle\Psi, v_b\rangle_{\Gamma_h} - h^{-1}\langle\Phi + \Phi', v_0 - v_b\rangle_{\Gamma_h} \\ &\quad +l_1(u, v_h) + l_2(u', v_h) + l_3(u, v_h) + l_3(u', v_h). \end{aligned} \tag{5.3.25}$$

Here, we have used Remark 5.3.4.

Now, subtracting equation (5.3.1) from equation (5.3.25) yields the desire result. This completes the rest of the proof. □

Remark 5.3.6. *Unlike the LDG methods where the interface conditions appears naturally in variational formulations, the WG-FEM approximation (5.3.1) is motivated by the work of Mu et al. [112] and equation (5.3.25). More precisely, we incorporate jump functions Φ and Ψ in the discrete formulation to avoid residue in the error equation.* □

Next, we recall following crucial estimates for the bilinear maps l_1, l_2 and l_3 from literature [112].

Lemma 5.3.4. *Assume that $\mathcal{T}_h$ is shape regular. Then, for $u \in H^1(J; H^{k+1}(\Omega_i))$, $i = 1, 2$ and $v_h = \{v_0, v_b\} \in V_h^0$, we have*

$$\begin{aligned} |l_1(u, v_h)| + |l_3(u, v_h)| &\leq Ch^k(\|u\|_{k+1,\Omega_1} + \|u\|_{k+1,\Omega_2})|||v_h|||, \\ |l_2(u', v_h)| + |l_3(u', v_h)| &\leq Ch^k(\|u'\|_{k+1,\Omega_1} + \|u'\|_{k+1,\Omega_2})|||v_h|||. \quad \square \end{aligned}$$

Now, we are ready to discuss the main results of this section.

Theorem 5.3.1. *Let $u_h \in V_h^0$ be the weak Galerkin finite element solution of the problem (5.1.1)-(5.1.3) arising from (5.3.1). Assume the exact solution $u \in H^1(J; H^{k+1}(\Omega_i))$, $i = 1, 2$. Then there exists a constant C such that*

$$\begin{aligned} \text{(a) } |||e_h(t)|||^2 + \int_0^t |||e_h(s)|||^2 ds &\leq Ch^{2k} \sum_{i=1}^{2} \|u\|^2_{H^1(0,t;H^{k+1}(\Omega_i))}, \\ \text{(b) } |||e_h'(t)|||^2 + \int_0^t |||e_h'(s)|||^2 ds &\leq Ch^{2k} \sum_{i=1}^{2} \|u\|^2_{H^1(0,t;H^{k+1}(\Omega_i))}. \end{aligned}$$

Proof. Putting $v_h = e_h$ in (5.3.18) and using the fact that $(\nabla_w e_h)' = \nabla_w e_h'$, we obtain

$$|||e_h|||_1^2 + \frac{1}{2}\frac{d}{dt}|||e_h|||_2^2 = l_1(u, e_h) + l_2(u', e_h) + l_3(u, e_h) + l_3(u', e_h).$$

By integration over the time period $[0, t]$ and use of Lemma 5.3.4 yields

$$\int_0^t |||e_h|||_1^2 ds + |||e_h(t)|||_2^2 \leq Ch^k \left\{ \sum_{i=1}^{2} \|u\|_{H^1(0,t;H^{k+1}(\Omega_i))} \right\} \int_0^t |||e_h||| ds.$$

Here, we have used the fact that $e_h(0) = Q_h u(0) - u_h(0) = Q_h u(0) - Q_h u(0) = 0$. Finally, Young's inequality leads to part (a).

For the second part, we set $v_h = e_h'$ in (5.3.18) and proceed in a similar fashion. This completes the rest of the proof. $\square$

Next, we want to estimate the error in L^2-norm. To obtain an optimal order error estimate in L^2-norm, we use duality argument. We consider the following interface problem that seeks $w \in H^1(J; \mathcal{Y})$ such that for *a. e.* $t \in J$,

$$\begin{aligned} -\nabla \cdot \left(\sigma(x)\nabla w - \epsilon(x)\nabla w'\right) &= e_0 \text{ in } \Omega, \qquad (5.3.26) \\ [w] = 0, \quad \left[\sigma \frac{\partial w}{\partial \nu} - \epsilon \frac{\partial w'}{\partial \nu}\right] &= 0 \text{ on } \Gamma \end{aligned}$$

and $w(\tau) = 0$, $\tau \in J$. Assume that there exists a unique solution $w \in H^1(J; \mathcal{Y})$ such that (cf. [9])

$$\|w\|_{H^1(J;\mathcal{Y})} \leq C\|e_0\|_{L^2(J;L^2(\Omega))}. \qquad (5.3.27)$$

Testing equation (5.3.26) with e_0' we obtain,

$$(e_0, e_0') = \big(-\nabla \cdot \big(\sigma(x)\nabla w - \epsilon(x)\nabla w'\big), e_0'\big).$$

Next, arguing as in (5.3.23) and (5.3.24), we obtain

$$(e_0, e_0') = \sum_{K\in\mathcal{T}_h} \big(\sigma\nabla_w Q_h w - \epsilon\nabla_w Q_h w', \nabla_w e_h'\big) - l_1(w, e_h') + l_2(w', e_h'), \tag{5.3.28}$$

where bilinear maps $l_1(\cdot,\cdot)$ and $l_2(\cdot,\cdot)$ are as defined in (5.3.18).

Now, for suitable $\tau \in (0, T]$, integrate the equation (5.3.28) in $[0, \tau]$ to obtain

$$\begin{aligned}
\frac{1}{2}\|e_0(\tau)\|^2 &= \sum_{K\in\mathcal{T}_h} \int_0^\tau \Big\{(\sigma\nabla_w Q_h w, (\nabla_w e_h)')_K - (\epsilon\nabla_w Q_h w', \nabla_w e_h')_K\Big\} ds \\
&\quad - \int_0^\tau l_1(w, e_h') ds + \int_0^\tau l_2(w', e_h') ds \\
&= -\sum_{K\in\mathcal{T}_h} \int_0^\tau \Big\{(\sigma(\nabla_w Q_h w)', \nabla_w e_h)_K + (\epsilon\nabla_w Q_h w', \nabla_w e_h')_K\Big\} ds \\
&\quad + \sum_{K\in\mathcal{T}_h} (\sigma\nabla_w Q_h w, \nabla_w e_h)_K(0) - \int_0^\tau \{l_1(w, e_h') - l_2(w', e_h')\} ds \\
&= -\int_0^\tau \{a_1(e_h, (Q_h w)') + a_2(e_h', (Q_h w)')\} ds \\
&\quad - \int_0^\tau \{l_1(w, e_h') - l_2(w', e_h')\} ds.
\end{aligned}$$

Here, we have used the fact that $\nabla_w v_h(t)|_{t=0} = \nabla_w v_h(0)$ for $v_h \in V_h^0$ and $e_h(0) = \{e_0(0), e_b(0)\} = 0$.

Now, using the error equation (5.3.18), we obtain

$$\begin{aligned}
\frac{1}{2}\|e_0(\tau)\|^2 &= \int_0^\tau s(e_h, Q_h w') ds + \int_0^\tau s(e_h', Q_h w') ds - \int_0^\tau l_1(u, Q_h w') ds \\
&\quad - \int_0^\tau l_2(u', Q_h w') ds - \int_0^\tau l_3(u, Q_h w') ds - \int_0^\tau l_3(u', Q_h w') ds \\
&\quad - \int_0^\tau l_1(w, e_h') ds + \int_0^\tau l_2(w', e_h') ds.
\end{aligned} \tag{5.3.29}$$

Next, we estimate each term of the equation (5.3.29) individually.

$$\begin{aligned}
|l_1(u, Q_h w')| &= C \sum_{K\in\mathcal{T}_h} \langle \sigma(\nabla u - \mathbb{Q}_h(\nabla u))\cdot\eta, Q_0 w' - Q_b w'\rangle_{\partial K} \\
&\le C \sum_{K\in\mathcal{T}_h} \|\nabla u - \mathbb{Q}_h(\nabla u)\|_{\partial K} \|Q_0 w' - w'\|_{\partial K} \\
&\le Ch^k \big(\|u\|_{k+1,\Omega_1} + \|u\|_{k+1,\Omega_2}\big) \Bigg(\sum_{K\in\mathcal{T}_h} h_K^{-1} \|Q_0 w' - w'\|_{\partial K}^2 \Bigg)^{\frac{1}{2}} \\
&\le Ch^k \big(\|u\|_{k+1,\Omega_1} + \|u\|_{k+1,\Omega_2}\big) \\
&\quad \times \Bigg(\sum_{K\in\mathcal{T}_h} \Big(h_K^{-2} \|Q_0 w' - w'\|_K^2 + \|\nabla(Q_0 w' - w')\|_K^2 \Big) \Bigg)^{\frac{1}{2}} \\
&\le Ch^k \big(\|u\|_{k+1,\Omega_1} + \|u\|_{k+1,\Omega_2}\big) h \big(\|w'\|_{2,\Omega_1} + \|w'\|_{2,\Omega_2}\big). \qquad (5.3.30)
\end{aligned}$$

In a similar way, other terms $l_2(\cdot,\cdot)$ and $l_3(\cdot,\cdot)$ can be estimated as

$$\begin{aligned}
&|l_2(u', Q_h w')| + |l_3(u, Q_h w')| + |l_3(u', Q_h w')| \\
&\le Ch^{k+1} \sum_{i=1}^{2} \|u\|_{k+1,\Omega_i} \sum_{i=1}^{2} \|u'\|_{k+1,\Omega_i} \sum_{i=1}^{2} \|w'\|_{2,\Omega_i}
\end{aligned}$$

and hence

$$\begin{aligned}
&\int_0^\tau \{|l_1(u, Q_h w')| + |l_2(u', Q_h w')| + |l_3(u, Q_h w')| + |l_3(u', Q_h w')|\} ds \\
&\le Ch^{k+1} \sum_{i=1}^{2} \|u\|_{H^1(0,\tau;H^{k+1}(\Omega_i))} \|e_0\|_{L^2(J;L^2(\Omega))}. \qquad (5.3.31)
\end{aligned}$$

For the last two terms appearing in (5.3.29), we use Lemma 5.3.4 to have

$$|l_1(w, e_h')| + |l_2(w', e_h')| \le Ch \|w'\|_{\mathcal{Y}} |||e_h'|||$$

which together with Theorem 5.3.1 yields

$$\begin{aligned}
&\int_0^\tau \{|l_1(w, e_h')| + |l_2(w', e_h')|\} ds \\
&\le Ch^{k+1} \sum_{i=1}^{2} \|u\|_{H^1(0,\tau;H^{k+1}(\Omega_i))} \|e_0\|_{L^2(J;L^2(\Omega))}. \qquad (5.3.32)
\end{aligned}$$

Also, we have following estimate for $s(e_h, Q_h w')$

$$\begin{aligned}
s(e_h, Q_h w') &= \sum_{K\in\mathcal{T}_h} h_K^{-1} \langle e_0 - e_b, Q_0 w' - Q_b w'\rangle_{\partial K} \\
&\le C|||e_h||| \Bigg(\sum_{K\in\mathcal{T}_h} h_K^{-1} \|Q_0 w' - w'\|_{\partial K}^2 \Bigg)^{\frac{1}{2}} \le Ch |||e_h||| \|w'\|_{\mathcal{Y}}. \qquad (5.3.33)
\end{aligned}$$

Similarly, we obtain

$$s(e_h', Q_h w') \leq Ch|||e_h'|||\|w'\|_{\mathcal{Y}}. \tag{5.3.34}$$

Combining the estimates (5.3.33)-(5.3.34) together with Theorem 5.3.1, we obtain

$$\begin{aligned}&\int_0^\tau \{s(e_h, Q_h w') + s(e_h', Q_h w')\}dt \\ &\leq Ch^{k+1}\sum_{i=1}^{2}\|u\|_{H^1(0,\tau;H^{k+1}(\Omega_i))}\|e_0\|_{L^2(J;L^2(\Omega))}.\end{aligned} \tag{5.3.35}$$

Using estimates (5.3.31), (5.3.32) and (5.3.35) in (5.3.29), we arrive at

$$\|e_0(\tau)\|^2 \leq Ch^{k+1}\sum_{i=1}^{2}\|u\|_{H^1(0,\tau;H^{k+1}(\Omega_i))}\|e_0\|_{L^2(J;L^2(\Omega))}. \tag{5.3.36}$$

Now, we select τ such that $\|e_0(\tau)\| = \max_{t\in J}\|e_0(t)\|$ so that estimate (5.3.36) finally leads to following optimal $L^\infty(L^2)$ norm estimate

Theorem 5.3.2. *Let $u_h \in V_h^0$ be the weak Galerkin finite element solution of the problem (5.1.1)-(5.1.3) arising from (5.3.1). Assume the exact solution $u \in H^1(J; H^{k+1}(\Omega_i))$, $i = 1, 2$. Then there exists a constant C such that*

$$\|e_0\|_{L^\infty(J;L^2(\Omega))} \leq Ch^{k+1}\sum_{i=1}^{2}\|u\|_{H^1(J;H^{k+1}(\Omega_i))}. \quad \square$$

5.4 Fully Discrete Method

In this section, we are going to formulate a fully discrete finite element scheme to approximate the solution of the interface problem (5.1.1)-(5.1.3). We shall use the backward Euler scheme for the time discretization.

We first divide the time interval $J = [0, T]$ into N equally spaced subintervals by using the following nodal points

$$0 = t^0 < t^1 < t^2 < \cdots < t^N = T,$$

where $t^n = n\kappa$ for $n = 1, 2, \cdots N-1$ and $\kappa = T/N$ being the time step. For any given sequence $\{w^n\}_{n=0}^N \in V_h$ and a function $g \in C(J; L^2(\Omega))$, we define

$$\bar{\partial}w^n = \frac{w^n - w^{n-1}}{\kappa}, \quad \bar{g}^n = \frac{1}{\kappa}\int_{t^{n-1}}^{t^n} g(\cdot, s)ds, \ n = 1, 2, 3, \cdots, N.$$

We denote by w^n the value of $w \in C(J; L^2(\Omega))$ at $t = t^n$.

Now, we propose a fully discrete finite element scheme to approximate the solution to the interface problem. Let $U_h^0 = Q_h u(0)$ and $U_h^n = \{U_0^n, U_b^n\} \in V_h^0$ be the fully discrete approximation of u at $t = t^n$ which we shall define through the following scheme: For given $U_h^0 \in V_h^0$, determine $U_h^n \in V_h^0,\ 1 \le n \le N$, satisfying

$$a(U_h^n, v_h) + b(\bar{\partial} U_h^n, v_h) = (\bar{f}^{\,n}, v_0) + \langle \bar{\Psi}^n, v_b\rangle_{\Gamma_h} + \langle \bar{\Phi}^n, \sigma(x)\nabla_w v_h \cdot \mathbf{n}\rangle_{\Gamma_h} + \langle \bar{\partial}\Phi^n, \epsilon(x)\nabla_w v_h \cdot \mathbf{n}\rangle_{\Gamma_h} - \frac{1}{h}\langle \bar{\Phi}^n + \bar{\partial}\Phi^n, v_0 - v_b\rangle_{\Gamma_h}, \tag{5.4.1}$$

for all $v_h = \{v_0, v_b\} \in V_h^0$.

We decompose the fully discrete error at $t = t^n$ as follows:

$$e^n := U_h^n - u^n = \theta^n + \xi^n, \text{ where } \theta^n := U_h^n - u_h^n \text{ and } \xi^n := u_h^n - u^n,$$

where $u_h : [0, T] \to V_h^0$ is the semidiscrete solution given by the equation (5.3.1).

Now, integrating the equation (5.3.1) from t^{n-1} to t^n with respect to t and dividing by κ, for all $v_h \in V_h^0$, we obtain

$$a(\bar{u}_h^n, v_h) + b(\bar{\partial} u_h^n, v_h) = (\bar{f}^{\,n}, v_0) + \langle \bar{\Psi}^n, v_b\rangle_{\Gamma_h} + \langle \bar{\Phi}^n, \sigma(x)\nabla_w v_h.\mathbf{n}\rangle_{\Gamma_h} + \langle \bar{\partial}\Phi^n, \epsilon(x)\nabla_w v_h.\mathbf{n}\rangle_{\Gamma_h} - \frac{1}{h}\langle \bar{\Phi}^n + \bar{\partial}\Phi^n, v_0 - v_b\rangle_{\Gamma_h}. \tag{5.4.2}$$

Now, we subtract (5.4.2) from (5.4.1) to have following error equation in θ

$$a(\theta^n, v_h) + b(\bar{\partial}\theta^n, v_h) = a(\bar{u}_h^n - u_h^n, v_h). \tag{5.4.3}$$

Putting $v_h = \theta^n$ in the equation (5.4.3), we obtain

$$|||\theta^n|||^2 \le C|||\theta^n|||\,|||\theta^{n-1}||| + C\kappa|||\bar{u}_h^n - u_h^n|||\,|||\theta^n|||.$$

Here, we have used continuity of $b(\cdot,\cdot)$, and positivity of the operators $a(\cdot,\cdot)$ and $b(\cdot,\cdot)$. Further, Young's inequality leads to following estimate

$$\begin{aligned} |||\theta^n|||^2 &\le C|||\theta^0|||^2 + C\kappa \sum_{j=1}^{n} |||\bar{u}_h^j - u_h^j|||^2 \\ &\le C\kappa^2 \sum_{j=1}^{n} \int_{t^{j-1}}^{t^j} |||u_{ht}|||^2 dt. \end{aligned} \tag{5.4.4}$$

Here, we have used the fact that $\theta^0 = U_h^0 - u_h^0 = Q_h u(0) - Q_h u(0) = 0$ and Taylor's series expansion.

Now, it follows from (5.3.4)-(5.3.5) that

$$\|\theta^n\| + \|\nabla\theta^n\| \le C|||\theta^n||| + C\|\theta^n\|_{1,h} \le C|||\theta^n||| \le C\kappa\|u_h\|_{H^1(0,t^n;|||\cdot|||)}. \tag{5.4.5}$$

In the last inequality, we have used (5.4.4).

Above estimate together with semidiscrete error estimates and (5.3.5) leads to following fully discrete error estimates.

Theorem 5.4.1. *Let $U_h \in V_h^0$ be the weak Galerkin finite element solution of the problem (5.1.1)-(5.1.3) arising from (5.4.1). Assume the exact solution $u \in H^1(J; H^{k+1}(\Omega_i))$ $i = 1, 2$. Then there exists a constant C such that*

$$\text{(a)} \quad \|U_h^n - u^n\| \leq Ch^{k+1} \sum_{i=1}^{2} \|u\|_{H^1(0,t^n;H^{k+1}(\Omega_i))} + C\kappa \|u_h\|_{H^1(0,t^n;|||\cdot|||)},$$

$$\text{(b)} \quad \|\nabla(U_h^n - u^n)\| \leq Ch^k \sum_{i=1}^{2} \|u\|_{H^1(0,t^n;H^{k+1}(\Omega_i))} + C\kappa \|u_h\|_{H^1(0,t^n;|||\cdot|||)}. \quad \square$$

5.5 Numerical Results

In this section, we present some numerical experiments to validate the theoretical findings presented in the previous section for weak Galerkin space $(\mathcal{P}_1(K),\ \mathcal{P}_1(\partial K),\ \left[\mathcal{P}_0(K)\right]^2)$ based on uniform triangulations of Ω_i, $i = 1, 2$. The nodes of the triangulations of Ω_1 and Ω_2 coincide on the interface Γ. All the numerical computations are done in the time interval $J = (0, 1]$ for the coupling $\kappa = \mathrm{O}(h^2)$.

To illustrate the flexibility of the method, different forms of interfaces along with a large scale of variation in the physical coefficients are considered. To mark the significance of the interface model problem (5.1.1), we take a set of specific thermal parameters from the paper by Rems *et al.* [121] given as

$$\sigma = \begin{cases} \sigma_1 = 0.25, \\ \sigma_2 = 5 \times 10^{-7}, \end{cases} \quad \& \quad \epsilon = \begin{cases} \epsilon_1 = 70, \\ \epsilon_2 = 4.5. \end{cases}$$

Example 5.5.1. For our first numerical example, we consider the two dimensional domain $\Omega = (-1, 1) \times (-1, 1)$ and the interface is taken to be the circle $r^2 := x^2 + y^2 = 1/4$. The source function f is taken as

$$f(x, y, t) = \begin{cases} 40(\sigma_1 \sin t + \epsilon_1 \cos t) & \text{if } r^2 \leq \frac{1}{4}, \\ \big\{(\sigma_2 t + \epsilon_2)\sin(\pi x)\sin(\pi y)(2\pi^2(\frac{1}{4} - r^2) & \\ \quad + 4\sin(\pi x)\sin(\pi y)) + 4\pi x \sin(\pi y)\cos(\pi x) & \\ \quad + 4\pi y \cos(\pi y)\sin(\pi x)\big\} & \text{if } r^2 > \frac{1}{4}. \end{cases}$$

And the exact solution of the problem is given by

$$u(x,y,t) = \begin{cases} 10(\frac{1}{4} - r^2)\sin t & \text{if } r^2 \leq \frac{1}{4}, \\ t(\frac{1}{4} - r^2)\sin(\pi x)\sin(\pi y) & \text{if } r^2 > \frac{1}{4}. \end{cases}$$

The Dirichlet boundary condition, initial data and interface functions are calculated from the exact solution. In Figure 5.1, we show the numerical solution at final time step and triangulation of the domain Ω with mesh size $h = 0.167378$.

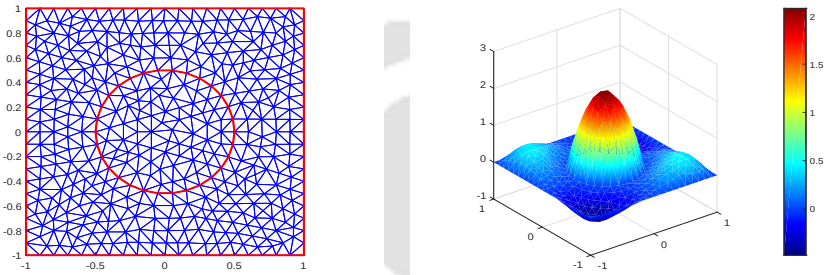

Figure 5.1: Numerical solution (right) and triangulation (left) of Ω for $h = 0.167378$ with circular interface (Test Example 5.5.1).

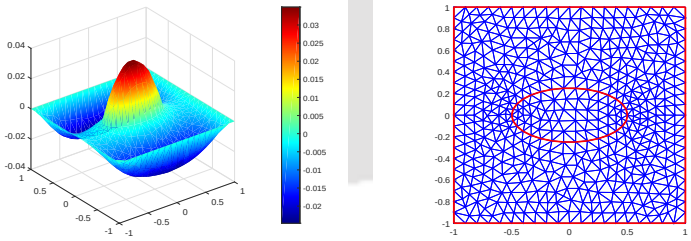

Figure 5.2: Numerical solution (left) and triangulation (right) of Ω for $h = 0.152069$ with elliptic interface (Test Example 5.5.2).

Example 5.5.2. For our second numerical example, we take the computational domain $\Omega = (-1,1) \times (-1,1)$ and the interface is the ellipse given by $r^2 := 4x^2 + 16y^2 = 1$. We select the data in (5.1.1)-(5.1.3) such that the exact solution is given by

$$u(x,y,t) = \begin{cases} \frac{1}{10}(1 - r^2)t^2 e^{-t} & \text{if } r^2 \leq 1, \\ \frac{1}{100}(1 - r^2)(x^2 - 1)(y^2 - 1)\sin\frac{\pi t}{4} & \text{if } r^2 > 1. \end{cases}$$

In Figure 5.2, we show the exact solution and triangulation of the domain Ω with mesh size $h = 0.152069$ at final time step.

For numerical implementation of the weak Galerkin algorithm (5.4.1), we have used linear WG-FEM space on triangular mesh $\mathcal{T}_h$ matched with the interface. By successive mesh refinements using piecewise linear finite elements, the convergence behavior of the fully discrete solution at final time $t = 1$ with various mesh parameters h and κ are reported in Figure 5.3. It is evident from the error plots that we have obtained optimal second order of convergence in L^2-norm and first order of convergence in H^1-norm which consolidates our theoretical findings in Theorem 5.4.1.

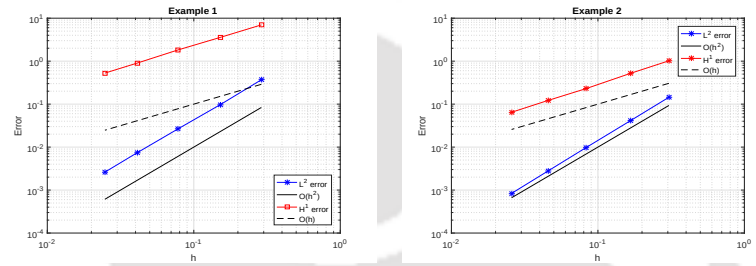

Figure 5.3: Log-log plot of the L^2-norm and H^1-norm errors versus the mesh size at time $t = 1$ for Examples 5.5.1-5.5.2.

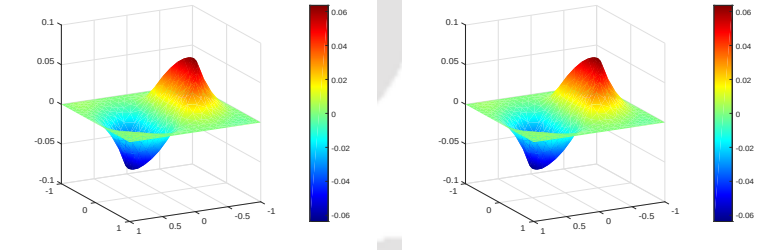

Figure 5.4: Numerical solutions at $t = t^1 = \kappa = 0.01$ (right) and at $t = t^M = 1$ (left) for $h = 0.167378$.

Example 5.5.3. (Conservation of voltage) We consider IBVP (5.1.1)-(5.1.3) in domain $\Omega \times (0, 1] = (-1, 1) \times (-1, 1) \times (0, 1]$ with initial data $u(x, y, 0) = \sin x$ and coefficients $(\beta_1, \beta_2) = (1, \frac{1}{2}) = (\epsilon_1, \epsilon_2)$. The interface is taken to be the circle $x^2 + y^2 = 1/4$. We define

$$\mathcal{A}_n := \sum_{K \in \mathcal{T}_h} \int_K U_h^n dx, \quad n = 1,\ 2, \ldots, N.$$

In the absence of source function and interface functions, we have numerically achieved that our approximate solution U_h satisfying (5.4.1) is conserved in the sense that difference $|\mathcal{A}_n - \mathcal{A}_{n-1}|$ $(1 \leq n \leq N)$ is sufficiently small. For instance, Figure 5.4 demonstrates the numerical solutions at time levels $t = t^1$ and $t = t^N$. It is easy to notice from Figure 5.4 that areas $\mathcal{A}_1$ and $\mathcal{A}_N$ under the curves U_h^1 and U_h^N in $\Omega = (-1,1)\times(-1,1)$ are preserved. In fact it is calculated that $|\mathcal{A}_1 - \mathcal{A}_N| \approx 0.061 \times 10^{-6}$.

6

Conclusions and Extensions

In this chapter, we highlight the significant and contribution of the current thesis work also techniques to derive them. We also provide possible extensions and scope for future investigations.

6.1 Critical Review of the Results

In this thesis, we proposed some time dependent interface problem with non homogeneous jump conditions. We have used non-conforming fitted finite element methods to study the convergence of weak Galerkin finite element solutions to the exact solutions.

In Chapter 2, we have presented a priori error estimates for the spatially semidiscrete scheme for the parabolic interface problem (2.1.1)-(2.1.3). In this chapter, we extend the work of [44, 112] to parabolic interface problem based on WG finite element space $(\mathcal{P}_k(K),\ \mathcal{P}_{k-1}(\partial K),\ \left[\mathcal{P}_{k-1}(K)\right]^2)$ with projected element-boundary discrepancy stabilizer (see, (1.4.13)). Optimal order error estimates in both $L^\infty(H^1)$ (see, Theorem 2.3.1) and $L^\infty(L^2)$ (see, Theorem 2.3.2) norms are established. To obtain optimal order error estimates in $L^\infty(H^1)$ norm, we have used usual splitting technique, where L^2 projection Q_h (defined as in (2.2.8)) of the exact solution has used as an intermediate operator. Further, the error equation (2.2.12) played a crucial role in the derivation of optimal error with respect to point-wise in time discrete H^1 norm. Then, elliptic type projection operator R_h has been introduced in (2.3.6) to obtain optimal order of convergence for semidiscrete solution with respect to $L^\infty(L^2)$ norm.

In Chapter 3, we have extended the spatially discrete a priori error analysis to the fully discrete approximation for the parabolic interface problem (3.1.1)-(3.1.3). First order backward Euler and second order Crank-Nicolson schemes are applied for the time discretization. We have obtained optimal order of convergence in L^2 norm (see, Theorem 3.2.2 and Theorem 3.3.2) for both fully discrete schemes. The basic error

analysis technique is borrowed from [131]. Finally, we have presented some numerical experiments to validate the theoretical estimates for fully discrete method based on Crank-Nicolson schemes.

In Chapter 4, we have presented a priori error analysis for wave interface problem (4.1.1)-(4.1.3) with non-homogeneous jump conditions along the interface. We have derived optimal order of convergence for both semidiscrete scheme and fully discrete scheme in $L^\infty(L^2)$ norm (see, Theorem 4.2.1 and Theorem wt51). The fully discrete error estimate is based on the stability of the semidiscrete solution and a reconstruction operator defined by (4.3.15) connecting both fully discrete and semidiscrete solutions. Finally, we have presented few numerical examples to validate our theoretical findings.

In Chapter 5, we have considered an electric interface model problem (5.1.1)-(5.1.3) with non-homogeneous jump conditions and solve it numerically using WG-FEM. We have presented error analysis for both semidiscrete and fully-discrete finite element schemes. Optimal order of convergence in $L^\infty(L^2)$ and $L^\infty(H^1)$ norms are established for the semidiscrete solution (see, Theorem 5.3.1 and Theorem 5.3.2). For the $L^\infty(H^1)$ norm error estimate for the semidiscrete solution, the splitting technique has been used, where the L^2 projection Q_h (defined as in (5.3.6)) of the exact solution has used to split the error into two parts. In fact, apart from the standard error splitting technique, the newly derived error equation (5.3.3) is also critical. The $L^\infty(L^2)$ norm error analysis is based on duality arguments. We have also proved stability of the semidiscrete solution and derive some estimates which are very crucial to prove the optimal convergence rate of the fully discrete solution. Further, optimal a priori error estimates for fully discrete scheme is proved in L^2 norm (see, Theorem 5.4.1). The fully discrete error analysis is based on standard ρ and θ technique. Finally, numerical results are reported to confirm our theoretical convergence rate.

6.2 Extensions and Remarks

Unfitted WG-FEMs for Interface Problems: In this thesis, we have considered fitted finite element method where the discretization is done in such a way that the grid line follows the actual interface. In unfitted finite element method, the discretization of the domain is independent of the interface. Unfitted FEMs are helpful in a number of context including multi-phase and multi-physics applications with moving interfaces or in situations in which one wants to avoid the generation of body-fitted meshes to reduce the computational cost. In future, one can consider unfitted WG-FEMs for parabolic interface problems. As parabolic error analysis depends on the error estimates of elliptic problems, one has to first analyze the unfitted FEMs for elliptic interface problems.

Non-Fourier Bio Heat Model Problem: Let Ω be a bounded domain in $\mathbb{R}^d (d = 2,\ 3)$ with Lipschitz boundary $\partial\Omega$ and $\Omega_1 \subset \Omega$ is an open domain with Lipschitz boundary $\Gamma = \partial\Omega_1$ and $\Omega_2 = \Omega \backslash \Omega_1$(see, Figure 1.1). In Ω, we consider the following non-Fourier bio heat transfer model in multi-layered media (*cf.* [150] and references therein)

$$u'' + \sigma u' - \nabla \cdot (\beta \nabla u) = f \quad \text{in } \Omega \times (0, T],\ T < \infty, \tag{6.2.1}$$

with initial and boundary conditions

$$u(x, 0) = u_0,\ \ u'(x, 0) = v_0 \ \text{ in } \Omega \ \ \& \ \ u(x, t) = 0 \quad \text{on } \partial\Omega \times (0, T]. \tag{6.2.2}$$

Here, $\sigma = \sigma(x)$ and $\beta = \beta(x)$ are non-negative real-valued functions, and f denotes the source. Further, u' and u'' denotes the first and second order time differentiation of u, respectively.

Equation (6.2.1) is also known as hyperbolic heat equation/Maxwell-Cattaneo (MC) equation/damped wave equation. As a model, we consider bio heat transfer model in non-homogeneous media. With advances in laser, microwave, radio-frequency and similar technologies, a variety of thermal methods have been proposed to analyze the bio heat transfer in living tissue. However, in applications involving samples with non-homogeneous internal structures, *e.g.* biological samples, it has been experimentally demonstrated that the Fourier law of heat conduction cannot accurately predict the thermal response of such samples (*e.g.* [150]). Biological tissue, along with a number of other common materials, exhibits a relaxation time. Relaxation time reflects the time between phonon collisions or it represents a time lag between the imposition of a temperature gradient and the creation of a thermal flux. Skin tissue has a "lengthy" relaxation time, which means it is desirable to develop a computational approach to examine the non-Fourier heat transfer process. For details, we refer to Xu *et al.* [150]. Due to implication of such relaxation time, heat conduction in biological media is generally not described by Fourier's law, but rather by the Maxwell-Cattaneo law. Thermal behavior or heat transfer in biological media is mainly a heat conduction process and since the thermal properties of biological media vary between different layers, so, it is natural to have heterogeneity in the underlying media. In particular, media parameters are discontinuous and piecewise constants in Ω. We write

$$(\sigma, \beta) = \begin{cases} (\sigma_1, \beta_1) & \text{in } \Omega_1, \\ (\sigma_2, \beta_2) & \text{in } \Omega_2. \end{cases}$$

The interfacial continuity conditions between layers are given by

$$[u] = \phi, \quad \left[\beta \frac{\partial u}{\partial \mathbf{n}}\right] = \psi \quad \text{along } \Gamma \times (0, T], \tag{6.2.3}$$

where the symbols $[v]$ and $\mathbf{n}$ are defined as before. The convergence analysis for the finite element methods for such problems with nonhomogeneous jump conditions and irregular interfaces are still open.

WG-FEMs for Westervelt's Equation: Consider the following nonlinear damped wave equation of the form

$$c^{-2}u_{tt} - \nabla \cdot (\nabla u + \beta \nabla u') = \gamma (u^2)_{tt} \text{ in } (0, T] \times \Omega. \tag{6.2.4}$$

The above equation (6.2.4) is known as Westervelt equation which is widely used to simulate high-intensity focused ultrasound fields generated by medical ultrasound transducers. High intensity focused ultrasound has numerous applications starting from treatment of kidney and bladder stones via thermotherapy, ultrasound cleaning, and welding to sonochemistry. Westervelt equation (6.2.4) with interfaces are motivated by lithotripsy where a silicone acoustic lens focuses the ultrasound traveling through a nonlinearity acoustic fluid to a kidney stone. Although substantial work has been dedicated to their analytical studies [62, 115] and their numerical treatment via finite element procedure (cf. [14, 62] just to name a few), rigorous error analysis for finite element methods of nonlinear acoustic phenomena is still largely missing from the literature. Recently, a priori error estimates for the classical finite element approximation of Westervelt's quasi-linear strongly damped wave equation (6.2.4) with linear elements have been discussed in [116]. Then, a high-order discontinuous Galerkin (DG) method for the equation (6.2.4) has been carried out in [14]. It is worthwhile to note that only the semidiscrete scheme (space discretization) has been discussed in [14, 116]. The fully discrete scheme (space-time discretization) error analysis is still open. It will be interesting and challenging to extend the present the analysis discuss in this thesis to the interface problems associated with nonlinear acoustic wave equation discussed in [115].

Bibliography

[1] R. Adams and J. Fournier, *Sobolev Spaces*, sec. ed, Academic Press, Amsterdam, 2003.

[2] M. O. Adewole, *Almost optimal convergence of FEM-FDM for a linear parabolic interface problem*, ETNA, 46 (2017), 337-358.

[3] S. Adjerid, R. Guo, and T. Lin, *High degree immersed finite element spaces by a least squares method*, Int. J. Numer. Anal. Model, 14 (2017), 604-626.

[4] S. Adjerid and T. Lin, *A p-th degree immersed finite element for boundary value problems with discontinuous coefficients*, Appl. Numer. Math., 59 (2009), 1303-1321.

[5] S. Adjerid, T. Lin and Q. Zhuang, *Error estimates for an immersed finite element method for second order hyperbolic equations in inhomogeneous media*, J. Sci. Comput., 84 (2020), 1-25.

[6] S. Adjerid and K. Moon, *A higher order immersed discontinuous Galerkin finite element method for the acoustic interface problem*, Adv. Appl. Math., 87 (2014), 57-69.

[7] ———, *An immersed discontinuous Galerkin method for acoustic wave propagation in inhomogeneous media*, SIAM J. Sci. Comput., 41 (2019), A139-A162.

[8] A. Aldroubi and M. Renardy, *Energy methods for a parabolic-hyperbolic interface problem arising in electromagnetism*, Z. Angew. Math. Phys., 39 (1988), 931-936.

[9] H. Ammari, D. H. Chen and J. Zou, *Well-posedness of an electric interface model*

and its finite element approximation, Math. Models Methods Appl. Sci., 26 (2016), 601-625.

[10] H. Ammari, J. Garnier, L. Giovangigli, W. Jing and J. K. Seo, *Spectroscopic imaging of a dilute cell suspension*, J. Math. Pure. Appl., 105 (2016), 603-661.

[11] N. An, X. Yu and C. Huang, *Local discontinuous Galerkin methods for parabolic interface problems with homogeneous and nonhomogeneous jump conditions*, Comput. Math. Appl., 74 (2017), 2572-2598.

[12] F. Andr and L. M. Mir, *DNA electrotransfer: its principles and an updated review of its therapeutic applications*, Gene Therapy, 11 (2004), S33-S42.

[13] A. Angersbach, V. Heinz and D. Knorr, *Effects of pulsed electric fields on cell membranes in real food systems*, Innov. Food Sci. Emerg. Techno., 1 (2000), 135-149.

[14] Antonietti, P. F., Mazzieri, I., Muhr, M., Nikolić, V. and Wohlmuth, B., *A high-order discontinuous Galerkin method for nonlinear sound waves*, J. Comput. Phys., 415 (2020), 109484.

[15] D. N. Arnold, F. Brezzi, B. Cockburn and L. D. Marini, *Unified analysis of discontinuous Galerkin methods for elliptic problems*, SIAM J. Numer. Anal., 39(2002), 1749-1779.

[16] G. A. Baker, *Error estimates for finite element methods for second order hyperbolic equations*, SIAM J. Numer. Anal., 13(1976), 564-576.

[17] G.A. Baker, V.A. Dougalis, On the L^{∞} convergence of Galerkin approximations for second-order hyperbolic equations, Math. Comp. 34 (1980) 401-424.

[18] A. Bamberger, R. Glowinski and Q. H. Tran, A domain decomposition method for the acoustic wave equation with discontinuous coefficients and grid change, SIAM J. Numer. Anal., 34 (1997), 603-639.

[19] J. W. Barrett and C. M. Elliott, *Fitted and unfitted finite element methods for elliptic equations with smooth interfaces*, IMA J. Numer. Anal., 7 (1987), 283-300.

[20] D. M. Boore, Seismology: Surface Waves and Earth Oscillations: B. A. Bolt (Ed.), *Finite Difference Methods for Seismic Wave Propagation in Heterogeneous Materials*, Academic Press, London, 1972, pp. 1-37.

[21] L. M. Brekhovskihk, *Waves in Layered Media*, Academic Press, New York, 1980.

[22] S. Brenner and R. Scott, *The Mathematical Theory of Finite Element Methods*, Vol. 15, Springer Science & Business Media, 2007.

[23] F. Brezzi, J. Douglas, Jr. and L. D. Marini, *Two families of mixed finite elements for second order elliptic problems*, Numer. Math., 47 (1985), 217-235.

[24] E. Burman and A. Ern, *An unfitted hybrid high-order method for elliptic interface problems*, SIAM J. Numer. Anal., 56 (2018), 1525-1546.

[25] C. R. Butson, C. C. McIntryre, *Tissue and electrode capacitance reduce neural activation volumes during deep brain stimulation*, Clinical Neuriphysiology, 116 (2005), 2490-2500.

[26] Z. Cai, X. Ye and S. Zhang, *Discontinuous Galerkin finite element methods for interface problems: a priori and a posteriori error estimations,* SIAM J. Numer. Anal., 49 (2011), 1761-1787.

[27] Z. Cai and S. Zhang, *Recovery-based error estimator for interface problems: mixed and nonconforming elements*, SIAM J. Numer. Anal, 48:1 (2010), 30-52.

[28] A. Cangiani, Z. Dong and E. H. Georgoulis, *hp-version space-time discontinuous Galerkin methods for parabolic problems on prismatic meshes*, SIAM J. Sci. Comput., 39 (2017), A1251-A1279.

[29] A. Cangiani, E. H. Georgoulis and P. Houston, *hp-version discontinuous Galerkin methods on polygonal and polyhedral meshes*, Math. Models Methods Appl. Sci., 24 (2014), 2009-2041.

[30] A. Cangiani and R. Natalini, *A spatial model of cellular molecular trafficking including active transport along microtubules*, J. Theoret. Biol., 267 (2010), 614-625.

[31] C. Carstensen, *Interface problems in viscoplasticity and plasticity*, SIAM J. Math. Anal., 25 (1994), 1468-1487.

[32] W. Chen, F. Wang and Y. Wang, *Weak Galerkin method for the coupled Darcy-Stokes flow*, IMA J. Numer. Anal. 36 (2016), 897-921.

[33] L. Chen, H. Wei and M. Wen, *An interface-fitted mesh generator and virtual element methods for elliptic interface problems*, J. Comput. Phys. 334 (2017), 327-348.

[34] Z. Chen and J. Zou, *Finite element methods and their convergence for elliptic and parabolic interface problems*, Numer. Math., 79 (1998), 175-202.

[35] S.-H. Chou, D. Y. Kwak and K. T. Wee, *Optimal convergence analysis of an immersed interface finite element method*, Adv. Comput. Math., 33 (2010), 149-168.

[36] P. G. Ciarlet, *The Finite Element Method for Elliptic Problems*, Vol. 40, SIAM, 2002.

[37] B. Cockburn, D. A. Di Pietro and A. Ern, *Bridging the hybrid high-order and hybridizable discontinuous Galerkin methods*, ESAIM Math. Model. Numer. Anal., 50 (2016), 635-650.

[38] B. Cockburn and V. Quenneville-Bélair, Uniform-in-time superconvergence of the HDG methods for the acoustic wave equation, Math. Comp., 83 (2014), 65-85.

[39] B. Cockburn, J. Gopalakrishnan and R. Lazarov, *Unified hybridization of discontinuous Galerkin, mixed, and continuous Galerkin methods for second order elliptic problems*, SIAM J. Numer. Anal., 47 (2009), 1319-1365.

[40] M. Cui and S. Zhang, *On the uniform convergence of the weak Galerkin finite element method for a singularly-perturbed biharmonic equation*, J. Sci. Comput. 82 (2020), Paper No. 5, 15 pp.

[41] W. Dai, H. Wang, P. M. Jordan, R. E. Mickens, A. Bejan, *A mathematical model for skin burn injury induced by radiation heating*, Int. Jour. Heat and Mass Transfer, 51 (2008), 5497-5510.

[42] R. Dautray and J.-L. Lions, *Mathematical Analysis and Numerical Methods for Science and Technology: I*, vol. 5, Springer-Verlag, Berlin, 1992

[43] B. Deka, *A priori $L^\infty(L^2)$ error estimates for finite element approximations to the wave equation with interface*, Appl. Numer. Math., 115 (2017), 142-159.

[44] _____, *A weak Galerkin finite elememnt method for elliptic interface problems with polynomial reduction*, Numer. Math. Theor. Meth. Appl., 11 (2018), 655-672.

[45] _____, *A posteriori error estimates for finite element approximations to the wave equation with discontinuous coefficients*, Numer. Methods Partial Differential Equations, 35 (2019), 1630-1653.

[46] B. Deka, T. Ahmed, *Convergence of finite element method for linear second order wave equations with discontinuous coefficients*, Numer. Methods Partial Differential Equations, 29 (2013), 1522-1542.

[47] B. Deka and R. C. Deka, *Quadrature based finite element methods for linear parabolic interface problems*, Bull. Korean Math. Soc., 51 (2014), 717-737.

[48] B. Deka and J. Dutta, *Convergence of finite element methods for hyperbolic heat conduction model with an interface*, Comput. Math. Appl. 79 (2020), 3139-3159.

[49] _____, *$L^\infty(L^2)$ and $L^\infty(H^1)$ norms error estimates in finite element methods for electric interface model*, Appl. Anal. 100 (2021), 1351-1370.

[50] B. Deka and N. Kumar, *Error estimates in weak Galerkin finite element methods for parabolic equations under low regularity assumptions*, Appl. Numer. Math. 162 (2021), 81-105.

[51] B. Deka and P. Roy, *Weak Galerkin finite element methods for parabolic interface problems with nonhomogeneous jump conditions*, Numer. Funct. Anal. Optim., 40 (2019), 259-279.

[52] _____ *A least-squares-based weak Galerkin finite element method for elliptic interface problems*, Proc. Indian Acad. Sci. Math. Sci. 129 (2019), no. 5, Paper No. 73, 8 pp.

[53] _____, *Weak Galerkin finite element methods for electric interface model with nonhomogeneous jump conditions*, Numer. Methods Partial Differential Equations, 36 (2020), 734-755.

[54] B. Deka, P. Roy and N. Kumar, *Weak Galerkin finite element methods combined with Crank-Nicolson scheme for parabolic interface problems*, J. Appl. Anal. Comput. 10 (2020), 1433-1442.

[55] _____, *Convergence of weak Galerkin finite element method for second order linear wave equation in heterogeneous media*, submitted.

[56] Z. Dong and A. Ern, *Hybrid high-order and weak Galerkin methods for the biharmonic problem*, arXiv preprint arXiv:2103.16404, 2021.

[57] H. Dong, B. Wang, Z. Xie, and L.-L. Wang, *An unfitted hybridizable discontinuous Galerkin method for the Poisson interface problem and its error analysis*, IMA J. Numer. Anal., 37 (2017), 444-476.

[58] T. Dupont, L^2 *estimates for Galerkin methods for second order hyperbolic equations*, SIAM J. Numer. Anal. 10 (1973) 880-889.

[59] J. Dutta and B. Deka, *Optimal a priori error estimates for the finite element approximation of dual-phase-lag bio heat model in heterogeneous medium*, J. Sci. Comput. 87 (2021), no. 2, Paper No. 58, 32 pp.

[60] H. Egger and B. Radu, *A mass-lumped mixed finite element method for acoustic wave propagation*, Numer. Math., 145 (2020), 239-269.

[61] L. C. Evans, *Partial Differential Equations*, vol. 19, American Mathematical Soc., 2010.

[62] Fritz, M., Nikolić, V. and Wohlmuth, B., *Well-posedness and numerical treatment of the Blackstock equation in nonlinear acoustics*, Math. Models Methods Appl. Sci., 28 (2018), 2557-2597.

[63] E. H. Georgoulis, O. Lakkis, C. G. Makridakis, *A posteriori* $L^\infty(L^2)$*-error bounds for finite element approximations to the wave equation*, IMA Jour. Numer. Anal. 33 (2013) 1245-1264.

[64] E. H. Georgoulis, O. Lakkis, C. G. Makridakis and J. M. Virtanen, A posteriori error estimates for leap-frog and cosine methods for second order evolution problems, SIAM J. Numer. Anal., 54 (2016), 120-136.

[65] Z. Gharibi and M Dehghan, *Convergence analysis of weak Galerkin flux-based mixed finite element method for solving singularly perturbed convection-diffusion-reaction problem*, Appl. Numer. Math., 163 (2021), 303-316.

[66] Y. Gong and Z. Li, *Immersed interface finite element methods for elliptic interface problems with non-homogeneous jump conditions*, SIAM J. Numer., Anal., 46 (2008), 472-495.

[67] W. M. Grill, *Modeling the effects of electric fields on nerve fibers: influence of tissue electrical properties*, IEEE Trans. Biomedical Engineering, 46 (1999), 918-928.

[68] M. J. Grote, A. Schneebeli and D. Schötzau, *Discontinuous Galerkin finite element method for the wave equation*, SIAM J. Numer. Anal. 44 (2006), 2408-2431.

[69] R. Guo and T. Lin, *A group of immersed finite-element spaces for elliptic interface problems*, IMA J. Numer. Anal. 39 (2019), 482-511.

[70] A. Hansbo and P. Hansbo, *An unfitted finite element method, based on Nitsche's method, for elliptic interface problems*, Comput. Methods Appl. Mech. Engrg., 191 (2002), 5537-5552.

[71] G. H. Hardy, J. E. Littlewood and G. Pólya, *Inequalities*, Cambridge Univ. Press, London, 1964.

[72] X. He, T. Lin, Y. Lin, and X. Zhang, *Immersed finite element methods for parabolic equations with moving interface*, Numer. Methods Partial Differential Equations, 29 (2013), 619-646.

[73] Y. Huang, J. Li and D Li, *Developing weak Galerkin finite element methods for the wave equation*, Numer. Methods Partial Differential Equations 33 (2017), 868-884.

[74] L. T. Ikelle and L. Amundsen, Introduction to Petroleum Seismology, Tulsa, Okla, USA: Society of Exploration Geophysicists, 2005.

[75] H. Ji, J. Chen and Z. Li, *A symmetric and consistent immersed finite element method for interface problems*, J. Sci. Comput., 61 (2014) 533-557.

[76] B. S. Jovanović and L. G. Vulkov, *Formulation and analysis of a parabolic transmission problem on disjoint intervals,* Publ. Inst. Math. (Beograd) (N.S.) 91(105) (2012), 111-123.

[77] O. Karakashian, C. Makridakis, *Convergence of a continuous Galerkin method with mesh modification for nonlinear wave equations*, Math. Comp. 74 (2005) 85-102.

[78] A. Khan, C. S. Upadhyay and M. Gerritsma, *Spectral element method for parabolic interface problems*, Comput. Methods Appl. Mech. Engrg., 337 (2018), 66-94.

[79] K. Kelly, R. Ward, S. Treitel and R. Alford, *Synthetic seismograms: a finite difference approach, Geophysics*, 41 (1976), 2-27.

[80] O. A. Ladyžhenskaya, V. A. Solonnikov and N. N. Ural'ceva, Linear and quasilinear equations of parabolic type, Translated from Russian by S. Smith. Translations of Mathematical Monograph, vol. 23, Am. Math. Soc., 1968.

[81] C. Lehrenfeld and A. Reusken, *Analysis of a high-order unfitted finite element method for elliptic interface problems*, IMA J. Numer. Anal., 38 (2018), 1351-1387.

[82] C. Lehrenfeld and A. Reusken, *L^2-error analysis of an isoparametric unfitted finite element method for elliptic interface problems*, J. Numer. Math., 27 (2019), 85-99.

[83] R. J. LeVeque and Z. Li, *The immersed interface method for elliptic equations with discontinuous coefficients and singular sources* , SIAM J. Numer. Anal., 31 (1994), 1019-1044.

[84] Z. Li, T. Lin, and X. Wu, *New cartesian grid methods for interface problems using the finite element formulation*, Numer. Math., 96 (2003), 61-98.

[85] J. Li, J. M. Melenk, B. Wohlmuth, and J. Zou, *Optimal a priori estimates for higher order finite elements for elliptic interface problems*, Appl. Numer. Math., 60 (2010), 19-37.

[86] H. Li, L. Mu and X. Ye, *Interior energy error estimates for the weak Galerkin finite element method*, Numer. Math. 139 (2018), 447-478.

[87] D. Li, Y. Nie and C. Wang, *Superconvergence of numerical gradient for weak Galerkin finite element methods on nonuniform Cartesian partitions in three dimensions*, Comput. Math. Appl., 78 (2019), 905-928.

[88] Q. H. Li and J. Wang, *Weak Galerkin finite element methods for parabolic equations*, Numer. Methods Partial Differential Equations, 29 (2013), 2004-2024.

[89] D. Li, C. Wang and J. Wang, *Superconvergence of the gradient approximation for weak Galerkin finite element methods on nonuniform rectangular partitions*, Appl. Numer. Math., 150 (2020), 396-417.

[90] J. Li, X. Ye and S. Zhang, *A weak Galerkin least-squares finite element method for div-curl systems*, J. Comput. Phys. 363 (2018), 79-86.

[91] T. Lin and D. Sheen, *The immersed finite element method for parabolic problems using the Laplace transformation in time discretization*, IJNAM, 10 (2013), 298-313.

[92] T. Lin, Y. Lin and X. Zhang, *Partially penalized immersed finite element methods for elliptic interface problems*, SIAM J. Numer. Anal., 53 (2015), 1121-1144.

[93] G. Lin, J. Liu, L. Mu and X. Ye, *Weak Galerkin finite element methods for Darcy flow: anisotropy and heterogeneity*, J. Comput. Phys. 276 (2014), 422-437.

[94] T. Lin, D. Sheen and X. Zhang, *A nonconforming immersed finite element method for elliptic interface problems*, J. Sci. Comput., 79 (2019), 442-463.

[95] T. Lin, Q. Yang and X. Zhang, *A priori error estimates for some discontinuous Galerkin immersed finite element methods*, J. Sci. Comput., 65 (2015), 875-894.

[96] ———, *Partially penalized immersed finite element methods for parabolic interface problems*, Numer. Methods Partial Differential Equations, 31 (2015), 1925-1947.

[97] R. Lin, X. Ye, S. Zhang and P. Zhu, *A weak Galerkin finite element method for singularly perturbed convection-diffusion-reaction problems*, SIAM J. Numer. Anal., 56 (2018), 1482-1497.

[98] J. Liu, S. Tavener and Z. Wang, *Lowest-order weak Galerkin finite element method for Darcy flow on convex polygonal meshes*, SIAM J. Sci. Comput. 40 (2018), B1229-B1252.

[99] R. C. MacCamy and M. Suri, *A time-dependent interface problem for two-dimensional eddy currents*, Quart. Appl. Math., 44 (1987), 675-690.

[100] G. H. Markxa and C. L. Daveyb, *The dielectric properties of biological cells at radio frequencies: applications in biotechnology*, Enzyme and Microbial Technology, 25 (1999), 161-171.

[101] R. Massjung, *An unfitted discontinuous Galerkin method applied to elliptic interface problems*, SIAM J. Numer. Anal., 50 (2012), 3134-3162.

[102] D. Miklavcic, N. Pavselj and F. X. Hart, *Electric properties of tissues*, Wiley Encyclopedia of Biomedical Engineering, 2006.

[103] L. Mu, *A uniformly robust H(div) weak Galerkin finite element methods for Brinkman problems*, SIAM J. Numer. Anal. 58 (2020), 1422-1439.

[104] ———, *Pressure robust weak Galerkin finite element methods for Stokes problems*, SIAM J. Sci. Comput. 42 (2020), B608-B629.

[105] L. Mu, J. Wang, Y. Wang and X. Ye, *A computational study of the weak Galerkin method for second-order elliptic equations*, Numer. Algorithms, 63 (2013), 753-777.

[106] ———, *A weak Galerkin mixed finite element method for biharmonic equations*, Numerical solution of partial differential equations: theory, algorithms, and their applications, 247-277, Springer Proc. Math. Stat., 45, Springer, New York, 2013.

[107] L. Mu, J. Wang, G. Wei, X. Ye, and S. Zhao, *Weak Galerkin methods for second order elliptic interface problems*, J. Comput. Phys. 250 (2013), 106-125.

[108] L. Mu, J. Wang and X. Ye, *Weak Galerkin finite element methods for the biharmonic equation on polytopal meshes*, Numer. Methods Partial Differential Equations 30 (2014), 1003-1029.

[109] ———, *Weak Galerkin finite element methods on polytopal meshes*, Int. J. Numer. Anal. Model., 12 (2015), 31-53.

[110] , ——— *A least-squares-based weak Galerkin finite element method for second order elliptic equations*, SIAM J. Sci. Comput. 39 (2017), A1531-A1557.

[111] ———, *Effective implementation of the weak Galerkin finite element methods for the biharmonic equation*, Comput. Math. Appl. 74 (2017), 1215-1222.

[112] L. Mu, J. Wang, X. Ye and S. Zhao, *A new weak Galerkin finite element method for elliptic interface problems*, J. Comput. Phys., 325 (2016), 157-173.

[113] L. Mu, X. Ye and S. Zhang, *A Stabilizer-free, pressure-robust, and superconvergence weak Galerkin finite element method for the Stokes equations on polytopal mesh*, SIAM J. Sci. Comput. 43 (2021), A2614-A2637.

[114] F. Müller, D. Schötzau and C. Schwab, *Discontinuous Galerkin methods for acoustic wave propagation in polygons*, J. Sci. Comput., 77 (2018), 1909-1935.

[115] Nikolić, V. and Kaltenbacher, B., *On higher regularity for the Westervelt equation with strong nonlinear damping*, Appl. Anal., 95 (2016), 2824-2840.

[116] Nikolić, V. and Wohlmuth, B., *A priori error estimates for the finite element approximation of Westervelt's quasi-linear acoustic wave equation*, SIAM J. Numer. Anal., 57 (2019), 1897-1918.

[117] Y. Polevaya, I. Ermolina, M. Schlesinger, B.-Z. Ginzburg and Y. Feldman, *Time domain dielectric spectroscopy study of human cells II. Normal and malignant white blood cells*, Biochimica et Biophysica Acta, 1419 (1999), 257-271.

[118] M. R. M. Rao, *Ordinary Differential Equations Theory and Aplications*, East-West Press Pvt. Ltd., 1980.

[119] J. Rauch, *On convergence of the finite element method for the wave equation*, SIAM J. Numer. Anal. 22 (1999) 245-249.

[120] P. A. Raviart and J. M. Thomas, *A mixed finite element method for 2-nd order elliptic problems*, in: A. Dold, B. Eckmann (Eds.), *Mathematical Aspects of Finite Element Methods, Lecture Notes in Mathematics Series*, Vol. 606, Springer, Berlin, 1977, 92-315.

[121] L. Rems, M. Ušaj, M. Kandušer, M. Reberšek, D. Miklavčič and G. Pucihar *Cell electrofusion using nanosecond electric pulses*, Sci. Rep., 3 (2013), 3382 (DOI: 10.1038/srep03382).

[122] A. Reusken and T. H. Nguyen, *Nitsche's method for a transport problem in two-phase incompressible flows*, J. Fourier Anal. Appl., 15 (2009), 663-683.

[123] J. C. Robinson, *Infinite-dimensional dynamical system: an introduction to dissipative parabolic PDEs and the theory of global attractors*, Cambridge Texts in Applied Mathematics, New York, USA, 2001.

[124] E. Salimi, *Nanosecond pulse electroporation of biological cells: the effect of membrane dielectric relaxation*, Thesis submitted to the University of Manitoba, Department of Electrical and Computer Engineering, 2011.

[125] K. H. Schoenbach, F. E. Peterkin, R. W. Alden and S. J. Beebe, *The effect of pulsed electric fields on biological cells: experiments and applications*, IEEE Trans. Plasma Sci., 25 (1997), 284-292.

[126] H. P. Schwan, *Mechanism responsible for electrical properties of tissues and cell suspensions*, Med.Prog. Technol., 19 (1993), 163-165.

[127] R. K. Sinha and B. Deka, *Optimal error estimates for linear parabolic problems with discontinuous coefficients*, SIAM J. Numer. Anal., 43 (2005), 733-749.

[128] ———, *An unfitted finite element method for elliptic and time dependent parabolic interface problems*, IMA J. Numer. Anal., 27 (2007), 529-549.

[129] L. Song, K. Liu and S. Zhao *A weak Galerkin method with an over-relaxed stabilization for low regularity elliptic problems*, J. Sci. Comput. 71 (2017), 195-218.

[130] L. Song, S. Zhao and K. Liu *A relaxed weak Galerkin method for elliptic interface problems with low regularity*, Appl. Numer. Math., 128 (2018) 65-80.

[131] V. Thomée, *Galerkin Finite Element Methods for Parabolic Problems*, Springer-Verlag, 1997.

[132] C. Tucci, M. Trujillo, E. Berjano, M. Iasiello, A. Andreozzi and G. P. Vanoli, *Pennes' bioheat equation vs. porous media approach in computer modeling of radiofrequency tumor ablation*, Sci. Rep., 11 (2021), 5272, https://doi.org/10.1038/s41598-021-84546-6.

[133] G. Vacca and L. Beirão da Veiga, *Virtual element methods for parabolic problems on polygonal meshes*, Numer. Methods Partial Differential Equations 31 (2015), 2110-2134.

[134] L. Beirão da Veiga, F. Brezzi, A. Cangiani, G. Manzini, L. D. Marini and A. Russo, *Basic principles of virtual element methods*, Math. Models Methods Appl. Sci. 23 (2013), 199-214.

[135] L. Beirão da Veiga and G. Manzini, *A virtual element method with arbitrary regularity*, IMA J. Numer. Anal. , 34 (2014), 759-781.

[136] Y. Wang, Y. Chen, Y. Huang and H. Yi, *A family of two-grid partially penalized immersed finite element methods for semi-linear parabolic interface problems*, J. Sci. Comput., 88 (2021), no. 3, Paper No. 80.

[137] X. Wang, F. Gao and Z. Sun, *Weak Galerkin finite element method for viscoelastic wave equations*, J. Comput. Appl. Math., 375 (2020), 112816, 10 pp.

[138] C. Wang and J. Wang, *A hybridized weak Galerkin finite element method for the biharmonic equation*, Int. J. Numer. Anal. Model. 12 (2015), 302-317.

[139] ———, *Discretization of div-curl systems by weak Galerkin finite element methods on polyhedral partitions*, J. Sci. Comput. 68 (2016), 1144-1171.

[140] ———, *A primal-dual weak Galerkin finite element method for second order elliptic equations in non-divergence form*, Math. Comp. 87 (2018), 515-545.

[141] K. Wang and N. Wang, *Analysis of a fully discrete finite element method for parabolic interface problems with nonsmooth initial data*, J. Comput. Math., article in press, doi:10.4208/jcm.2101-m2020-0075.

[142] J. Wang, R. Wang, Q. Zhai and R. Zhang, *A systematic study on weak Galerkin finite element methods for second order elliptic problems*, J. Sci. Comput., 74 (2018), 13691396.

[143] J. Wang and X. Ye, *A weak Galerkin finite element method for second-order elliptic problems*, J. Comput. Appl. Math., 241 (2013), 103-115.

[144] _____, *A weak Galerkin mixed finite element method for second order elliptic problems*, Math. Comp., 83 (2014), 2101-2126.

[145] _____, *A weak Galerkin finite element method for the Stokes equations*, Adv. Comput. Math., 42 (2016), 155-174.

[146] J. Wang, Q. Zhai, R. Zhang, S. Zhang, *A weak Galerkin finite element scheme for the Cahn-Hilliard equation*, Math. Comp. 88 (2019), 211-235.

[147] X. Wang and J. Zou, *Identification of conductivity and permittivity in a pulsed electric field model*, Appl. Anal., 95 (2016), 2736-2749.

[148] J. C. Weaver and Y. Chizmadzhev, *Theory of electroporation: A review*, Bioelectrochemistry and Bioenergetics, 41 (1996), 135-160.

[149] S. Xie, P. Zhu and X. Wang, *Error analysis of weak Galerkin finite element methods for time-dependent convection-diffusion equations*, Appl. Numer. Math., 137 (2019), 19-33.

[150] F. Xu, T. J. Lu, K. A. Seffen and E. Y. K. Ng, *Mathematical modeling of skin bioheat transfer*, Appl. Mech. Rev., 62 (2009), 050801.

[151] F. Xu, T. J. Lu and K. A. Seffen, *Non-Fourier analysis of skin biothermomechanics*, Int. Jour. Heat and Mass Transfer, 51 (2008), 2237-2259.

[152] C. Yang, *Convergence of a linearized second-order BDF-FEM for nonlinear parabolic interface problems*, Comput. Math. Appl., 70 (2015), 265-281.

[153] L. Yang, *Electrical impedance spectroscopy for detection of bacterial cells in suspensions using interdigitated microelectrodes*, Talanta, 74 (2008), 1621-1629.

[154] Q. Yang, *Numerical analysis of partially penalized immersed finite element methods for hyperbolic interface problems*, Numer. Math. Theor. Methods Appl., 11 (2018), 272-298.

[155] Q. Yang and X. Zhang, *Discontinuous Galerkin immersed finite element methods for parabolic interface problems*, J. Comput. Appl. Math., 299 (2016), 127-139.

[156] X. Ye and S. Zhang, *A stabilizer free weak Galerkin method for the biharmonic equation on polytopal meshes*, SIAM J. Numer. Anal. 58 (2020), 2572-2588.

[157] S. Zhang, *Robust and local optimal a priori error estimates for interface problems with low regularity: mixed finite element approximations*, arXiv:1902.10901.

[158] Z. -J. Zhang and X.-J. Yu, Local discontinuous Galerkin method for parabolic interface problems, Acta Math. Appl. Sin. Engl. Ser., 31 (2015), 453-466.

[159] R. Zhang and Q. Zhai, *A weak Galerkin finite element scheme for the biharmonic equations by using polynomials of reduced order*, J. Sci. Comput. 64 (2015), 559-585.

[160] H. Zhang, Y. Zou, Y. Xu, Q. Zhai and H. Yue, *Weak Galerkin finite element method for second order parabolic equations*, Int. J. Numer. Anal. Model. 13 (2016), 525-544.

[161] S. Zhou, F. Gao, B. Li and Z. Sun, *Weak Galerkin finite element method with second-order accuracy in time for parabolic problems*, Appl. Math. Lett. 90 (2019), 118-123.

[162] C. Zhou, Y. Zou, S. Chai, Q. Zhang and H. Zhu, *Weak Galerkin mixed finite element method for heat equation*, Appl. Numer. Math. 123 (2018), 180-199.